

Copyright

by

Carrie Lynn Peterson

2010

**The Dissertation Committee for Carrie Lynn Peterson Certifies that this is the  
approved version of the following dissertation:**

**Simulation and Experimental Analyses of Human Movement:  
Application to Post-stroke Hemiparetic Gait**

**Committee:**

---

Richard R. Neptune, Supervisor

---

Lawrence D. Abraham

---

Ronald E. Barr

---

Steven A. Kautz

---

Raul G. Longoria

**Simulation and Experimental Analyses of Human Movement:  
Application to Post-stroke Hemiparetic Gait**

**by**

**Carrie Lynn Peterson, B.E.; M.S.E.**

**Dissertation**

Presented to the Faculty of the Graduate School of  
The University of Texas at Austin  
in Partial Fulfillment  
of the Requirements  
for the Degree of

**Doctor of Philosophy**

**The University of Texas at Austin  
August 2010**

## **Dedication**

This dissertation is dedicated to my sisters, Eliza and Amy, and to my parents, Jane and Paul, for their encouragement, laughter and love.

## **Acknowledgements**

I am grateful to have had Dr. Richard Neptune as an advisor for my graduate studies and research. The collaborative, productive and fun research environment he provided is one I hope to experience again and replicate for others. Dr. Steven Kautz has also been an excellent mentor throughout my graduate work and I appreciate his support and shared knowledge.

I would like to acknowledge members of the Neuromuscular Biomechanics Lab for their assistance and helpful comments, and for contributing to an enjoyable research environment. Special thanks to Nick Fey for making my time at The University of Texas at Austin even better than I expected. I would like to thank our collaborators at the University of Florida for their help with data collection and processing. I would also like to acknowledge Dr. Alaa Ahmed and Dr. James Ashton-Miller for introducing me to biomechanics and for their mentorship during my undergraduate research at the University of Michigan.

Finally, I am very grateful to have received financial support through the National Science Foundation Graduate Research Fellowship Program and a Thrust 2000 Graduate Fellowship.

# **Simulation and Experimental Analyses of Human Movement: Application to Post-stroke Hemiparetic Gait**

Publication No. \_\_\_\_\_

Carrie Lynn Peterson, PhD

The University of Texas at Austin, 2010

Supervisor: Richard R. Neptune

Stroke is the leading cause of long term disability with improved walking being an important goal following stroke. Understanding deficits that result in reduced walking performance by hemiparetic subjects is important for the design of effective rehabilitation strategies. The goal of this research was to investigate muscle coordination and mechanical work in hemiparetic walking and mechanisms of acceleration and deceleration in nondisabled walking as a framework for investigating non-steady state walking in hemiparetic subjects.

Musculoskeletal modeling and simulation analyses were used to compare individual muscle contributions to important walking subtasks and muscle mechanical work by representative hemiparetic subjects (limited community and community walkers) during pre-swing with a representative speed and age-matched control. Simulation analyses identified decreased paretic soleus and gastrocnemius contributions to forward propulsion and power generation as the primary impairment in the limited

community walker compared to the control. Comparison of mechanical work showed that total paretic and non-paretic fiber work was increased in the limited community walker, which was primarily related to decreased fiber and tendon work by paretic soleus and gastrocnemius. The decreased output by the ankle plantar flexors required compensatory work by other muscles. Also, the experimental analyses of accelerated and decelerated walking showed that the ankle plantar flexor moment was positively related to braking and propulsive impulses, which increased with speed. Thus, deficits of the paretic plantar flexors limit forward propulsion and increase mechanical work during pre-swing, and would limit the ability of hemiparetic walkers to accelerate and decelerate, which are essential tasks in daily living activities.

For the community walker, simulation analyses showed that deficits in paretic swing initiation are a primary impairment. Specifically, the paretic gastrocnemius and hip flexors contributed less to swing initiation in the community walker compared to the control subject. Total paretic and non-paretic fiber work was increased in the community walker, primarily due to increased work by the hip abductors and adductors. Because step length and step frequency were positively related to walking speed in accelerated and decelerated walking, impaired paretic swing initiation would likely limit the community walker's ability to accelerate and decelerate.

## Table of Contents

List of Tables .....	x
List of Figures .....	xii
Introduction.....	1
Background.....	1
Study Goals.....	3
Chapter 1 .....	6
Introduction.....	6
Methods.....	9
Results.....	14
Discussion.....	21
Conclusion .....	24
Chapter 2 .....	26
Introduction.....	26
Methods.....	28
Results.....	30
Discussion.....	39
Conclusion .....	43
Chapter 3 .....	45
Introduction.....	45
Methods.....	47
Results.....	50
Discussion.....	54
Conclusion .....	57



Conclusions.....	59
Summary .....	59
Future Work .....	61
Appendix 1.....	65
Appendix 2.....	81
Appendix 3.....	82
References.....	100
Vita .....	106

## List of Tables

Table 1-1: The 43 musculotendon actuators per leg were combined into 18 groups after analysis according to their anatomical classification and contributions to the walking subtasks.....	14
Table 1-2: The average error between the experimental and simulated kinematics and ground reaction forces (GRFs) compared to the average standard deviations of the experimental data (in parentheses below).....	15
Table 3-1: Linear mixed regression model coefficients (Coeff.) and intercepts (Int.) to predict braking impulses, propulsive impulses, step length and step frequency from walking speed during accelerated and decelerated walking. Model coefficients for the main effect of walking speed are shown in the top row. Interaction effects due to rate were determined with respect to deceleration at $0.12 \text{ m/s}^2$ . For example, the braking impulse (BI) at $0.03 \text{ m/s}^2$ can be predicted from walking speed (WS) with the following equation: $\text{BI} = (0.019 - 0.0034) + (0.0099 + 0.0016) \cdot \text{WS}$ . Significance of the model coefficients are indicated by * ( $p < 0.05$ ), and † ( $p < 0.001$ ).....	51
Table 3-2: Linear mixed model coefficients and intercepts (Int.) to predict braking and propulsive impulses from joint moment impulses generated during accelerated and decelerated walking. Significance of the model coefficients are indicated by * ( $p < 0.05$ ), and † ( $p < 0.001$ ).....	54
Table A1-1: Fitting equations for musculotendon lengths ( $L_{mt}$ ) and moment arms ( $R_i$ ) depending on the number of generalized coordinates (GCs) from Menegaldo et al. (2004). .....	67
Table A1-2: Generalized coordinates and the range of motion over which data were sampled to compute regression coefficients. ....	68
Table A1-3: Selected muscle groups according to dependence on the same generalized coordinates (GCs). ....	68
Table A1-4: Regression coefficients for Group 1 muscles dependent on 3 generalized coordinates to estimate musculotendon lengths ( $L_{mt}$ ) and hip flexion, hip abduction, and hip rotation moment arms ( $R_{HF}$ , $R_{HA}$ , $R_{HR}$ ) using the equations (Eq.) given in Table A1-1. ....	69
Table A1-5: Regression coefficients for Group 2 muscles dependent on 4 generalized coordinates to estimate musculotendon lengths ( $L_{mt}$ ) and hip flexion, hip abduction, hip rotation, and knee angle moment arms ( $R_{HF}$ , $R_{HA}$ , $R_{HR}$ , $R_{KA}$ ) using the equations (Eq.) given in Table A1-1. ....	74

Table A1-6: Regression coefficients for Group 3 muscles dependent on 1 generalized coordinate to estimate musculotendon lengths ( $L_{mt}$ ) and knee angle moment arms ( $R_{KA}$ ) using the equations (Eq.) given in Table A1-1. .... 76

Table A1-7: Regression coefficients for Group 4 muscles dependent on 3 generalized coordinates to estimate musculotendon lengths ( $L_{mt}$ ) and knee, ankle and subtalar angle moment arms ( $R_{KA}$ ,  $R_{AA}$ ,  $R_{SA}$ ) using the equations (Eq.) given in Table A1-1. .... 76

Table A1-8: Regression coefficients for Group 5 muscles dependent on 2 generalized coordinates to estimate musculotendon lengths ( $L_{mt}$ ) and ankle and subtalar angle moment arms ( $R_{AA}$ ,  $R_{SA}$ ) using the equations (Eq.) given in Table A1-1. .... 78

Table A1-9: Regression coefficients for Group 6 muscles dependent on 3 generalized coordinates to estimate musculotendon lengths ( $L_{mt}$ ) and ankle, subtalar and metatarsal angle moment arms ( $R_{AA}$ ,  $R_{SA}$ ,  $R_{MA}$ ) using the equations (Eq.) given in Table A1-1. .... 79

## List of Figures

Figure 1-1: Experimental data of the gait cycle with minimum difference in joint angles and ground reaction forces (GRFs) compared to the subject's average for the limited community walker at self-selected speed (with  $\pm 1$  standard deviation (S.D.) of the 30 s walking trial) and the control walking at 0.6 m/s. Data are normalized to the paretic (ipsilateral) gait cycle. Joint angle subtitles correspond to positive directions. Positive pelvic obliquity, rotation and tilt correspond to positive rotations about the X, Y and Z pelvis segment axes, respectively (see bottom right)..... 10

Figure 1-2: Experimental data of the gait cycle with minimum difference in joint angles and ground reaction forces (GRFs) compared to the subject's average for the community walker at self-selected speed (with  $\pm 1$  standard deviation (S.D.) of the 30 s walking trial) and the control walking at 1.0 m/s. Data are normalized to the paretic (ipsilateral) gait cycle. Joint angle subtitles correspond to positive directions. Positive pelvic obliquity, rotation and tilt correspond to positive rotations about the X, Y and Z pelvis segment axes, respectively (see bottom right). ..... 11

Figure 1-3: Primary muscle contributors to forward propulsion (i.e., average horizontal pelvis acceleration) and the total average pelvis acceleration and deceleration (Total) and net by all paretic (ipsilateral for control) and non-paretic (contralateral for control) muscles during pre-swing. (A) For the limited community walker, forward propulsion provided by paretic and non-paretic muscles were decreased and increased, respectively, compared to the speed-matched control. (B) Forward propulsion provided by paretic muscles (i.e., SOL and GMED) was increased in the community walker relative to the speed-matched control. .... 17

Figure 1-4: Primary muscle contributors to average swing initiation during pre-swing by paretic (ipsilateral for control) and non-paretic (contralateral for control) leg muscles. (A) For the limited community walker, swing initiation by paretic muscles was similar to the ipsilateral control leg, but paretic muscles absorbed less power compared to the control. (B) For the community walker, swing initiation by the paretic GAS, IL and SAR was decreased and paretic AM was increased compared to the control. Paretic muscles absorbed much more power from the paretic leg compared to the ipsilateral control leg. 19

Figure 1-5: Average power generated by paretic (ipsilateral for control) and non-paretic (contralateral for control) leg muscles during pre-swing. (A) Paretic muscles generated less power in the limited community walker relative to the speed-matched control as paretic GAS generated much less power. (B) The community walker generated and absorbed much power with the paretic and non-paretic leg muscles, although power generated by the paretic SOL and GAS was decreased relative to the control..... 20

Figure 2-1: For the limited community walker and control subject at 0.6 m/s, paretic (ipsilateral for control) and non-paretic (contralateral for control) EMG and optimized

excitation timings (bars below the EMG indicate when a muscle is excited) normalized to the paretic leg (ipsilateral for control) gait cycle. Average EMG is shown with  $\pm$  one standard deviation of the 30 s walking trial. Muscle excitations were optimized from mid-stance to toe-off corresponding to 36 to 84% of the paretic gait cycle for the limited community walker and 33 to 72% of the ipsilateral gait cycle for the control subject..... 31

Figure 2-2: For the community walker and control subject at 1.0 m/s, paretic (ipsilateral for control) and non-paretic (contralateral for control) EMG and optimized excitation timings (bars below the EMG indicate when a muscle is excited) normalized to the paretic leg (ipsilateral for control) gait cycle. Average EMG is shown with  $\pm$  one standard deviation of the 30 s walking trial. Muscle excitations were optimized from mid-stance to toe-off corresponding to 35 to 74% of the paretic gait cycle for the community walker and 36 to 74% of the ipsilateral gait cycle for the control subject..... 32

Figure 2-3: For the limited community walker and speed-matched control, musculotendon (MT), muscle fiber, and tendon work by all paretic (ipsilateral for control) and non-paretic (contralateral for control) muscles during paretic (ipsilateral for control) pre-swing. (A) Paretic leg negative musculotendon work was increased and positive tendon work was decreased relative to the ipsilateral control leg. (B) Net and total non-paretic musculotendon work was increased compared to the contralateral control leg. ....34

Figure 2-4: Net musculotendon (MT), fiber and tendon work by individual muscles during paretic (ipsilateral for control) pre-swing for the limited community walker and control subject at 0.6 m/s. (A) Paretic VAS and RF had increased negative fiber work and paretic IL and SAR had increased positive fiber work compared to the ipsilateral control leg. Positive tendon work by paretic SOL and GAS were decreased relative to the ipsilateral control leg. (B) Non-paretic and contralateral GMAX and HAM did much positive work in the limited community walker and control, respectively. Non-paretic SOL and GAS had increased positive fiber work and negative tendon work compared to the contralateral control leg. .... 35

Figure 2-5: For the community walker and speed-matched control, musculotendon (MT), muscle fiber, and tendon work by all paretic (ipsilateral for control) and non-paretic (contralateral for control) muscles during paretic (ipsilateral for control) pre-swing. (A) Paretic leg positive fiber work and negative tendon work was increased relative to the ipsilateral control leg. (B) Net non-paretic fiber and tendon work were similar to the contralateral control leg, but total non-paretic fiber and tendon work was increased relative to the contralateral leg..... 37

Figure 2-6: Net musculotendon (MT), fiber and tendon work by individual muscles during paretic (ipsilateral for control) pre-swing for the community walker and control subject at 1.0 m/s. (A) Positive fiber work was increased and positive tendon work was decreased in paretic GAS compared to the ipsilateral control leg. Paretic GMED, GMIN,

AM and QFEM generated more fiber and tendon work in the community walker compared to the ipsilateral control leg. (B) Fiber work by non-paretic GMED, GMIN and PIRI was increased and fiber work by non-paretic VAS, GMAX, and HAM was decreased in the community walker relative to the contralateral control leg. .... 38

Figure 3-1: Hip, knee and ankle moment impulses were computed for each step during the braking (light shaded) and propulsive (dark shaded) phases in order to identify relationships between joint moment impulses with the braking and propulsive impulses, respectively. Anterior-posterior ground reaction forces (AP GRFs) and joint moments were normalized by subject body weight (BW). .... 49

Figure 3-2: Anterior-posterior (AP) ground reaction force impulses increased with walking speed during accelerated and decelerated walking. The braking (negative) impulse had a greater relationship with walking speed than the propulsive impulse at each rate. Linear mixed regression models were generated from data collected from ten subjects and are compared to individual steps from three trials for a representative subject at each rate and their mean AP impulses (error bars are  $\pm 3$  standard deviations) at steady-state speeds. ....52

Figure 3-3: Step length (normalized by leg length (LL)) and frequency increased with walking speed during accelerated and decelerated walking. Linear mixed models generated from data across ten subjects well predicted mean step lengths and frequencies (error bars are  $\pm 3$  standard deviations) by a representative subject at steady-state speeds compared with individual steps during three trials at each rate..... 53

Figure A1-1: Schematic of a simulated annealing algorithm that determined the muscle excitation patterns that minimized differences between simulated and experimentally measured kinematics and ground reaction forces. .... 65

Figure A2-1: Kinematic and GRF data were collected during treadmill walking at the VA-UF Human Motor Performance Laboratory, VA Medical Center at Gainesville, Florida. Marker trajectories were recorded with a twelve-camera motion capture system (Vicon) and GRF data were measured as subjects walked on a split-belt instrumented treadmill. A safety harness that did not provide body weight support was worn during all trials to protect subjects in case of a loss of balance..... 81

Figure A3-1: Anterior-posterior ground reaction forces (AP GRFs), hip, knee and ankle moments across speeds of 0.8 to 1.2 m/s during a representative acceleration and deceleration trial at  $0.03 \text{ m/s}^2$ ..... 82

Figure A3-2: Anterior-posterior ground reaction forces (AP GRFs), hip, knee and ankle moments across speeds of 0.8 to 1.2 m/s during a representative acceleration and deceleration trial at  $0.06 \text{ m/s}^2$ ..... 83

Figure A3-3: Anterior-posterior ground reaction forces (AP GRFs), hip, knee and ankle moments across speeds of 0.8 to 1.2 m/s during a representative acceleration and deceleration trial at 0.09 m/s <sup>2</sup> .....	84
Figure A3-4: Anterior-posterior ground reaction forces (AP GRFs), hip, knee and ankle moments across speeds of 0.8 to 1.2 m/s during a representative acceleration and deceleration trial at 0.12 m/s <sup>2</sup> .....	85
Figure A3-5: Linear mixed regression models were generated from data collected from ten subjects and are compared to individual steps for subject 01 at each rate and subject 01's mean anterior-posterior ground reaction force (AP) impulses (error bars are $\pm 3$ standard deviations) at steady-state speeds. Subject 01's self-selected walking speed was 1.1 m/s.....	86
Figure A3-6: Linear mixed regression models were generated from data collected from ten subjects and are compared to individual steps for subject 02 at each rate and subject 02's mean anterior-posterior ground reaction force (AP) impulses (error bars are $\pm 3$ standard deviations) at steady-state speeds. Subject 02's self-selected walking speed was 1.2 m/s.....	87
Figure A3-7: Linear mixed regression models were generated from data collected from ten subjects and are compared to individual steps for subject 03 at each rate and subject 03's mean anterior-posterior ground reaction force (AP) impulses (error bars are $\pm 3$ standard deviations) at steady-state speeds. Subject 03's self-selected walking speed was 1.2 m/s.....	88
Figure A3-8: Linear mixed regression models were generated from data collected from ten subjects and are compared to individual steps for subject 04 at each rate and subject 04's mean anterior-posterior ground reaction force (AP) impulses (error bars are $\pm 3$ standard deviations) at steady-state speeds. Subject 04's self-selected walking speed was 1.4 m/s.....	89
Figure A3-9: Linear mixed regression models were generated from data collected from ten subjects and are compared to individual steps for subject 06 at each rate and subject 06's mean anterior-posterior ground reaction force (AP) impulses (error bars are $\pm 3$ standard deviations) at steady-state speeds. Subject 06's self-selected walking speed was 1.15 m/s.....	90
Figure A3-10: Linear mixed regression models were generated from data collected from ten subjects and are compared to individual steps for subject 07 at each rate and subject 07's mean anterior-posterior ground reaction force (AP) impulses (error bars are $\pm 3$ standard deviations) at steady-state speeds. Subject 07's self-selected walking speed was 1.15 m/s.....	91

Figure A3-11: Linear mixed regression models were generated from data collected from ten subjects and are compared to individual steps for subject 08 at each rate and subject 08's mean anterior-posterior ground reaction force (AP) impulses (error bars are $\pm 3$ standard deviations) at steady-state speeds. Subject 08's self-selected walking speed was 1.1 m/s.....	92
Figure A3-12: Linear mixed regression models were generated from data collected from ten subjects and are compared to individual steps for subject 09 at each rate and subject 09's mean anterior-posterior ground reaction force (AP) impulses (error bars are $\pm 3$ standard deviations) at steady-state speeds. Subject 09's self-selected walking speed was 1.25 m/s.....	93
Figure A3-13: Linear mixed regression models were generated from data collected from ten subjects and are compared to individual steps for subject 10 at each rate and subject 10's mean anterior-posterior ground reaction force (AP) impulses (error bars are $\pm 3$ standard deviations) at steady-state speeds. Subject 10's self-selected walking speed was 1.1 m/s.....	94
Figure A3-14: Linear models generated from data across ten subjects compared to mean step lengths (normalized by leg length (LL)) and frequencies ( $\pm 3$ standard deviations) by subject 01 at steady-state speeds and individual steps.....	95
Figure A3-15: Linear models generated from data across ten subjects compared to mean step lengths (normalized by leg length (LL)) and frequencies ( $\pm 3$ standard deviations) by subject 02 at steady-state speeds and individual steps.....	95
Figure A3-16: Linear models generated from data across ten subjects compared to mean step lengths (normalized by leg length (LL)) and frequencies ( $\pm 3$ standard deviations) by subject 03 at steady-state speeds and individual steps.....	96
Figure A3-17: Linear models generated from data across ten subjects compared to mean step lengths (normalized by leg length (LL)) and frequencies ( $\pm 3$ standard deviations) by subject 04 at steady-state speeds and individual steps.....	96
Figure A3-18: Linear models generated from data across ten subjects compared to mean step lengths (normalized by leg length (LL)) and frequencies ( $\pm 3$ standard deviations) by subject 06 at steady-state speeds and individual steps.....	97
Figure A3-19: Linear models generated from data across ten subjects compared to mean step lengths (normalized by leg length (LL)) and frequencies ( $\pm 3$ standard deviations) by subject 07 at steady-state speeds and individual steps.....	97



Figure A3-20: Linear models generated from data across ten subjects compared to mean step lengths (normalized by leg length (LL)) and frequencies ( $\pm 3$  standard deviations) by subject 08 at steady-state speeds and individual steps..... 98

Figure A3-21: Linear models generated from data across ten subjects compared to mean step lengths (normalized by leg length (LL)) and frequencies ( $\pm 3$  standard deviations) by subject 09 at steady-state speeds and individual steps..... 98

Figure A3-22: Linear models generated from data across ten subjects compared to mean step lengths (normalized by leg length (LL)) and frequencies ( $\pm 3$  standard deviations) by subject 10 at steady-state speeds and individual steps..... 99

## **Introduction**

### **BACKGROUND**

Stroke is the leading cause of long-term disability in the United States (American Heart Association, 1997). Because improving walking is the goal most often stated by patients following a stroke, rehabilitation to increase walking speed is important. A central disability associated with post-stroke hemiparesis is that muscle excitation is impaired, and thus muscles fail to produce properly graded and timed force (i.e., muscle coordination). The influence of muscle coordination on walking speed can be determined using dynamic musculoskeletal-based simulations to quantify the contribution of each muscle force to a set of biomechanical subtasks: forward propulsion (i.e., acceleration of the trunk forward), swing initiation (i.e., acceleration of the leg forward) and power generation (i.e., production or absorption of mechanical energy). Modeling and simulation techniques have been used to quantify muscle contributions to these subtasks in nondisabled subjects walking at self-selected (Neptune et al., 2001; Neptune et al., 2004a; Liu et al., 2006) and across increasing steady-state speeds (Neptune et al., 2008; Liu et al., 2008). However, the relationships between impaired muscle coordination and walking speed in persons with hemiparesis are unknown. Because hemiparetic walking speed likely depends largely on the person's ability to coordinate the paretic leg during pre-swing (i.e. period from non-paretic leg heel strike to paretic toe-off) when much propulsion is generated in nondisabled walking, understanding these relationships during paretic pre-swing would be extremely beneficial for the design of effective rehabilitation strategies.

In addition to impaired muscle coordination, the metabolic cost of hemiparetic walking is up to two times the cost of nondisabled walking at slow speeds ( $< 0.4$  m/s) and ranges from normal to 1.7 times greater for hemiparetic subjects that walk at mild to moderate speeds (Zamparo et al., 1995). Recently, analyses showed that the greater cost of hemiparetic walking was related to an increase in total positive mechanical work, with more work done by the non-paretic leg than the paretic leg (Detrembleur et al., 2003). However, it is not clear from these measures of total work which muscles are contributing to the increased mechanical work. Previous studies have used experimental methods to compute joint moment work in hemiparetic subjects (Olney et al., 1991; Chen and Patten, 2008), but these methods are limited in their ability to account for co-contraction and elastic energy storage and return such that mechanical work is most likely over or under estimated (Sasaki et al., 2009). However, modeling and simulation analyses overcome these limitations since both positive and negative work production by individual muscles can be precisely quantified and provide important insight into the increased metabolic cost of hemiparetic walking.

The impaired muscle coordination and increased metabolic cost is compounded by the inability to accelerate and decelerate during walking and remains a challenge for hemiparetic subjects. Daily living is mainly comprised of short duration walking bouts with approximately forty percent of all walking bouts for nondisabled adult individuals in typical urban environments consisting of less than twelve consecutive steps (Orendurff et al., 2008a). Thus, the ability to accelerate and decelerate is important for walking in daily life and is likely more demanding than maintaining a constant speed. Forward propulsion of the body center of mass is a central task of walking that depends on the generation of appropriate anterior-posterior ground reaction forces (AP GRFs). However, to date no study has investigated AP GRFs in accelerated and decelerated walking over a wide

range of speeds. As a first step, understanding how nondisabled subjects modulate AP GRFs, step length and step frequency to accelerate and decelerate would provide a framework for which to investigate non steady-state walking in hemiparetic populations.

## **STUDY GOALS**

The overall goal of this work was to investigate muscle coordination and mechanical work production during pre-swing in hemiparetic walking and mechanisms of acceleration and deceleration in nondisabled walking. This goal was achieved via three specific studies.

The purpose of the first study was to use modeling and simulation analyses to compare individual muscle contributions to the walking subtasks of forward propulsion, swing initiation and power generation by two representative hemiparetic subjects with different levels of walking function classified by self-selected speed (i.e., limited community = 0.4-0.8 m/s and community walkers = >0.8 m/s) (Perry et al., 1995) to speed and age-matched controls during pre-swing. Simulation analyses of nondisabled adults walking at their self-selected speed showed that ankle plantar flexor force production is critical to power generation, forward propulsion and swing initiation during pre-swing (Neptune et al., 2001). Because experimental studies have reported deficits in kinetic (Nadeau et al., 1999; Lamontagne et al., 2002; Chen et al., 2005a) and electromyographic (EMG) (Turns et al., 2007) measures of the paretic plantar flexors during pre-swing, these paretic muscles were expected to contribute less to the walking subtasks in the hemiparetic walkers compared to the speed-matched controls. Also, because paretic hip flexor moments and powers seem to be reduced for slow walkers and increased for fast walkers with respect to nondisabled controls (Nadeau et al., 1999), the

hip flexors were expected to compensate for lower gastrocnemius force in the community walker, but not in the limited community walker.

The purpose of the second study was to compare individual musculotendon work generated by two representative hemiparetic subjects to a speed and age-matched control. Muscle mechanical work performed by representative hemiparetic walkers at two different levels were analyzed because metabolic cost is more increased compared to speed-matched controls for hemiparetic walkers at slower self-selected speeds than for hemiparetic walkers with faster self-selected speeds (Zamparo et al., 1995). Recently, muscle mechanical work generated by nondisabled walkers was quantified across a wide range of steady-state speeds using simulation analyses (Neptune et al., 2008). The plantar flexors and hip extensors produced the most positive muscle work during stance, and the knee extensors the most negative work during stance (Neptune et al., 2008). An experimental study of hemiparetic walking found that ankle plantar flexor work during pre-swing is greatly reduced compared to speed and age-matched controls (Chen and Patten, 2008). Thus, it was expected that the paretic plantar flexors would produce less positive work relative to the speed-matched controls. Further, because differences in hip flexor and knee extensor moment work in the paretic leg have been found to partially offset the reduction in plantar flexor work during pre-swing (Chen and Patten, 2008), it was expected that the paretic hip flexors would produce more positive work and the knee extensors more negative work in stance relative to speed-matched controls.

The purpose of the third study was to identify relationships between walking speed with AP impulses (i.e., time integral of the AP GRF), step length and step frequency during accelerated and decelerated walking by nondisabled subjects across moderate speeds (0.4 to 1.8 m/s). Braking (negative AP impulse) and propulsive (positive AP impulse) impulses regulate walking speed. Increasing step frequency decreases the

AP impulse, whereas increasing step length, and thereby peak AP GRF, presumably increases the AP impulse. Previously, braking and propulsive impulses were found to increase with steady-state speeds from 1.0 to 2.0 m/s (Nilsson and Thorstensson, 1989). Thus, it was expected that step length would influence AP GRFs more than step frequency such that AP impulses would increase with walking speed. Another purpose of the third study was to identify relationships between braking and propulsive impulses with joint moment impulses. Based on previous simulation analyses of nondisabled walking across steady-state speeds (Neptune et al., 2008; Liu et al., 2008), it was expected that increased hip and knee extensor moments during early stance would increase the braking impulse and increased plantar flexor moments during stance would increase both braking and propulsive impulses.

## **Chapter 1**

### **Muscle Function during Pre-swing in Hemiparetic Walking**

#### **INTRODUCTION**

A central disability associated with post-stroke hemiparesis is impaired muscle excitation, which inhibits the generation of properly graded and timed muscle force (i.e., muscle coordination) necessary to perform important subtasks of walking. Of particular interest are those subtasks related to improving walking speed, which include forward propulsion (i.e., acceleration of the pelvis forward), swing initiation (i.e., power delivered to the swing leg) and power generation (i.e., production or absorption of mechanical energy). Recent studies have quantified muscle contributions to these subtasks in nondisabled subjects at self-selected and increasing steady-state speeds (Neptune et al., 2004a; Neptune et al., 2008) and found that pre-swing (i.e., double support phase proceeding toe-off) is a critical region of the gait cycle for muscles to accomplish these subtasks. Clinical studies of hemiparetic walking have shown pre-swing abnormalities in the paretic leg, including prolonged duration of the phase relative to the total gait cycle, reduced peak hip extension, and reduced hip and knee flexion velocities (De Quervain et al., 1996), suggesting that paretic muscle contributions to these subtasks are different than those of nondisabled walkers. Because walking speed depends largely on the person's ability to coordinate the paretic leg during pre-swing, understanding the relationships between impaired muscle coordination and walking speed in hemiparetic subjects during pre-swing would be extremely beneficial for designing effective locomotor interventions.

Due to dynamic coupling arising from the multiarticular nature of the musculoskeletal system (Zajac, 1993), individual muscle function is difficult to assess via

experimental techniques that use an inverse dynamics approach (Zajac et al., 2002). However, modeling and simulation techniques can quantify individual muscle contributions to body segment accelerations and power distribution. For example, simulation analyses of nondisabled walking have shown that soleus (SOL) and gastrocnemius (GAS) force output are both critical to power generation, while SOL is the primary contributor to forward propulsion and GAS is the primary contributor to swing initiation (Neptune et al., 2001; Zajac et al., 2003; Neptune et al., 2008). The hip flexors (e.g., iliacus, psoas (IL)) were also found to contribute to leg swing initiation (Neptune et al., 2004a; Neptune et al., 2008).

Experimental studies of hemiparetic walking have reported several abnormalities during paretic pre-swing including deficits in electromyography (EMG) (Lamontagne et al., 2002; Knutsson and Richards, 1979; Den Otter et al., 2007) and kinetic measures (Nadeau et al., 1999; Lamontagne et al., 2002; Chen et al., 2005a) of the paretic plantar flexors. EMG recorded from paretic SOL and GAS show reduced and early excitation compared to nondisabled EMG patterns (Knutsson and Richards, 1979; Den Otter et al., 2007). Chen et al. (2005a) found differences in kinetic leg energy in hemiparetic subjects and speed-matched controls that suggest impaired paretic leg swing initiation. Other experimental studies have hypothesized that some hemiparetic subjects are able to compensate for paretic plantar flexor deficits and achieve faster walking speeds via the paretic hip flexors (Nadeau et al., 1999) and/or non-paretic leg force production (Bowden et al., 2006). For example, Nadeau et al. (1999) found weakness of the plantar flexors was correlated with gait speed limitations in a group of hemiparetic subjects, and some of these subjects who attained faster speeds produced an increased hip flexor moment. Bowden et al. (2006) reported that hemiparetic subjects with high and moderate severity relied heavily on the non-paretic leg to generate propulsion, which may do so during



paretic pre-swing due to the changed orientation of the non-paretic leg. Specifically, in many hemiparetic subjects, the non-paretic foot is not as far forward at heel contact (relative to the pelvis) and flat for an extended time during paretic pre-swing compared to nondisabled walkers (Hsu et al., 2003; Chen et al., 2005a; Balasubramanian et al., 2007). Because simulation analyses of nondisabled walking showed that the gluteus maximus (GMAX), vasti group (VAS) and hamstrings (HAM) each contribute to forward propulsion and power generation during foot flat (Neptune et al., 2004a), these non-paretic muscles may do so during paretic pre-swing.

The purpose of this study was to compare individual muscle contributions to forward propulsion, swing initiation and power generation of two representative hemiparetic subjects with different levels of walking function classified by self-selected speed (i.e., limited community = 0.4-0.8 m/s and community walkers = >0.8 m/s) (Perry et al., 1995) and speed and age-matched controls during pre-swing. I expected that: 1) GAS contribution to swing initiation, SOL contribution to forward propulsion and SOL and GAS power generation would be decreased; 2) swing initiation and power generation by the paretic hip flexors (e.g., IL) would be decreased for the limited community walker; and 3) forward propulsion and power generation provided by non-paretic GMAX, VAS and HAM during paretic leg pre-swing (i.e., early stance of the non-paretic leg) would be increased relative to controls. Because the stroke population is very heterogeneous, this study is a first step toward understanding the various impairments and compensatory mechanisms in post-stroke hemiparetic walking.

## METHODS

### *Experimental Data*

Experimental data were collected from 51 hemiparetic subjects walking at self-selected speeds without use of an assistive device or ankle-foot orthosis and 21 nondisabled elderly subjects walking at self-selected speeds and speeds of 0.3, 0.6 and 0.9 m/s at the VA Brain Rehabilitation Research Center at the University of Florida as part of a larger study. A safety harness mounted to the ceiling that provided no body weight support protected the subjects in the event of loss of balance. All subjects signed informed consent and the Institutional Review Boards of the University of Florida and the University of Texas approved the protocol. Three-dimensional (3D) ground reaction forces (GRFs) and kinematics, and bilateral EMG from eight lower limb muscles (medial gastrocnemius, soleus, tibialis anterior, rectus femoris, vastus lateralis, biceps femoris, semimembranosus, and gluteus medius) were recorded at 2000 Hz, 100 Hz and 2000 Hz, respectively, during 30 s walking trials on a split-belt instrumented treadmill (Tecmachine) and were processed using Visual 3D (C-Motion, Inc.). Raw kinematic and GRF data were low-pass filtered using a fourth-order zero-lag Butterworth filter with cutoff frequencies of 6 Hz and 20 Hz, respectively. All data were time normalized to 100% of the paretic (ipsilateral, right for control) gait cycle and averaged across consecutive gait cycles within each subject at each speed. From this data set, walking trials of a representative subject from each functional group (limited community: male, left hemiparesis, single cerebrovascular infarction, age = 53 years, time post stroke = 2 years 1 month, self-selected treadmill speed = 0.45 m/s; community: male, left hemiparesis, single cerebrovascular infarction, age = 60 years, time post stroke = 8 years

5 months, self-selected treadmill speed = 0.9 m/s) and an age matched control subject (female, age = 59 years) walking at speeds of 0.6 and 1.0 m/s were selected for the simulation analysis. For these trials, the individual gait cycle with the minimum difference in joint angles and GRFs compared to the average data was used as tracking data (Figs. 1-1 and 1-2).

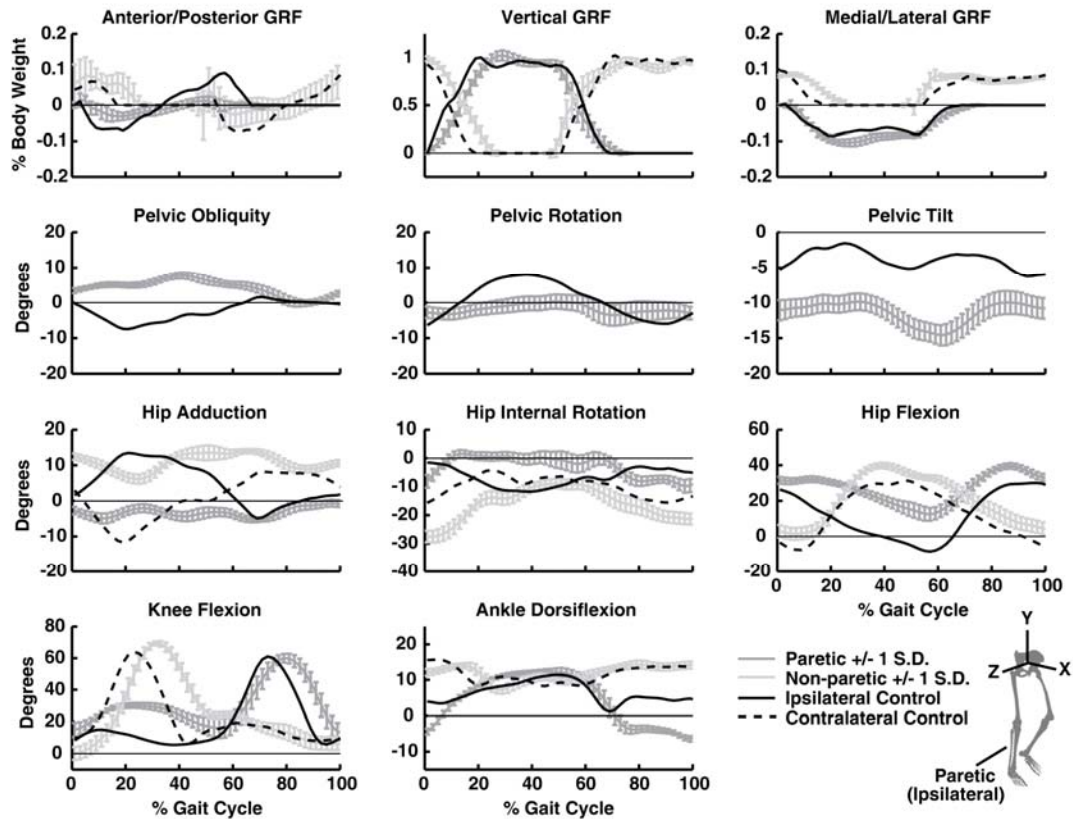


Figure 1-1: Experimental data of the gait cycle with minimum difference in joint angles and ground reaction forces (GRFs) compared to the subject's average for the limited community walker at self-selected speed (with  $\pm 1$  standard deviation (S.D.) of the 30 s walking trial) and the control walking at 0.6 m/s. Data are normalized to the paretic (ipsilateral) gait cycle. Joint angle subtitles correspond to positive directions. Positive pelvic obliquity, rotation and tilt correspond to positive rotations about the X, Y and Z pelvis segment axes, respectively (see bottom right).

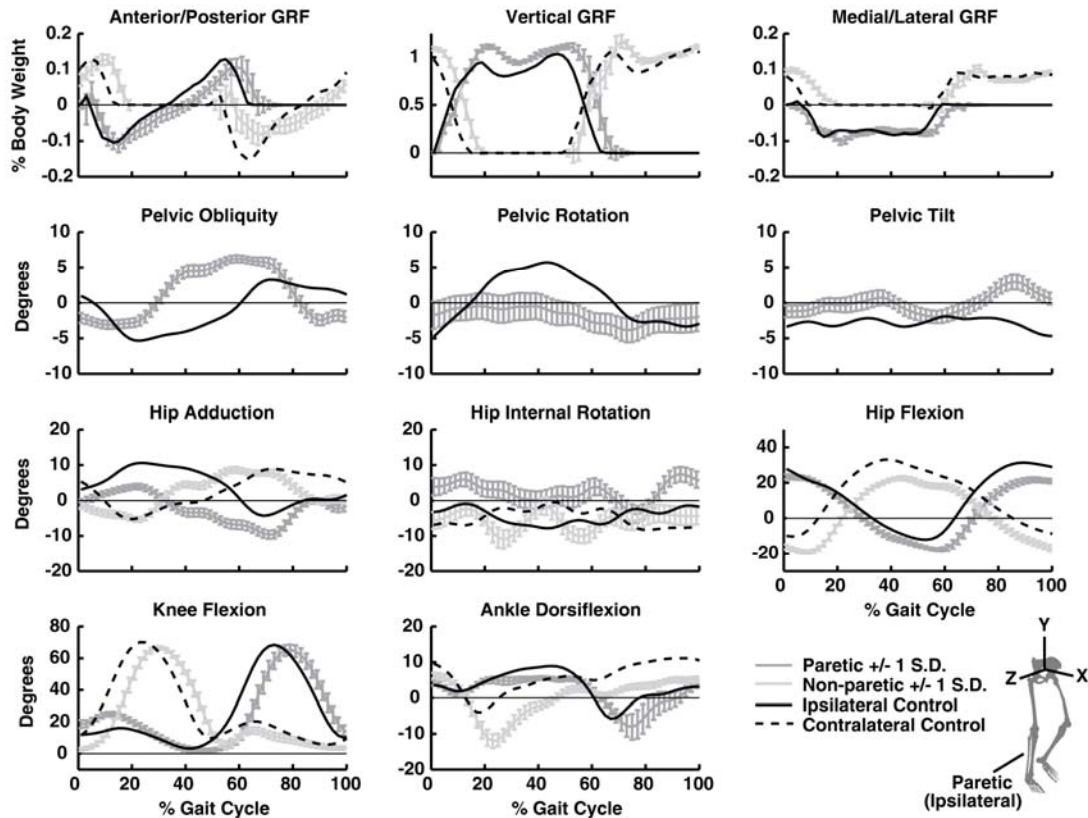


Figure 1-2: Experimental data of the gait cycle with minimum difference in joint angles and ground reaction forces (GRFs) compared to the subject's average for the community walker at self-selected speed (with  $\pm 1$  standard deviation (S.D.) of the 30 s walking trial) and the control walking at 1.0 m/s. Data are normalized to the paretic (ipsilateral) gait cycle. Joint angle subtitles correspond to positive directions. Positive pelvic obliquity, rotation and tilt correspond to positive rotations about the X, Y and Z pelvis segment axes, respectively (see bottom right).

For the hemiparetic subjects walking with self-selected overground and treadmill speeds within each functional group range, the subject with the average percent of paretic propulsion value (Bowden et al., 2006) closest to the functional group average was selected to represent each group.

### ***Musculoskeletal Model***

A previously developed 2D model and optimization framework (Neptune et al., 2001; Neptune et al., 2004a; Neptune et al., 2008) were adapted to simulate 3D walking. The model was developed using SIMM (MusculoGraphics, Inc.) with musculoskeletal geometry based on Delp et al. (1990) and consisted of rigid body segments representing the trunk, pelvis, and thigh, shank, talus, calcaneus and toes of each leg. The pelvis was allowed to translate and rotate with respect to the ground with six degrees-of-freedom (df) and the trunk was allowed to rotate relative to the pelvis with three df. Each hip joint was modeled with a spherical joint and each knee, ankle, subtalar, and metatarsal joint was modeled with a single df, yielding a total of 23 df in the model. The contact between the foot and ground was modeled with 31 independent visco-elastic elements on the bottom of each foot (Neptune et al., 2000). Passive torques representing the forces applied by ligaments, passive tissue and joint structures were applied at each joint (Anderson, 1999). The dynamical equations-of-motion were derived using SD/FAST (PTC) and forward dynamics simulations were produced using Dynamics Pipeline (MusculoGraphics, Inc.).

The model had 43 Hill-type musculotendon actuators per leg. Muscle contraction dynamics were governed by Hill-type muscle properties (Zajac, 1989) and muscle activation dynamics were modeled using a nonlinear first-order differential equation (Raasch et al., 1997) with activation and deactivation time constants derived from Winters and Stark (1988). Polynomial equations were used to estimate musculotendon lengths and moment arms (Menegaldo et al., 2004).

### ***Dynamic Optimization***

Forward dynamic simulations from paretic mid-stance to paretic toe-off (right for controls) were generated using dynamic optimization to test the hypotheses related to the pre-swing (double support) phase. A simulated annealing algorithm varied the muscle excitation patterns until differences between simulated and experimentally measured joint angles and GRFs were minimized (Goffe, 1994). Total muscle stress (muscle force/cross-sectional area of muscle) was also included in the cost function to minimize co-contraction while reproducing the experimental kinematics and GRFs equally well. Bimodal patterns (Eq. 1-1) were used to define the muscle excitations,  $u(t)$ , and were described by six optimization parameters including the onset, offset, and amplitude (A) of each mode  $i$ , at time  $t$ , for each muscle.

$$u(t) = \sum_{i=1}^2 \frac{A_i}{2} \left[ 1 - \cos \left( 2\pi \cdot \frac{t - onset_i}{offset_i - onset_i} \right) \right] \quad \text{Eq. 1-1}$$

### ***Simulation Analyses***

Previously described muscle-induced acceleration and segment power analyses (Fregly and Zajac, 1996; Neptune et al., 2001) were used to quantify individual muscle contributions to forward propulsion (i.e., average horizontal acceleration of the pelvis), swing initiation (i.e., average mechanical power generated to the leg) and power generation (i.e., average musculotendon power) during paretic (right) leg pre-swing for each of the hemiparetic (control) simulations. After analysis, contributions by individual muscles were grouped according to their anatomical classification and how they contributed to the walking subtasks (Table 1-1).

Table 1-1: The 43 musculotendon actuators per leg were combined into 18 groups after analysis according to their anatomical classification and contributions to the walking subtasks.

<b>Muscle name</b>	<b>Analysis Group</b>
Iliacus, Psoas	IL
Adductor Longus, Adductor Brevis, Pectineus	AL
Quadratus Femoris	QF
Superior, Middle and Inferior Adductor Magnus	AM
Sartorius	SAR
Rectus Femoris	RF
Vastus Medialis, Lateralis, and Intermedius	VAS
Anterior, Middle and Posterior Gluteus Medius	GMED
Piriformis	PIRI
Gemellus	GEM
Anterior, Middle and Posterior Gluteus Minimus	GMIN
Tensor Fascia Lata	TFL
Anterior, Middle, and Posterior Gluteus Maximus	GMAX
Semitendinosus, Semimembranosus, Gracilis, Biceps Femoris Long Head	HAM
Biceps Femoris Short Head	BFSH
Medial and Lateral Gastrocnemius	GAS
Soleus, Tibialis Posterior, Peroneus Brevis, Flexor Digitorum Longus, Flexor Hallucis Longus	SOL
Tibialis Anterior, Extensor Digitorum Longus, Peroneus Tertius, Extensor Hallucis Longus	TA

## RESULTS

Simulations of limited community and community hemiparetic walkers and speed-matched controls were generated such that simulated GRFs and kinematics from mid-stance to toe-off were near  $\pm$  two standard deviations of the experimental data (Table 2). For clarification, the right and left leg of the control simulations are referred to as the ipsilateral and contralateral leg, respectively, for comparison with the paretic and non-paretic legs. Paretic (ipsilateral) and non-paretic (contralateral) muscle excitation timings compared well with the experimental EMG and with data available in the literature (Den Otter et al., 2004; Den Otter et al., 2007).

Table 1-2: The average error between the experimental and simulated kinematics and ground reaction forces (GRFs) compared to the average standard deviations of the experimental data (in parentheses below).

			Limited Community	Control at 0.6 m/s	Community	Control at 1.0 m/s	
Kinematic Angles (degrees)	Pelvis		Obliquity	1.623 (2.193)	0.580 (1.150)	0.298 (1.364)	1.083 (1.207)
			Rotation	1.249 (4.967)	2.532 (2.457)	1.775 (3.223)	0.570 (2.657)
			Tilt	1.635 (2.946)	0.420 (1.481)	0.492 (1.893)	0.467 (1.442)
	Trunk		Obliquity	2.118 (2.154)	0.848 (1.540)	5.162 (3.178)	0.962 (1.364)
			Rotation	1.236 (1.544)	0.671 (0.463)	1.776 (2.131)	0.272 (0.520)
			Tilt	1.830 (1.605)	2.343 (1.240)	4.852 (1.445)	1.126 (2.130)
	Paretic/ Ipsilateral Leg		Hip Adduction	1.020 (2.370)	2.731 (1.886)	1.435 (2.366)	3.660 (1.634)
			Hip Rotation	2.441 (4.568)	0.715 (2.532)	2.922 (5.058)	0.846 (2.170)
			Hip Flexion	2.100 (6.227)	1.706 (3.905)	0.752 (3.911)	1.379 (3.347)
			Knee Flexion	8.319 (9.909)	1.629 (5.059)	2.808 (6.409)	2.802 (4.012)
			Ankle Dorsiflexion	3.783 (2.565)	0.643 (1.775)	1.108 (2.159)	1.889 (1.866)
	Non-paretic/ Contralateral Leg		Hip Adduction	1.399 (2.575)	1.156 (1.955)	0.293 (1.853)	1.701 (1.911)
			Hip Rotation	3.123 (4.296)	0.533 (3.272)	0.815 (4.732)	1.344 (2.659)
			Hip Flexion	3.380 (5.264)	1.159 (2.617)	0.552 (3.230)	1.341 (2.612)
			Knee	3.892 (7.138)	3.741 (6.434)	3.403 (6.163)	1.804 (5.120)
			Ankle Dorsiflexion	1.286 (1.989)	0.457 (1.239)	0.491 (1.850)	0.646 (1.148)
Forces (%BW)	Paretic/ Ipsilateral Leg		A/P GRF	0.264 (0.620)	0.646 (2.111)	0.533 (2.689)	2.675 (2.450)
			Vertical GRF	7.324 (11.365)	2.327 (7.479)	6.031 (14.027)	6.983 (11.959)
			M/L GRF	3.024 (1.311)	1.834 (0.938)	1.133 (1.248)	3.019 (1.540)
	Non-paretic/ Contralateral Leg		A/P GRF	0.655 (2.455)	1.368 (1.997)	0.505 (2.394)	1.174 (2.585)
			Vertical GRF	8.365 (12.697)	3.975 (7.721)	4.181 (13.522)	6.391 (10.426)
			M/L GRF	2.192 (1.632)	1.579 (1.103)	0.665 (1.563)	2.414 (1.997)
Average Angle Error (degrees)			2.527	1.367	1.808	1.368	
Average GRF Error (%BW)			3.637	1.955	2.175	3.776	



### ***Forward Propulsion***

Paretic muscles contributed less to forward propulsion in the limited community hemiparetic walker compared to the ipsilateral leg of the speed-matched control (Fig. 1-3A, Net). For the limited community walker, forward propulsion by paretic SOL, GAS and GMED was decreased compared to the ipsilateral leg (Fig. 1-3A). The net effect of non-paretic muscles was to decelerate the pelvis during paretic pre-swing, in contrast with the net effect of the contralateral muscles of the control, which accelerated the pelvis forward (Fig. 1-3A). Non-paretic and contralateral VAS and RF in early stance contributed substantially to pelvis acceleration (Fig. 1-3A). Non-paretic and contralateral HAM contributed to pelvis deceleration, though much more in the limited community walker (Fig. 1-3A).

For the community hemiparetic walker, paretic SOL strongly accelerated the pelvis forward to provide more forward propulsion than ipsilateral SOL of the speed-matched control (Fig. 1-3B). Paretic and ipsilateral GAS provided forward propulsion secondary to SOL in the community walker and control (Fig. 1-3B). The total average pelvis acceleration and deceleration by paretic muscles was increased for the community walker compared to the ipsilateral leg due to increased acceleration by paretic GMED and increased deceleration by paretic AM (Fig. 1-3B). Non-paretic leg muscles contributed to forward propulsion in the community walker similar to the contralateral leg with HAM, VAS and RF being the primary contributors (Fig. 1-3B).

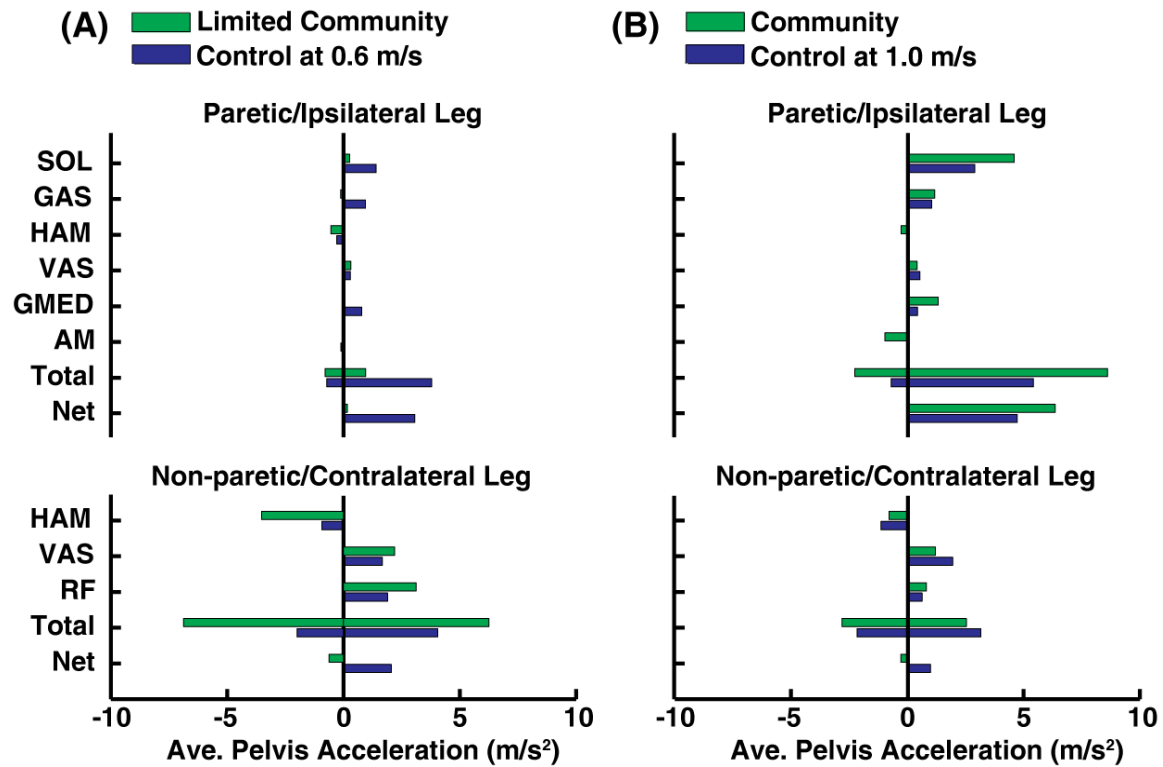


Figure 1-3: Primary muscle contributors to forward propulsion (i.e., average horizontal pelvis acceleration) and the total average pelvis acceleration and deceleration (Total) and net by all paretic (ipsilateral for control) and non-paretic (contralateral for control) muscles during pre-swing. (A) For the limited community walker, forward propulsion provided by paretic and non-paretic muscles were decreased and increased, respectively, compared to the speed-matched control. (B) Forward propulsion provided by paretic muscles (i.e., SOL and GMED) was increased in the community walker relative to the speed-matched control.

### *Swing Initiation*

For the limited community walker, paretic muscles contributed more to swing initiation compared to the ipsilateral control leg (Fig. 1-4A, Net). Paretic and ipsilateral GAS was a primary contributor to swing initiation in both the limited community walker and control (Fig. 1-4A). Paretic IL contributed less to swing initiation and SAR

contributed more to swing initiation in the limited community walker compared to the ipsilateral leg. Negative paretic swing initiation (i.e., power absorbed from the paretic leg by paretic muscles) was decreased relative to the ipsilateral leg due to reduced absorption by paretic SOL and GMED (Fig. 1-4A). Non-paretic leg muscles contributed to swing initiation in the limited community walker similar to the contralateral leg with HAM being the primary positive contributor and RF being the primary negative contributor (Fig. 1-4A).

For the community walker, paretic GAS, IL and SAR provided less and paretic AM provided more swing initiation compared to the ipsilateral leg (Fig. 1-4B). The total average power absorbed by paretic leg muscles of the community walker was increased relative to the ipsilateral leg as paretic SOL and GMED absorbed more power from the paretic leg, such that the net effect of paretic muscles was to absorb power from the paretic leg during pre-swing (Fig. 1-4B, Net). Similar to the control, non-paretic HAM and RF were primary contributors to swing initiation in the community walker (Fig. 1-4B).

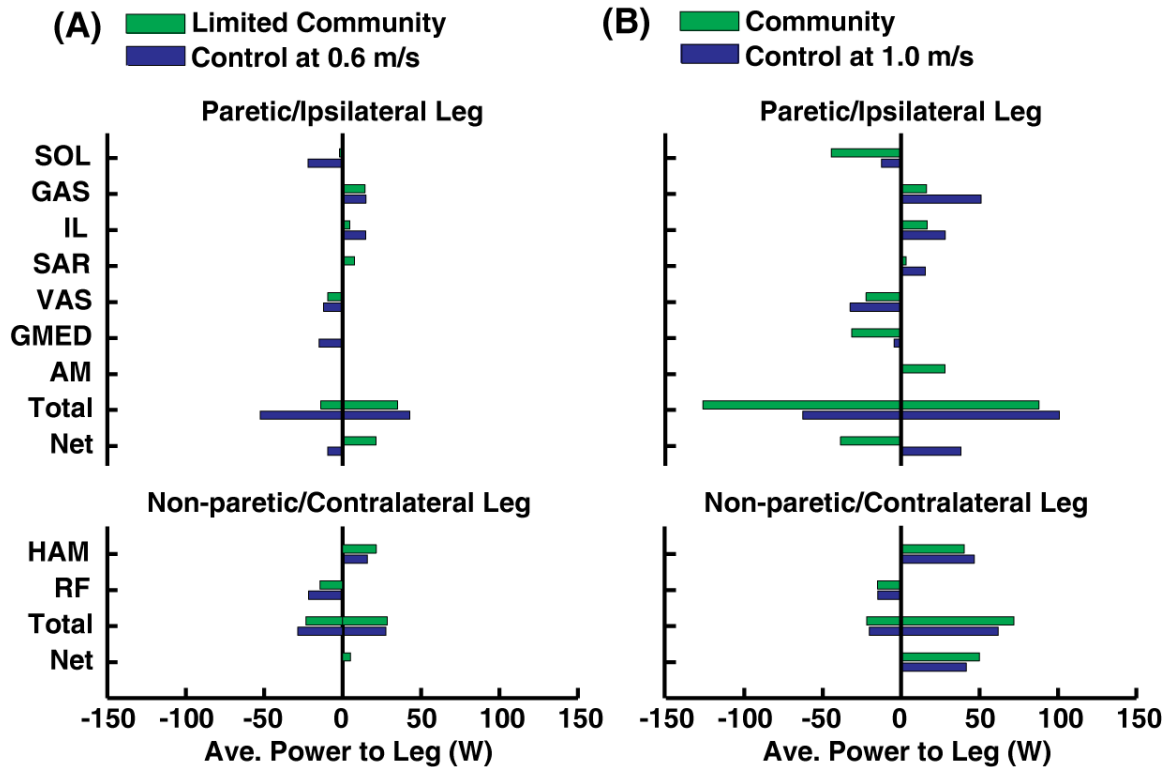


Figure 1-4: Primary muscle contributors to average swing initiation during pre-swing by paretic (ipsilateral for control) and non-paretic (contralateral for control) leg muscles. (A) For the limited community walker, swing initiation by paretic muscles was similar to the ipsilateral control leg, but paretic muscles absorbed less power compared to the control. (B) For the community walker, swing initiation by the paretic GAS, IL and SAR was decreased and paretic AM was increased compared to the control. Paretic muscles absorbed much more power from the paretic leg compared to the ipsilateral control leg.

### ***Power Generation***

For the limited community walker, paretic muscles generated less power compared to the ipsilateral control leg (Fig. 1-5A: Total), specifically with the paretic GAS generating much less power (Fig. 1-5A). Paretic SOL and GMED absorbed power in the limited community walker, while ipsilateral SOL and GMED generated power in

the control (Fig. 1-5A). Power generated by non-paretic and contralateral muscles was similar for the limited community walker and control (Fig. 1-5A: Total).

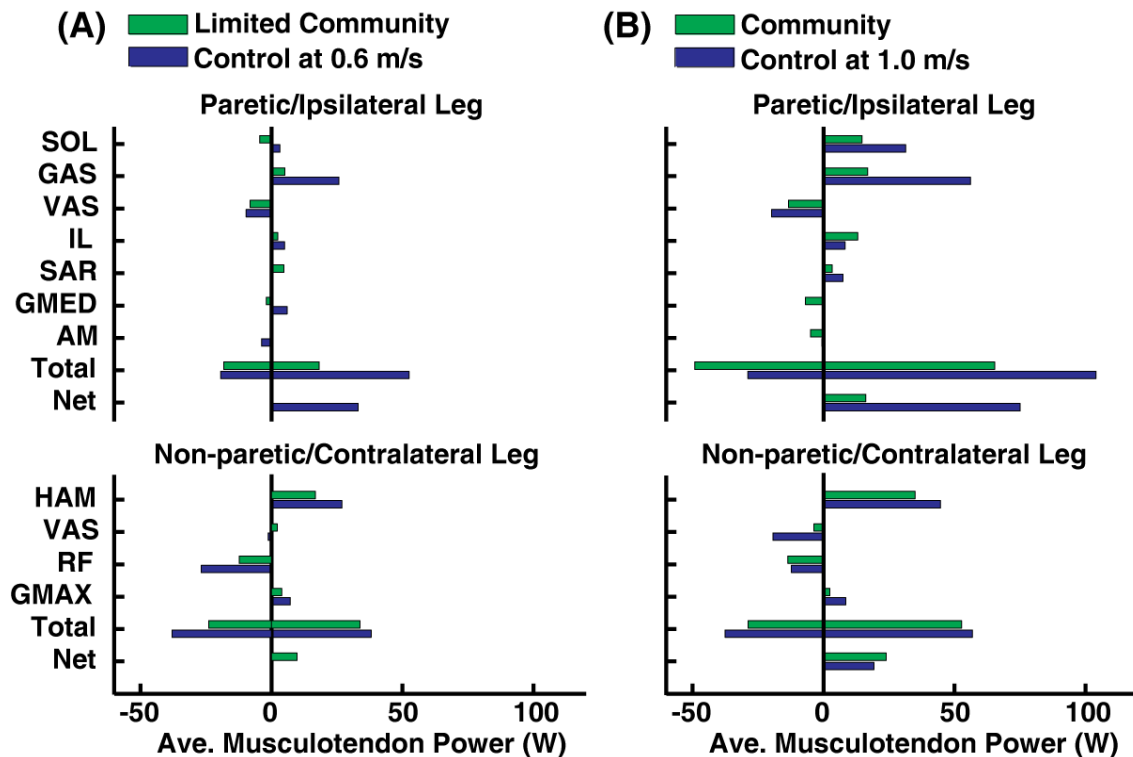


Figure 1-5: Average power generated by paretic (ipsilateral for control) and non-paretic (contralateral for control) leg muscles during pre-swing. (A) Paretic muscles generated less power in the limited community walker relative to the speed-matched control as paretic GAS generated much less power. (B) The community walker generated and absorbed much power with the paretic and non-paretic leg muscles, although power generated by the paretic SOL and GAS was decreased relative to the control.

The community walker also generated less power with paretic leg muscles compared to the control (Fig. 1-5B: Total) with the primary deficits in power generation by the paretic SOL and GAS (Fig. 1-5B). Power absorption by paretic muscles was increased in the community walker compared to the control (Fig. 1-5B: Total) as the

paretic GMED and AM absorbed power in addition to the paretic VAS (Fig. 1-5B). Power generated by non-paretic and contralateral muscles was similar for the community walker and control (Fig. 1-5B: Total).

## **DISCUSSION**

The simulation analyses identified decreased forward propulsion and power generation by paretic muscles in the limited community hemiparetic walker compared to the control. For the community hemiparetic walker, paretic leg muscles contributed less to swing initiation and generated less power compared to the control.

### ***Limited Community Hemiparetic Walker: Forward propulsion is primary impairment***

I expected that the SOL contribution to forward propulsion and power generation would be decreased in the paretic leg relative to the controls. Indeed for the limited community hemiparetic walker, paretic SOL contributed less to forward propulsion compared to the speed-matched control (Fig. 1-3A). In addition to SOL, the paretic GAS and GMED contributed less to forward propulsion (Fig. 1-3A) and paretic SOL, GAS and GMED each generated less power (Fig. 1-5A). Because SOL is the primary contributor to forward propulsion and GAS also accelerates the trunk during pre-swing in nondisabled walking (Neptune et al., 2001; McGowan et al., 2008), these results suggest that the decreased paretic SOL and GAS contribution to forward propulsion is likely an important factor limiting walking speed for the limited community walker, consistent with previous experimental studies of hemiparetic walking (Nadeau et al., 1999; Jonkers et al., 2009).

Also, it was expected that non-paretic GMAX, VAS and HAM contributions to forward propulsion and power generation during the paretic leg pre-swing would be

increased relative to controls. For the limited community walker, the net non-paretic leg contribution to forward propulsion was negative as non-paretic HAM contributed more to negative forward propulsion compared to the contralateral control leg. Thus, the non-paretic leg did not compensate for decreased forward propulsion by paretic muscles during pre-swing. Because the net forward propulsion by both legs (Fig. 1-3A, sum of paretic and non-paretic Net) was near zero ( $-0.462 \text{ m/s}^2$ ) for the limited community walker during paretic pre-swing, forward propulsion must be generated during another phase of the gait cycle (e.g., non-paretic pre-swing) to maintain walking speed (Morita et al., 1995).

I expected that GAS and hip flexor contributions to swing initiation and power generation would be decreased in the paretic leg of the limited community walker relative to the control. In contrast to my expectation, paretic muscles contributed to swing initiation similar to the ipsilateral leg (Fig. 1-4A, Total), including paretic GAS and the hip flexors (i.e., sum of IL and SAR) (Fig. 1-4A). Negative contributions to swing initiation by paretic muscles (Fig. 1-4A, primarily paretic SOL and GMED) were decreased relative to the ipsilateral leg. In the control subject walking at  $0.6 \text{ m/s}$ , ipsilateral SOL and GMED absorbed much energy from the ipsilateral leg to control the leg during slow walking.

### ***Community Hemiparetic Walker: Swing initiation is primary impairment***

Paretic muscles had the net effect to absorb energy from the paretic leg during pre-swing suggesting that paretic swing initiation is impaired in the community hemiparetic walker. Paretic GAS, IL and SAR contributed less to paretic swing initiation, paretic AM contributed more, and paretic SOL and GMED absorbed much more power from the paretic leg in the community walker relative to the control (Fig. 1-4B). The

decreased paretic GAS and hip flexor contributions to swing initiation and increased paretic AM and GMED contributions to positive and negative swing initiation, respectively, is consistent with an experimental study that found impaired swing initiation of the paretic leg that was related to compensatory strategies (e.g., pelvic hiking) during swing among hemiparetic subjects and speed-matched controls (Chen et al., 2005a). Also, the mechanism of SOL to decelerate the leg during pre-swing as it transfers energy from the leg to the trunk was observed in a previous 2D simulation of nondisabled walking (Neptune et al., 2001). This mechanism was found in the present 3D simulation of the community walker by paretic SOL to strongly decelerate the paretic leg (i.e., SOL transferred energy from the leg to the pelvis), and also by GMED (Fig. 1-4B).

The community walker was not limited by the ability to generate forward propulsion with the paretic leg, consistent with adequate paretic propulsive impulses generated by low severity hemiparetic subjects reported previously (Bowden et al., 2006). The community walker relied heavily on the paretic SOL to provide forward propulsion as it contributed more to forward propulsion compared to the control (Fig. 1-3B). Paretic muscles contributed more to positive and negative forward propulsion (Fig. 1-3B, Total) for the community walker compared to the control, primarily due to increased contributions by paretic GMED and AM (Fig. 1-3B). Paretic GAS contributed to forward propulsion in the community walker similar to ipsilateral GAS in the control (Fig. 1-3B), though its contribution was less than SOL, which is consistent with previous studies of nondisabled walking (Neptune et al., 2001; McGowan et al., 2008).

### ***Limitations***

Walking on a treadmill was analyzed, which induces higher metabolic cost in hemiparetic and elderly nondisabled subjects compared to walking at matched speeds



overground (Brouwer et al., 2009; Parvataneni et al., 2009). However, the contributions of individual muscles to the subtasks are unlikely to be different overground because they are completely determined by the state (i.e., positions and velocities of the body segments) of the system (Zajac et al., 2003). A potential limitation with any modeling study is the use of necessary assumptions and constraints (Zajac et al., 2003). In this study, parameters based on nondisabled subjects were used to model both the control and hemiparetic subjects. However, because muscle force is scaled by the excitation magnitude, which is determined by the optimization algorithm to emulate the experimental data, the simulated muscle forces used to assess muscle function are relatively insensitive to model parameters. Furthermore, the muscle excitation timings in the optimization were constrained to match closely with measured EMG timing. Because muscle coordination deficits of hemiparetic subjects result in various patterns of walking dysfunction, it is not known how well the results from the two representative hemiparetic subjects generalize to other hemiparetic subjects of their functional walking status. Others walking with similar kinematics and kinetics are expected to exhibit similar deficits during paretic pre-swing as observed in the current study.

## **CONCLUSION**

Deficits in paretic muscle contributions to forward propulsion and swing initiation during paretic pre-swing were found compared to the speed-matched control in the limited community and community hemiparetic subjects, respectively. Rehabilitation strategies aimed at diminishing these deficits have much potential to improve walking function in these hemiparetic subjects and those with similar deficits. Future work should focus on developing simulations of more hemiparetic subjects including other regions of

the gait cycle to provide additional insight into impairments in muscle function in the post-stroke hemiparetic population.

## **Chapter 2**

### **Muscle Mechanical Work during Pre-swing in Hemiparetic Walking**

#### **INTRODUCTION**

Muscle mechanical work, a measure that cannot be directly measured, is likely affected by gait abnormalities observed in hemiparetic walking. Increased co-contraction between antagonist muscles (Knutsson and Richards, 1979; Perry, 1993) and increased reliance on medial-lateral muscles for stability compared to nondisabled subjects (Corriveau et al., 2004; Niam et al., 1999) each can result in increased mechanical work without a corresponding increase in walking speed. Furthermore, increased stance limb knee flexion observed in the paretic leg of some hemiparetic subjects (De Quervain et al., 1996) likely increases mechanical work of the paretic muscles, as the knee extensor muscles have a lower mechanical advantage in a flexed-knee position and must generate greater forces to support body weight when the stance limb is more flexed during walking (Biewener et al., 2004). Recently, muscle mechanical work done by muscles was found to be consistent with metabolic cost during each region of the gait cycle in nondisabled walking (Umberger, 2010). Thus, since muscle mechanical work may partly explain the increased metabolic cost of walking in hemiparetic subjects compared to nondisabled controls at matched speeds (Zamparo et al., 1995), understanding differences in muscle work between hemiparetic and nondisabled subjects is important.

Olney et al. (1991) reported that the paretic leg performed less positive and negative joint moment work compared to the non-paretic leg. Chen and Patten (2008) compared joint work produced by the paretic hip, knee and ankle during paretic leg pre-swing to age and speed-matched control subjects and found that paretic ankle plantar flexor work was greatly reduced compared to the controls. Increased paretic hip flexor

and knee extensor moment work partially offset the reduction in paretic ankle work, but the net joint moment work in the paretic leg was still significantly reduced compared to nondisabled controls. Although results of these experimental studies suggest that muscle work may be decreased in the paretic leg, paretic work may have been underestimated since experimental approaches based on net joint moments do not account for co-contraction of antagonist muscles (Sasaki et al., 2009), which may be increased in the paretic leg. Also, it remains unknown whether the non-paretic leg does more work compared to control subjects at matched speeds and how work generation may differ between hemiparetic subjects walking with different self-selected speeds.

Other studies have investigated mechanical work by computing external work (i.e., work done to move the body center of mass) and internal work (work done to move the body segments relative to the body center of mass). However, external and internal work are not independent (Kautz and Neptune, 2002) and only indirectly related to the mechanical energetic cost of muscles (Sasaki et al., 2009). In addition, internal work is limited in its ability to account for co-contraction and elastic energy storage and return (Neptune et al., 2004b; Sasaki et al., 2009). One approach to overcome these limitations is to use modeling and simulation techniques to estimate individual musculotendon (i.e., muscle fiber and in-series tendon) work that can be partitioned into positive and negative work. Simulation analyses of nondisabled walking have found that muscle co-contractions produce substantial positive and negative work in stance and muscles store and release substantial elastic energy (Neptune et al., 2004b; Sasaki et al., 2009).

Therefore, the purpose of this study was to use musculoskeletal modeling and simulation analyses to compare individual musculotendon work generated by two representative hemiparetic subjects classified according to functional walking status (Perry et al) (i.e., limited community = 0.4-0.8 m/s and community walkers = > 0.8 m/s)

to speed and age-matched controls. Muscle mechanical work performed by representative hemiparetic walkers at two different speeds were analyzed because metabolic cost is more increased compared to speed-matched controls for hemiparetic walkers with slower self-selected speeds than for hemiparetic walkers with faster self-selected speeds (Zamparo et al., 1995). As a first step in understanding differences between the hemiparetic and control subjects, the paretic leg pre-swing phase was analyzed because many abnormalities secondary to stroke occur during this important double support phase of the gait cycle (De Quervain et al., 1996).

## **METHODS**

### ***Musculoskeletal Model***

The previously described (Chapter 1) forward dynamics simulations of two representative hemiparetic subjects (limited community: male, left hemiparesis, single cerebrovascular infarction, age = 53 years, time post stroke = 2 years 1 month, self-selected treadmill speed = 0.45 m/s; community: male, left hemiparesis, single cerebrovascular infarction, age = 60 years, time post stroke = 8 years 5 months, self-selected treadmill speed = 0.9 m/s) and an age-matched control (female, age = 59 years) walking at 0.6 and 1.0 m/s were analyzed. The three-dimensional model had 23 degrees-of-freedom and was developed using SIMM (MusculoGraphics, Inc.) with musculoskeletal geometry based on Delp et al. (1990). The model was driven by 43 Hill-type musculotendon actuators per leg with muscle contraction dynamics governed by Hill-type properties (Zajac, 1989) and activation dynamics modeled using a nonlinear first-order differential equation (Raasch et al., 1997). Muscle specific activation and deactivation time constants were derived from Winters and Stark (1988). Polynomial

equations were used to estimate musculotendon lengths and moment arms (Menegaldo et al., 2004). The foot-ground contact was modeled with 31 independent visco-elastic elements on the bottom of each foot (Neptune et al., 2000). Passive torques representing the forces applied by ligaments, passive tissue and joint structures were applied at each joint (Audu and Davy, 1985; Anderson, 1999). The dynamical equations-of-motion were derived using SD/FAST (PTC).

### ***Dynamic Optimization***

Forward dynamics simulations from paretic mid-stance to paretic toe-off (right leg for control simulations) were generated using a simulated annealing optimization algorithm (Goffe, 1994) that varied the muscle excitation patterns until differences between simulated and experimentally measured walking data were minimized. Total muscle stress (muscle force/muscle cross-sectional area) was also included in the cost function to minimize co-contraction while reproducing the experimental kinematics and GRFs equally well. Bimodal patterns were used to define the muscle excitations (Eq. 1-1).

### ***Work Calculations***

Musculotendon (MT), fiber (parallel active and passive components) and tendon (series-elastic element) power were computed as the product of corresponding force and velocity vectors obtained from the Hill-type muscle model. Fiber ( $F_{\text{Fiber}}$ ) and tendon forces ( $F_{\text{Tendon}}$ ) were determined from musculotendon forces ( $F_{\text{MT}}$ ) according to the Hill-type model for pennate muscles (i.e.,  $F_{\text{MT}} = F_{\text{Tendon}} = F_{\text{Fiber}} \cdot \cos(\text{pennation angle})$ ). Fiber velocity ( $v_{\text{Fiber}}$ ) was determined using an inverse muscle force-velocity relationship and tendon velocity ( $v_{\text{Tendon}}$ ) was computed as the difference between the musculotendon ( $v_{\text{MT}}$ )

and fiber velocities (i.e.,  $V_{Tendon} = V_{MT} - V_{Fiber} \cdot \cos(\text{pennation angle})$ ). Net MT, fiber and tendon work were computed by integrating the corresponding power over the paretic (ipsilateral for control) pre-swing phase. Positive and negative work were computed by integrating the positive and negative portions of the power trajectories over pre-swing and summed (i.e., positive work plus absolute value of negative work) to determine the total MT, fiber and tendon work. Work quantities were summed for muscles that were grouped according to anatomical classification (Table 1-1).

## **RESULTS**

Simulated GRFs and kinematics of the limited community and community hemiparetic walkers and speed-matched controls from mid-stance to toe-off were within or near  $\pm 2$  standard deviations of the experimental data (Table 1-2). The right and left leg of the control simulations are referred to as the ipsilateral and contralateral leg, respectively, for comparison with the paretic and non-paretic legs. Paretic (ipsilateral for control) and non-paretic (contralateral for control) muscle excitation timing compared well with the experimental EMG (Figs. 2-1 and 2-2) and with data available in the literature (Den Otter et al., 2004; Den Otter et al., 2007).

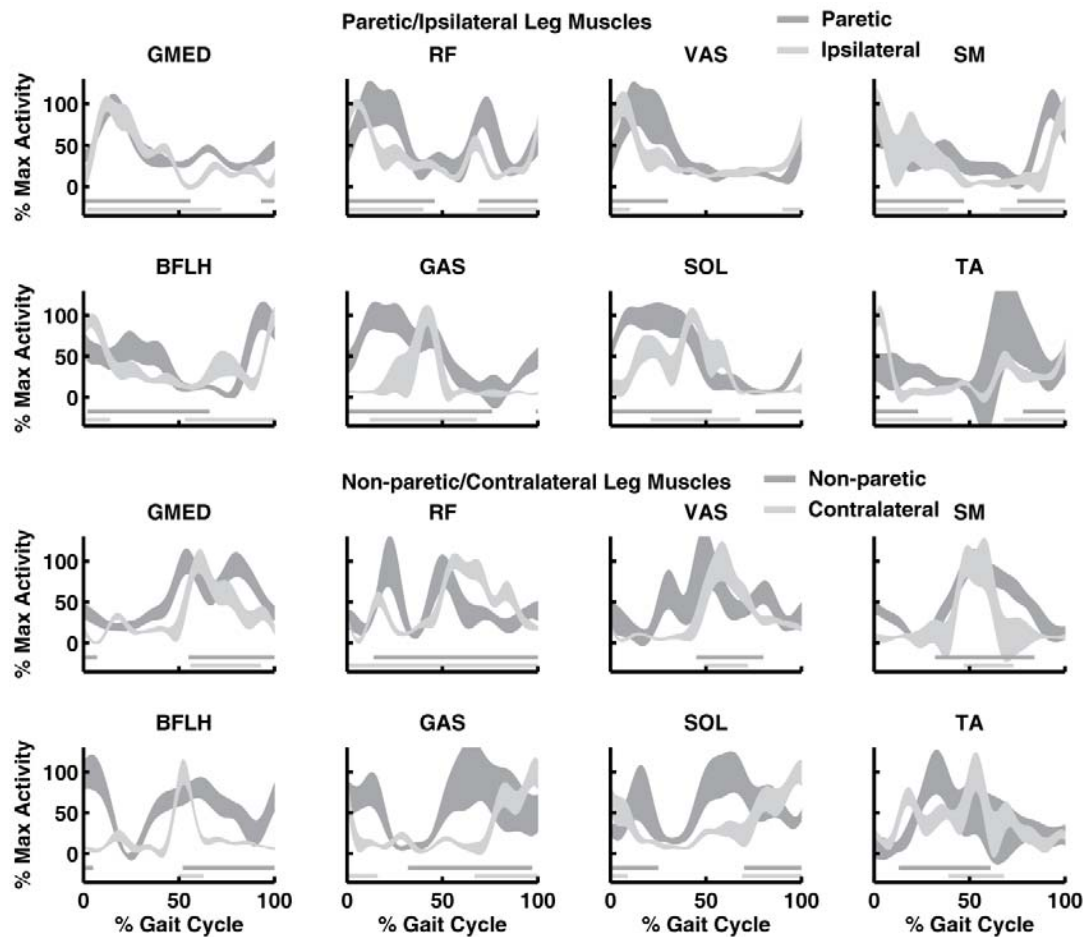


Figure 2-1: For the limited community walker and control subject at 0.6 m/s, paretic (ipsilateral for control) and non-paretic (contralateral for control) EMG and optimized excitation timings (bars below the EMG indicate when a muscle is excited) normalized to the paretic leg (ipsilateral for control) gait cycle. Average EMG is shown with  $\pm$  one standard deviation of the 30 s walking trial. Muscle excitations were optimized from mid-stance to toe-off corresponding to 36 to 84% of the paretic gait cycle for the limited community walker and 33 to 72% of the ipsilateral gait cycle for the control subject.



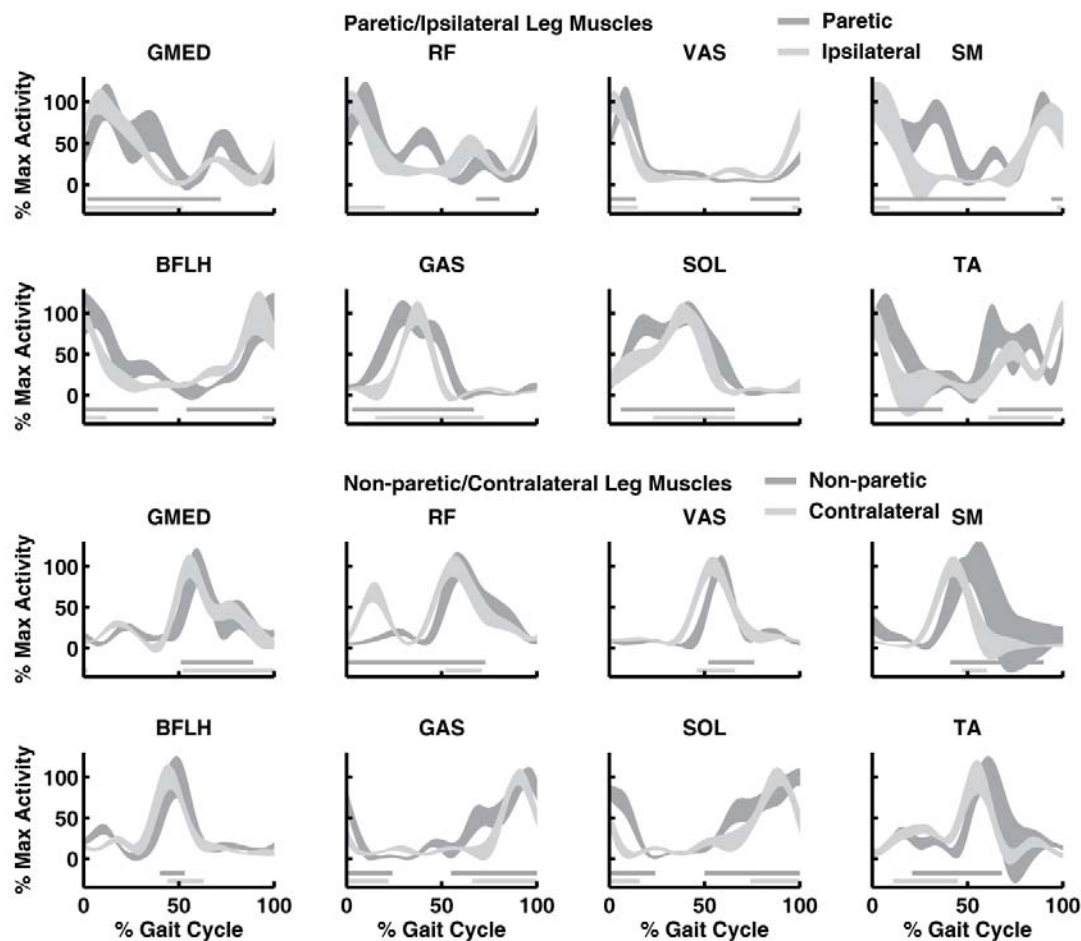


Figure 2-2: For the community walker and control subject at 1.0 m/s, paretic (ipsilateral for control) and non-paretic (contralateral for control) EMG and optimized excitation timings (bars below the EMG indicate when a muscle is excited) normalized to the paretic leg (ipsilateral for control) gait cycle. Average EMG is shown with  $\pm$  one standard deviation of the 30 s walking trial. Muscle excitations were optimized from mid-stance to toe-off corresponding to 35 to 74% of the paretic gait cycle for the community walker and 36 to 74% of the ipsilateral gait cycle for the control subject.

### *Musculotendon Work by the Limited Community Hemiparetic Walker and Control*

The limited community hemiparetic walker had increased total (absolute sum of positive and negative) paretic leg MT work during pre-swing compared to the ipsilateral

leg of the control subject walking at 0.6 m/s (Fig. 2-3A). Negative paretic MT work was increased and positive paretic MT work decreased, such that the net paretic MT work was decreased compared to the ipsilateral leg (Fig. 2-3A). Primary differences between paretic and ipsilateral leg fiber work occurred in VAS, RF, IL, SAR and the plantar flexors (Fig. 2-4A). Paretic VAS and RF had increased negative fiber work in the limited community walker relative to the ipsilateral control leg (Fig. 2-4A). Also, paretic IL and SAR had increased positive fiber work compared to the ipsilateral control leg (Fig. 2-4A). Positive tendon work was decreased in the paretic leg of the limited community walker compared to the ipsilateral control leg (Fig. 2-3A) primarily due to decreased positive tendon work by paretic GAS, but also by SOL (Fig. 2-4A).

Net and total non-paretic leg MT work during paretic pre-swing was increased relative to the contralateral control leg (Fig. 2-3B). Total fiber and tendon work were increased in the non-paretic leg largely because non-paretic positive fiber work and negative tendon work were increased relative to the contralateral control leg (Fig. 2-3B). Non-paretic and contralateral GMAX and HAM did much positive work in the limited community walker and control, respectively (Fig. 2-4B). Non-paretic SOL and GAS had increased positive fiber work and negative tendon work relative to the contralateral control leg (Fig. 2-4B).

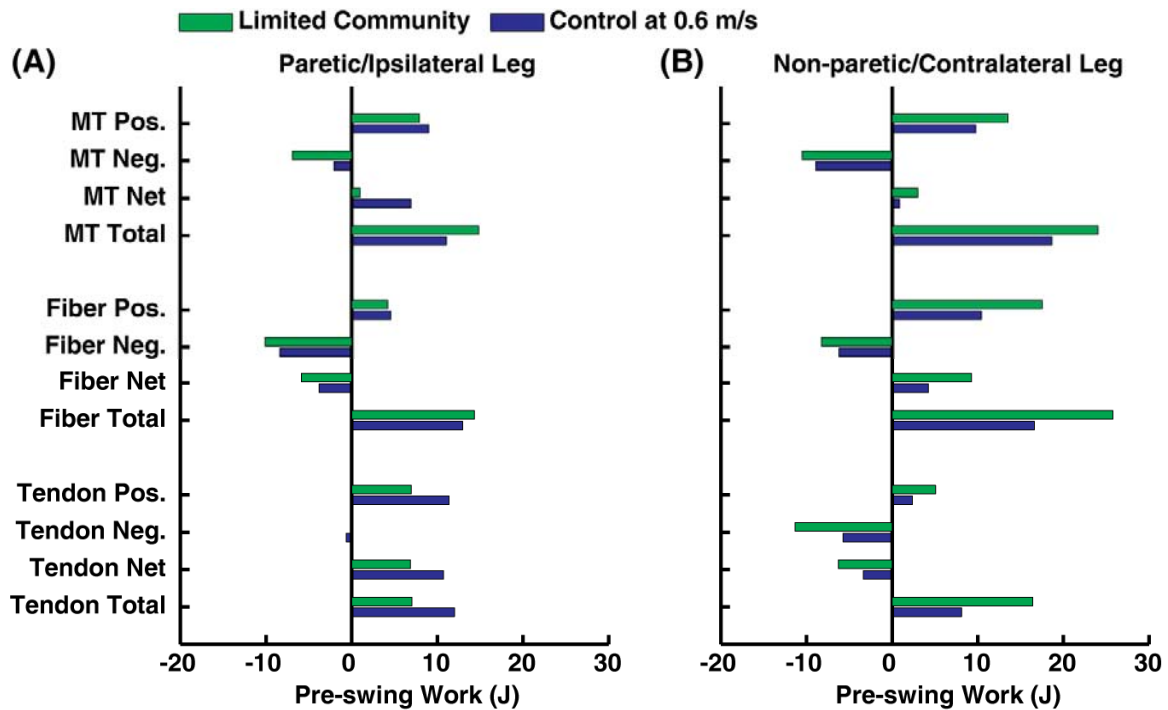


Figure 2-3: For the limited community walker and speed-matched control, musculoskeletal (MT), muscle fiber, and tendon work by all paretic (ipsilateral for control) and non-paretic (contralateral for control) muscles during paretic (ipsilateral for control) pre-swing. (A) Paretic leg negative musculoskeletal work was increased and positive tendon work was decreased relative to the ipsilateral control leg. (B) Net and total non-paretic musculoskeletal work was increased compared to the contralateral control leg.

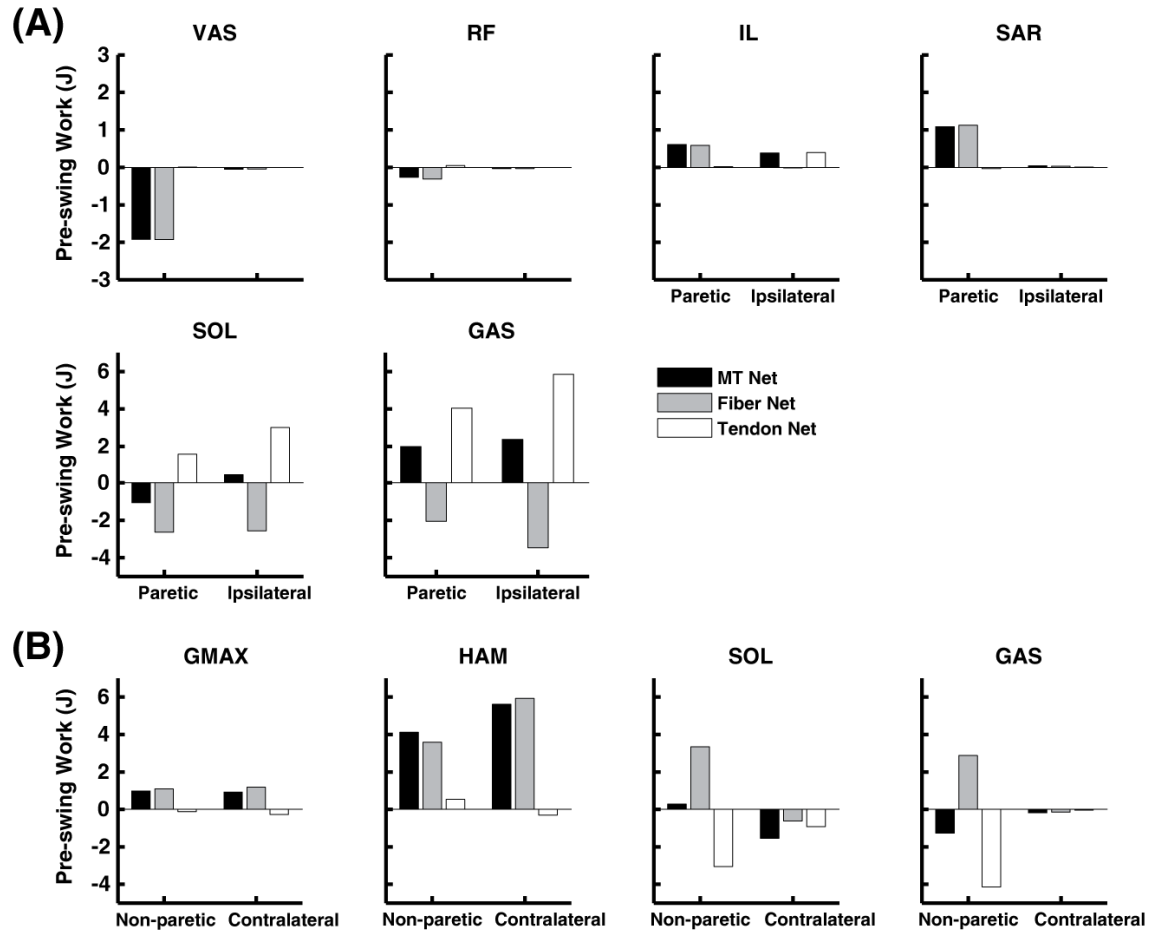


Figure 2-4: Net musculotendon (MT), fiber and tendon work by individual muscles during paretic (ipsilateral for control) pre-swing for the limited community walker and control subject at 0.6 m/s. (A) Paretic VAS and RF had increased negative fiber work and paretic IL and SAR had increased positive fiber work compared to the ipsilateral control leg. Positive tendon work by paretic SOL and GAS were decreased relative to the ipsilateral control leg. (B) Non-paretic and contralateral GMAX and HAM did much positive work in the limited community walker and control, respectively. Non-paretic SOL and GAS had increased positive fiber work and negative tendon work compared to the contralateral control leg.

### ***Musculotendon Work by the Community Hemiparetic Walker and Control***

Paretic leg net MT work by the community hemiparetic walker during pre-swing was similar to the ipsilateral leg of the control subject walking at 1.0 m/s, though the total paretic MT work was decreased (Fig. 2-5A). The paretic leg had increased positive fiber work compared to the ipsilateral control leg (Fig. 2-5A), primarily due to increased positive fiber work by paretic SOL and GAS, and also by GMED, GMIN and AM (Fig. 2-6A). Negative fiber work by paretic QF was increased compared to the ipsilateral control leg (Fig. 2-6A). Positive tendon work by paretic GAS was much decreased relative to the ipsilateral GAS (Fig. 2-6A). Paretic leg negative tendon work in the community walker was increased relative to the ipsilateral control leg (Fig. 2-5A) since paretic AM, GMIN and GMED generated negative tendon power during much of the paretic pre-swing phase (Fig. 2-6A).

Net and total non-paretic leg MT work by the community hemiparetic walker during paretic pre-swing was decreased compared to the contralateral control leg (Fig. 2-5B). Net fiber and tendon work was similar between the non-paretic and contralateral legs, although the total non-paretic fiber and tendon work were increased for the community walker relative to the contralateral control leg (Fig. 2-5B). Non-paretic GMED, GMIN and PIRI did more and non-paretic VAS, GMAX and HAM did less fiber work during pre-swing compared to the contralateral control leg (Fig. 2-6B).

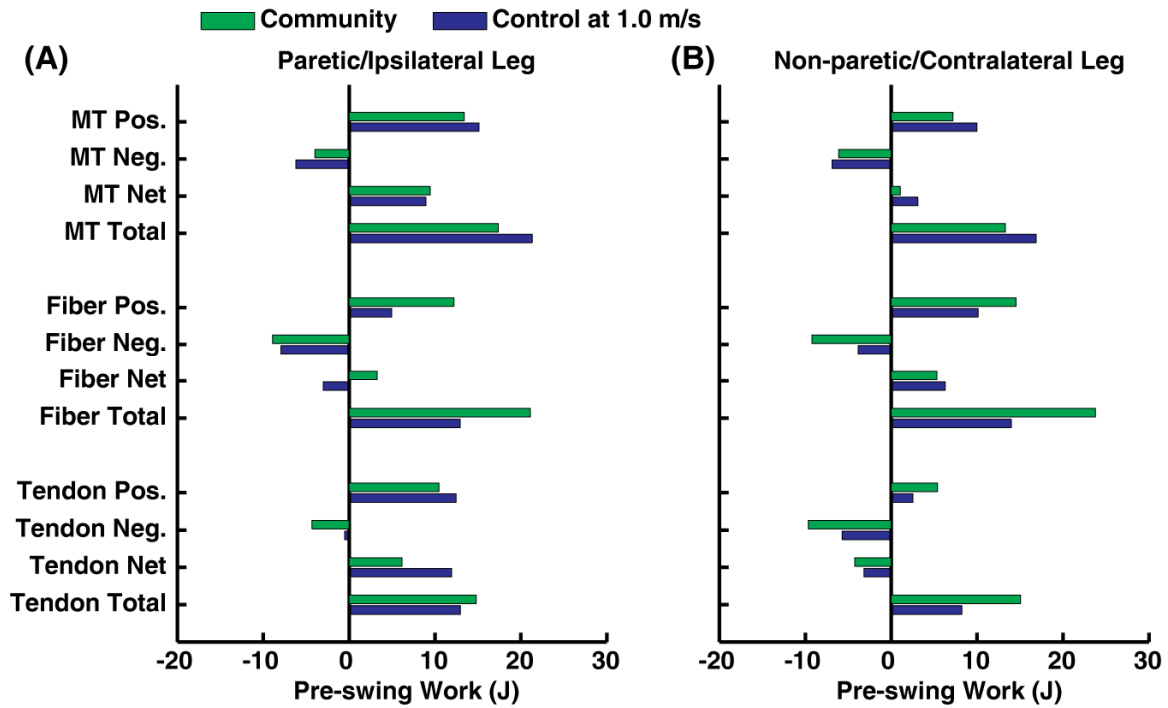


Figure 2-5: For the community walker and speed-matched control, musculotendon (MT), muscle fiber, and tendon work by all paretic (ipsilateral for control) and non-paretic (contralateral for control) muscles during paretic (ipsilateral for control) pre-swing. (A) Paretic leg positive fiber work and negative tendon work was increased relative to the ipsilateral control leg. (B) Net non-paretic fiber and tendon work were similar to the contralateral control leg, but total non-paretic fiber and tendon work was increased relative to the contralateral leg.

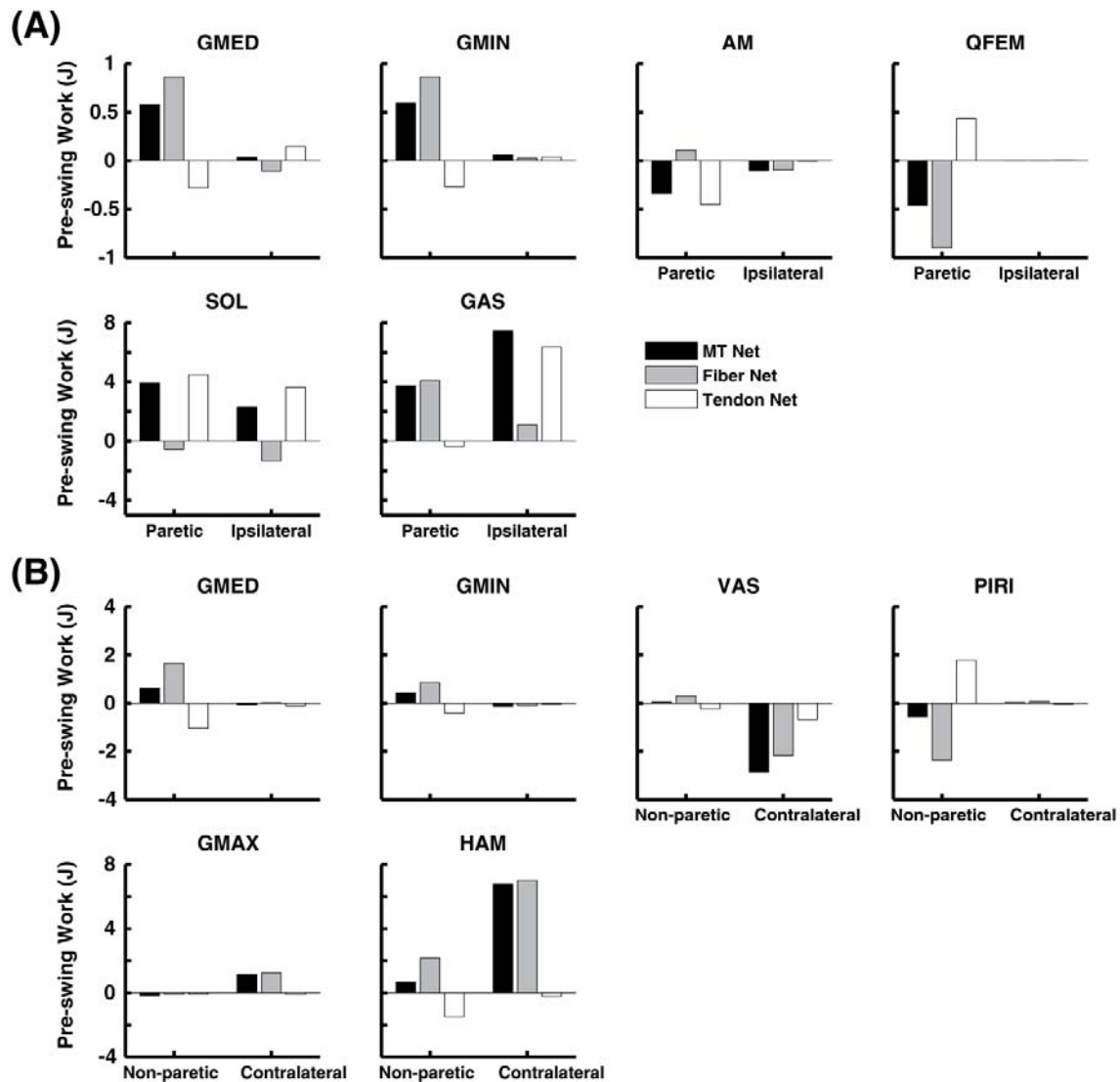


Figure 2-6: Net musculotendon (MT), fiber and tendon work by individual muscles during pre-swing for the community walker and control subject at 1.0 m/s. (A) Positive fiber work was increased and positive tendon work was decreased in paretic GAS compared to the ipsilateral control leg. Paretic GMED, GMIN, AM and QF generated more fiber and tendon work in the community walker compared to the ipsilateral control leg. (B) Fiber work by non-paretic GMED, GMIN and PIRI was increased and fiber work by non-paretic VAS, GMAX, and HAM was decreased in the community walker relative to the contralateral control leg.

## DISCUSSION

The purpose of this study was to compare musculotendon (MT) work generated by limited community and community hemiparetic walkers to speed and age-matched controls during pre-swing. For the limited community walker, net MT work by the paretic leg was decreased relative to the ipsilateral leg of the control subject walking at 0.6 m/s, which was consistent with an experimental study that found decreased net paretic joint moment work during paretic pre-swing by hemiparetic subjects compared to speed-matched controls (Chen and Patten, 2008). However, total paretic and non-paretic fiber work was increased. For the community walker whose self-selected speed was similar to that of the age matched control, net paretic MT work was similar to the ipsilateral leg of the control subject. However, similar to the limited community walker, total paretic and non-paretic fiber work was increased. Thus, if the hemiparetic walkers and control subjects perform work with the same mechanical efficiency, the hemiparetic walkers would expend more metabolic energy during paretic pre-swing compared to the controls during ipsilateral pre-swing.

### ***Limited community walker: Increased work related to paretic plantar flexor deficits***

More fiber work was required from paretic and non-paretic muscles of the limited community walker to achieve a similar speed as the control largely due to paretic plantar flexor deficits. Consistent with experimental and simulation studies of nondisabled walking (Ishikawa et al., 2005; Neptune et al., 2008), SOL and GAS recovered the most elastic energy (i.e., positive tendon work) among paretic and ipsilateral muscles for the limited community walker and control, respectively, although paretic SOL and GAS recovered less energy compared to the control (Fig. 2-4A). Because tendon is a passive tissue that uses little metabolic energy, the limited community walker's decreased ability



to exploit elastic energy recovery via the paretic ankle plantar flexors would contribute to increasing their metabolic cost of walking compared to the speed-matched control. As a result, increased MT work by other paretic muscles occurred to compensate for paretic plantar flexor deficits. Specifically, increased negative work by paretic VAS and RF (Fig. 2-4A) suggests weakness of paretic SOL, which is consistent with a simulation analysis of potential compensatory mechanisms in nondisabled walking that found increased negative MT work by VAS and RF in response to SOL weakness (Goldberg and Neptune, 2007). Similarly, increased positive work by paretic IL (Fig. 2-4A) likely compensated for weakness of paretic GAS (Goldberg and Neptune, 2007). Also, although SAR was not included in the 2D analysis by Goldberg and Neptune (2007), increased positive work by paretic SAR (Fig. 2-4A) may have compensated for paretic SOL and GAS weakness by contributing to the paretic hip flexor moment, a compensation previously observed in experimental studies of hemiparetic walking (Nadeau et al., 1999). Paretic IL and SAR generated positive work actively (i.e., positive work by the contractile element) incurring a metabolic cost, in contrast to the ipsilateral IL that generated much positive work via recovery of elastic energy in the tendon (Fig. 2-4A). Reduced paretic hip extension, which has been previously shown to limit propulsion generated by the paretic leg during pre-swing (Peterson et al., 2010), also limited the recovery of elastic energy by the paretic hip flexors in the limited community walker.

Increased fiber work by non-paretic muscles by the limited community walker during paretic pre-swing would also increase the metabolic cost of walking. The non-paretic leg did more fiber work than the contralateral control leg, with the greatest difference in positive fiber work, likely to provide body support in response to paretic plantar flexor deficits. The plantar flexors contribute to body support and forward propulsion during pre-swing in nondisabled walking (Neptune et al., 2001; McGowan et

al., 2008) and the non-paretic leg was shown not to compensate for decreased forward propulsion by the paretic leg (Chapter 1). While non-paretic and contralateral GMAX and HAM did much positive work in the community walker and control, respectively, consistent with previous simulation analyses of nondisabled walking (Neptune et al., 2004b), non-paretic SOL and GAS also did much positive work while active during paretic pre-swing with the non-paretic knee more flexed during paretic pre-swing (Fig. 2-4B). However, non-paretic SOL and GAS also stored much more elastic energy, which may allow for this energy to be recovered during another phase of the gait cycle.

***Community walker: Increased work by hip abductors and adductors***

For the community walker, paretic hip abductors and adductors did more work and paretic GAS did more positive fiber work while recovering less elastic energy compared to the control (Fig. 2-6A). Paretic GMED and GMIN fibers generated force while shortening early in pre-swing and then lengthened later in pre-swing at which time AM fibers generated force while shortening. The QF fibers generated force while lengthening during much of pre-swing. Previously, it was shown that paretic GMED and AM had offsetting contributions and GMIN and QF had only small contributions to swing initiation in the community walker (Chapter 1), these muscles performed work that did not contribute to forward propulsion. Although paretic GAS did contribute to an increased walking speed, (i.e., previously found to contribute to forward propulsion and swing initiation; Chapter 1) increased positive fiber work by paretic GAS was necessary since it recovered less elastic energy, which would contribute to increase metabolic cost compared to the control.

Also for the community walker, non-paretic hip abductors did more work compared to the contralateral control leg during pre-swing. Instead of positive work by

GMAX as seen in the contralateral leg, non-paretic GMED and GMIN did much positive fiber work in addition to HAM (Fig. 2-6B). Piriformis did the most negative fiber work of all non-paretic muscles in the community walker, while VAS did the most negative fiber work of all contralateral muscles in the control (Fig. 2-6B), which is in agreement with previous simulation analyses of nondisabled walking (Neptune et al., 2004b). Non-paretic hip abductors likely did more fiber work compared to the contralateral leg likely to enhance stability during paretic pre-swing (Corriveau et al., 2004).

### ***Limitations***

Musculotendon parameters based on nondisabled subjects were used to model both the control and hemiparetic subjects, although paretic and non-paretic fiber and tendon stiffness may be altered post-stroke (Svantesson et al., 2000). However, the mechanical work quantities are relatively insensitive to model parameters since they are derived from musculotendon forces and velocities, which are robust for a given movement. Simulated musculotendon forces are scaled by the excitation magnitude, which is determined by the optimization algorithm to emulate the experimental data, while musculotendon velocities depend on the of the body segment velocities, which agree with the experimental data. Thus, the decreased tendon work by paretic SOL and GAS of the limited community walker and by paretic GAS of the community walker was due to decreased force generated by these muscles and this finding would not differ with changes in muscle and tendon parameters. Another limitation was that metabolic cost was inferred from muscle mechanical work. However, a recent simulation study of nondisabled walking that included a metabolic cost model (Umberger, 2010) found that the metabolic energy expended was consistent with muscle mechanical work during each region of the gait cycle (Neptune et al., 2004b). Also, this study was limited to the pre-

swing (double support) phase and differences in mechanical work production between hemiparetic and nondisabled walkers likely exist during other phases of the gait cycle. Although the metabolic power during pre-swing is low compared to other phases of the gait cycle (Umberger, 2010), the decreased cost during pre-swing is attributed to the recovery of elastic energy by the plantar flexors, which the present study found to be an important deficit in the hemiparetic walkers. Nonetheless, quantifying mechanical work production during other phases of the gait cycle and using metabolic cost models to understand the relationships between muscle mechanical work and efficiency are important areas of future work to provide insight into the increased metabolic cost of hemiparetic walking. Finally, although similar mechanical work values are expected from subjects walking with similar kinematics and kinetics as the two representative hemiparetic subjects, the hemiparetic population is very heterogeneous such that analyses of more subjects are needed to fully understand the relationships between energy expenditure and functional walking status in hemiparetic subjects.

## **CONCLUSION**

Total paretic and non-paretic fiber work was increased in both the limited community and community hemiparetic walkers compared to an age-matched control subject walking at similar speeds. Increased fiber work in the limited community walker was primarily related to decreased fiber and tendon work by the paretic plantar flexors requiring compensatory work by other muscles. Increased fiber work in the community walker was primarily related to increased work by the hip abductors and adductors. Thus, if the hemiparetic and control subjects were to perform work with the same mechanical efficiency, the hemiparetic walkers would expend more metabolic energy during pre-swing. These results may partly explain why hemiparetic walkers have an

increased metabolic cost compared to nondisabled walkers at matched speeds and suggest that post-stroke rehabilitation strategies that promote walking kinematics and kinetics similar to nondisabled walkers may be beneficial for decreasing the metabolic cost. Future work using detailed models of muscle metabolic cost to analyze the entire gait cycle will provide further understanding of the relationships between muscle mechanical work and efficiency in hemiparetic walking.

## **Chapter 3**

### **Mechanisms of Accelerated and Decelerated Walking**

#### **INTRODUCTION**

Daily living is mainly comprised of short duration walking bouts. Approximately forty percent of all walking bouts for nondisabled adult individuals in typical urban environments consist of less than twelve consecutive steps (Orendurff et al., 2008a). Thus, the ability to accelerate and decelerate is important for walking in daily life and is likely more demanding than maintaining a constant speed. Walking speed is regulated by anterior-posterior ground reaction force (AP GRF) impulses. Few studies have investigated AP GRFs during accelerated and decelerated walking and most were conducted at very fast walking speeds near the walk-to-run transition (Thorstensson and Roberthson, 1987; Diedrich and Warren, 1995; Li and Hamill, 2002; Segers et al., 2006). Only one study was conducted across moderate speeds to examine acceleration and deceleration and found that walking speed was altered in early stance by reducing (acceleration) or increasing (deceleration) the braking impulse (i.e., time integral of the negative AP GRF) (Orendurff et al., 2008b). However, only a small speed increase and decrease (1.0 to 1.4 m/s) could be investigated due to the subjects walking overground across two force plates.

As a result, current insights into how healthy subjects accelerate and decelerate are based on comparisons across steady-state speeds. Step length and frequency influence AP impulses and increase with increasing steady-state speeds (Nilsson and Thorstensson, 1987). Increases in peak AP GRFs and AP impulses occur with increasing step length when walking at a constant speed (Martin and Marsh, 1992). Increasing step frequency presumably decreases the AP impulse (i.e., the AP GRF is integrated over a short time).

Nilsson and Thorstensson (1989) found propulsive (i.e., positive AP impulse) and braking impulses increased with steady-state speeds from 1.0 to 2.0 m/s, but braking and propulsive impulses decreased from 2.0 to 3.0 m/s. Thus, it appears as walking speed increased from 1.0 to 2.0 m/s, step length influenced AP impulses more than step frequency, whereas step frequency influenced AP impulses more than step length from 2.0 m/s to 3.0 m/s, possibly because subjects could not further increase their step length. During acceleration and deceleration across moderate walking speeds where saturation of step length is not likely to occur, it remains unclear how step length and frequency will influence the AP impulses.

Identifying relationships between joint moments with braking and propulsive impulses would provide further insight into mechanisms of accelerated and decelerated walking. At self-selected speeds, simulation analyses have shown the ankle plantar flexor moment is the largest contributor to AP acceleration (Kepple et al., 1997). Other simulation analyses have quantified individual muscle contributions to AP acceleration at self-selected speeds (Neptune et al., 2004a; Liu et al., 2006) and across steady-state speeds (Neptune et al., 2008; Liu et al., 2008). Neptune et al. (2004a; 2008) quantified AP acceleration of the trunk and Liu et al. (2006; 2008) quantified AP acceleration of the body center of mass. In agreement, these studies found that the hip extensors and vasti group are the main contributors to AP deceleration in early stance and soleus and gastrocnemius are the main contributors to AP acceleration in late stance. Furthermore, these contributions increased with walking speed. Neptune et al. (2001) also found that SOL and GAS each contribute to the AP deceleration in mid-stance, though Liu et al. (2006) did not. However, Liu et al. (2006) found that if they excited SOL during mid-stance, in agreement with previous EMG studies (Hunt et al., 2001; Den Otter et al., 2004), SOL contributes to AP deceleration.

The primary purpose of this study was to identify the relationships between walking speed and AP impulses, step length, and step frequency in nondisabled subjects accelerating and decelerating across a speed range of 0.4 to 1.8 m/s. The hypothesis that braking and propulsive impulses, step length and step frequency would increase with walking speed was tested. In addition, relationships between AP impulses and joint moment impulses were analyzed and the hypotheses that the ankle plantar flexor moment impulse would positively relate to braking and propulsive impulses and that the hip and knee extensor moment impulses would positively relate to the braking impulse were tested.

## **METHODS**

Kinematic and GRF data were collected from ten healthy subjects (5 females, 5 males; age =  $28.7 \pm 5.8$  yrs) during treadmill walking at the VA-UF Human Motor Performance Laboratory, VA Medical Center at Gainesville, Florida. All participants signed a written informed consent and the Institutional Review Board approved the protocol. Reflective markers were placed on the head (top, left and right temple, and back), trunk (C7, T10, clavicle, sternum and right scapula), and arms (left and right shoulder, elbow and wrist). Clusters of reflective markers were attached to the pelvis and left and right thigh, shank, and foot segments. Marker trajectories were recorded at 100 Hz with a twelve-camera motion capture system (Vicon, Oxford, UK) and GRF data were measured at 2000 Hz as subjects walked on a split-belt instrumented treadmill (Bertec Corporation, Columbus, OH). All data were collected using Vicon Workstation v4.5 software (Vicon, Oxford, UK). A safety harness that did not provide body weight support was worn during all trials to protect subjects in case of a loss of balance.



At the beginning of each test session, each subject completed a 30 s walking trial at their self-selected speed, followed by 30 s walking trials at steady-state speeds of 0.4, 0.8, 1.2, 1.6 and 1.8 m/s in random order. Subjects then completed randomized blocks of acceleration and deceleration trials at rates of 0.03, 0.06, 0.09, and 0.12 m/s<sup>2</sup>. Data were collected during three trials at each rate as subjects accelerated from 0 to 1.8 m/s, maintained a speed of 1.8 m/s for approximately 10 s (data was not collected during this time), and then decelerated from 1.8 to 0 m/s. Data at different rates were collected to provide a framework for investigating acceleration and deceleration in patient populations (e.g., post-stroke hemiparetic patients) that likely accelerate and decelerate at decreased rates compared to nondisabled walkers.

All data were processed using Visual3D (C-motion, Inc., Germantown, MD) and analyzed within the speed range of 0.4 to 1.8 m/s using MATLAB (The Mathworks, Inc. Natick, MA). Kinematic and GRF data were low pass filtered with a fourth order Butterworth filter with cutoff frequencies of 6 and 20 Hz, respectively. A standard inverse dynamics analysis was performed to determine the intersegmental joint moments using Visual3D. Kinetic data (GRFs and joint moments) were normalized by each subject's body weight. Step length and step frequency were determined for each step from heel marker trajectories and GRF data. Step lengths were normalized by each subject's leg length, which was computed as the vertical distance from the greater trochanter to the ankle joint center during the static calibration trial. Braking and propulsive impulses and flexor and extensor joint moment impulses (i.e., time integral of the flexor and extensor joint moment trajectories, respectively) for the hip, knee and ankle joints were computed for each step during the braking and propulsive phases (Fig. 3-1). The absolute values of negative impulses (e.g., braking) were computed.

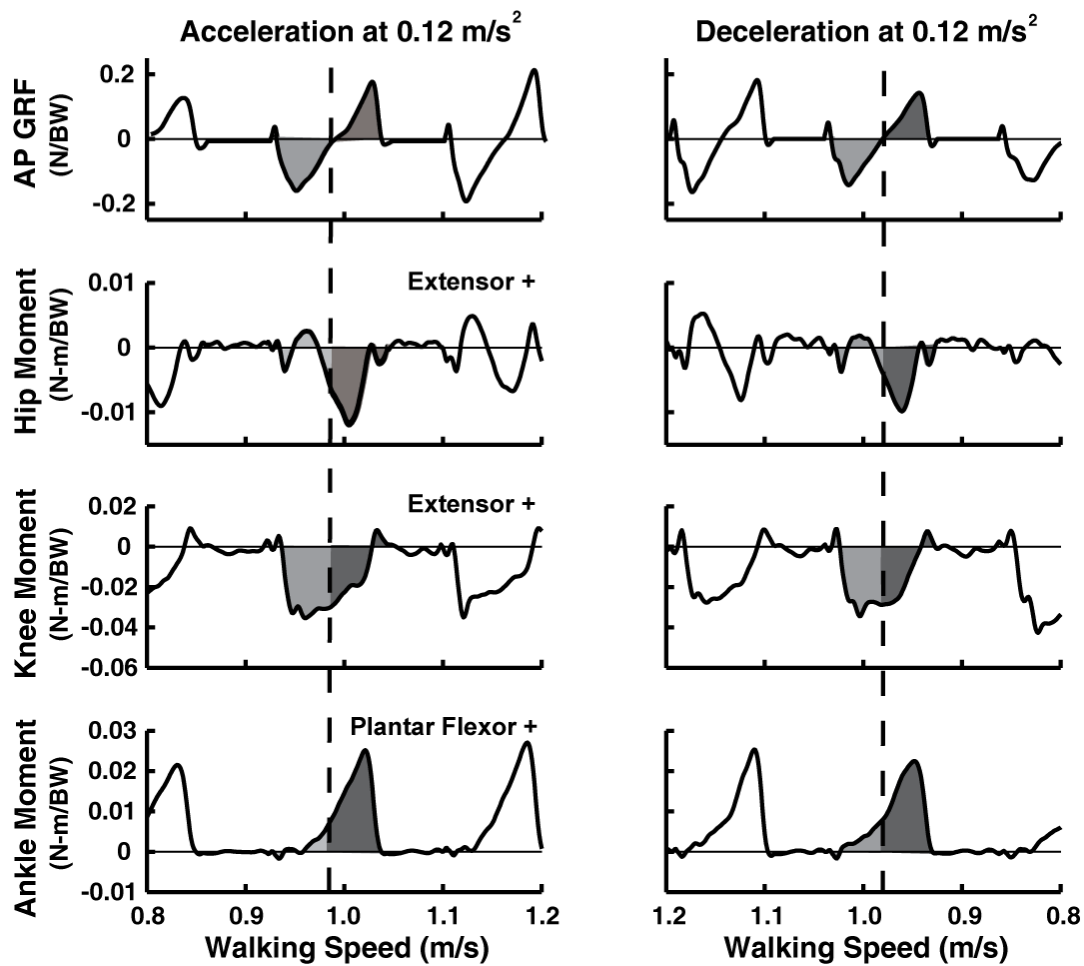


Figure 3-1: Hip, knee and ankle moment impulses were computed for each step during the braking (light shaded) and propulsive (dark shaded) phases in order to identify relationships between joint moment impulses with the braking and propulsive impulses, respectively. Anterior-posterior ground reaction forces (AP GRFs) and joint moments were normalized by subject body weight (BW).

Linear mixed regression models were generated using SPSS 16.0 GP Statistical Software (SPSS Inc., Chicago, IL) to determine relationships between walking speed with braking impulses, propulsive impulses, step length and step frequency. In addition, linear mixed models were generated to determine relationships between braking and

propulsive impulses each with hip, knee and ankle joint moment impulses during the braking and propulsive phases, respectively. Each model was generated with rate of acceleration or deceleration as a fixed factor and the intercept (i.e., value of the dependent variable when walking speed is 0 m/s) as a random effect. Models were generated to predict the dependent variable (Y) (Eq. 3-1) where the intercept<sup>Main</sup> and coefficient<sup>Main</sup> represent main effects of the variable (X) on Y, and intercept<sup>Rate</sup> and coefficient<sup>Rate</sup> represent the effect of rate and X. For example, a model to predict the braking impulse (Y) was generated where intercept<sup>Main</sup> and coefficient<sup>Main</sup> account for the main effect of walking speed on the braking impulse, and intercept<sup>Rate</sup> and coefficient<sup>Rate</sup> account for differences in the prediction of braking impulse due to rate. Significance of model coefficients were set at  $p < 0.05$ .

$$Y = (Intercept^{Main} + Intercept^{Rate}) + (Coefficient^{Main} + Coefficient^{Rate})X \quad \text{Eq. 3-1}$$

## RESULTS

The braking impulse was positively related to walking speed (i.e., the braking impulse became more negative as walking speed increased) (Table 3-1, coefficient = 0.0099,  $p < 0.001$ ). Compared to the braking impulse while subjects decelerated at the highest rate (i.e., -0.12 m/s<sup>2</sup>), braking impulses at acceleration rates of 0.06, 0.09 and 0.12 m/s<sup>2</sup> and deceleration at rates of 0.06 and 0.09 m/s<sup>2</sup> had greater positive coefficients with walking speed (Table 3-1). Propulsive impulses were positively related to walking speed (Table 3-1, coefficient = 0.0042,  $p < 0.001$ ). Compared to the propulsive impulse while subjects decelerated at -0.12 m/s<sup>2</sup>, the propulsive impulse during acceleration and deceleration at rates of 0.03, 0.06 and 0.09 m/s<sup>2</sup> had greater positive coefficients with

walking speed (Table 3-1). Average braking and propulsive impulses generated during steady-state walking trials were predicted by the model at each rate of acceleration or deceleration (Fig. 3-2, data shown for a representative subject).

Table 3-1: Linear mixed regression model coefficients (Coeff.) and intercepts (Int.) to predict braking impulses, propulsive impulses, step length and step frequency from walking speed during accelerated and decelerated walking. Model coefficients for the main effect of walking speed are shown in the top row. Interaction effects due to rate were determined with respect to deceleration at 0.12 m/s<sup>2</sup>. For example, the braking impulse (BI) at 0.03 m/s<sup>2</sup> can be predicted from walking speed (WS) with the following equation: BI = (0.019 - 0.0034) + (0.0099 + 0.0016)\*WS. Significance of the model coefficients are indicated by \* (p < 0.05), and † (p < 0.001).

	Braking Impulse		Propulsive Imp.		Step Length		Step Frequency	
	Coeff.	Int.	Coeff.	Int.	Coeff.	Int.	Coeff.	Int.
<b>Speed</b>	<b>0.0099†</b>	0.019	<b>0.0042†</b>	0.031	<b>0.34†</b>	0.44	<b>0.73†</b>	0.79
<b>Rate</b> <b>(m/s<sup>2</sup>)</b>								
<b>0.03</b>	0.0016	-0.0034	<b>0.0038†</b>	-0.0055	<b>-0.036†</b>	0.038	<b>0.070†</b>	-0.041
<b>0.06</b>	<b>0.0044†</b>	-0.0074	<b>0.0022*</b>	-0.0027	0.0029	-0.0078	<b>0.065†</b>	-0.044
<b>0.09</b>	<b>0.0027*</b>	-0.0045	<b>0.0040†</b>	-0.0077	<b>-0.024*</b>	-0.0025	0.015	0.033
<b>0.12</b>	<b>0.0038†</b>	-0.0048	0.0014	-0.0018	0.014	-0.011	<b>0.041*</b>	-0.028
<b>-0.03</b>	0.0019	-0.0030	<b>0.0030*</b>	-0.0056	-0.017	-0.0050	0.011	0.034
<b>-0.06</b>	<b>0.0029*</b>	-0.0033	<b>0.0022*</b>	-0.0033	0.016	-0.018	0.024	0.0015
<b>-0.09</b>	<b>0.0026*</b>	-0.0033	<b>0.0030*</b>	-0.0055	-0.019	-0.0021	0.0016	0.048
<b>-0.12</b>	--	--	--	--	--	--	--	--

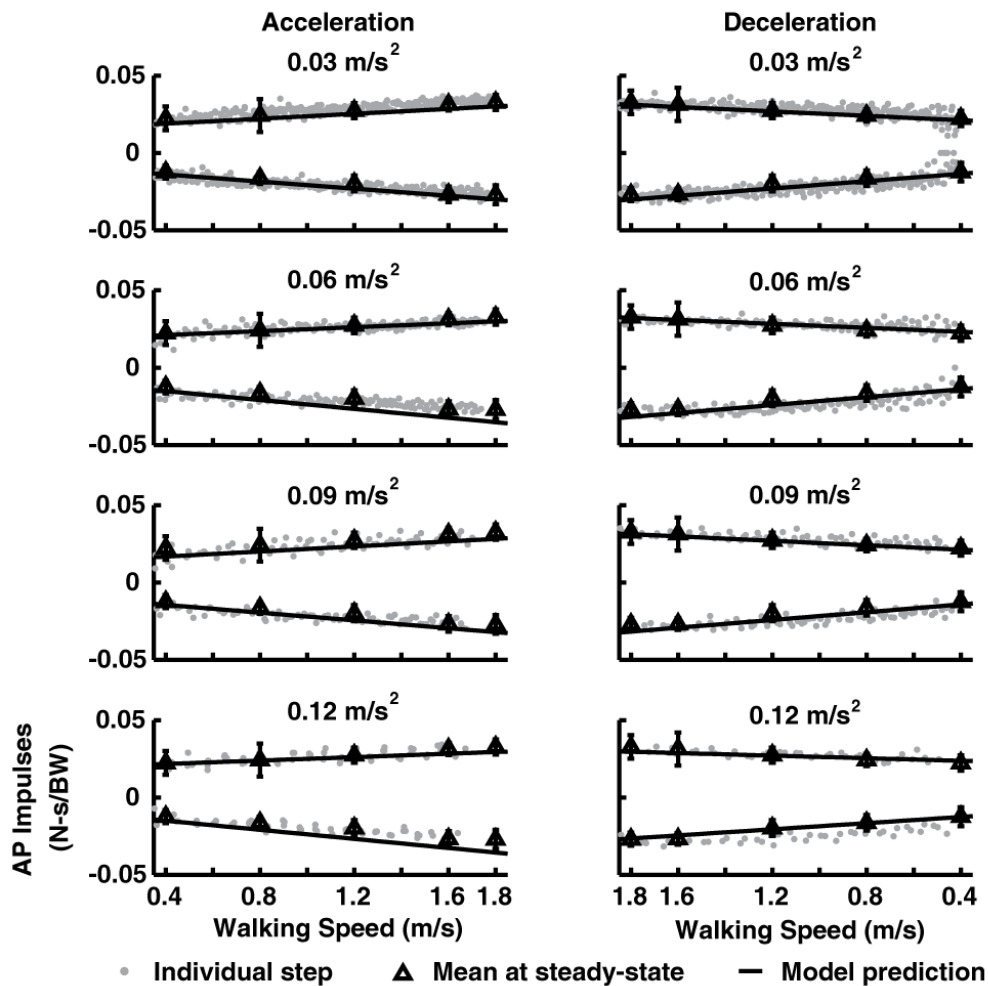


Figure 3-2: Anterior-posterior (AP) ground reaction force impulses increased with walking speed during accelerated and decelerated walking. The braking (negative) impulse had a greater relationship with walking speed than the propulsive impulse at each rate. Linear mixed regression models were generated from data collected from ten subjects and are compared to individual steps from three trials for a representative subject at each rate and their mean AP impulses (error bars are  $\pm 3$  standard deviations) at steady-state speeds.

Step length was positively related to walking speed (Table 3-1, coefficient = 0.34,  $p < 0.001$ ) and had smaller positive relationships for acceleration at rates of 0.03 and 0.09 m/s<sup>2</sup> compared to deceleration at 0.12 m/s<sup>2</sup> (Table 3-1). Step frequency was positively

related to walking speed (Table 3-1, coefficient = 0.73,  $p < 0.001$ ) and had greater positive relationships for acceleration at rates of 0.03, 0.09 and 0.12  $\text{m/s}^2$  compared to deceleration at 0.12  $\text{m/s}^2$  (Table 3-1). Average step lengths and frequencies during steady-state trials were predicted by the model for accelerated and decelerated walking, with only a few exceptions for some subjects (Fig. 3-3, data shown for a representative subject).

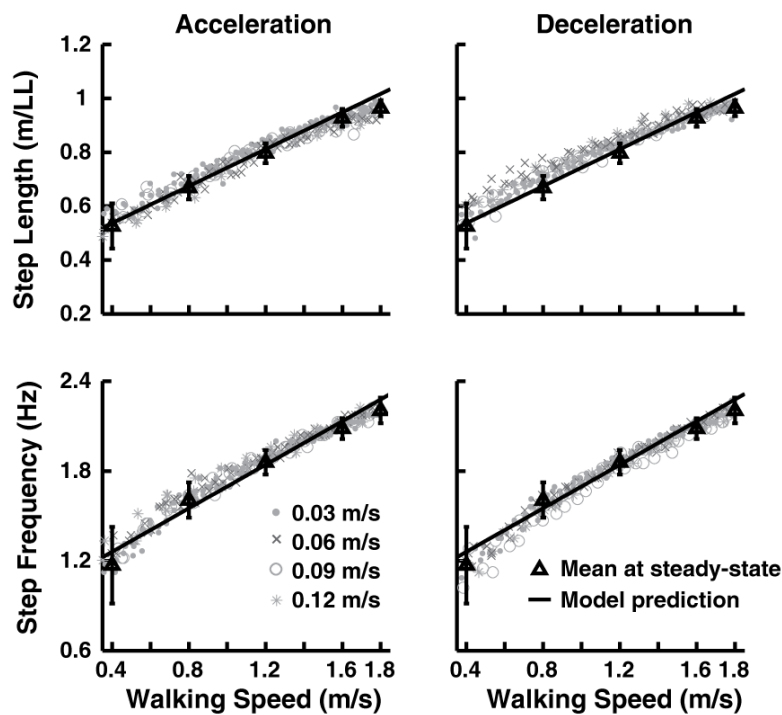


Figure 3-3: Step length (normalized by leg length (LL)) and frequency increased with walking speed during accelerated and decelerated walking. Linear mixed models generated from data across ten subjects well predicted mean step lengths and frequencies (error bars are  $\pm 3$  standard deviations) by a representative subject at steady-state speeds compared with individual steps during three trials at each rate.

The hip extensor moment impulse during the braking phase was positively related to the braking impulse (i.e., the braking impulse became more negative as the hip

extensor moment increased) (Table 3-2, coefficient = 0.064,  $p < 0.001$ ). The knee extensor moment impulse was positively related to the braking impulse (Table 3-2, coefficient = 0.12,  $p = 0.004$ ). The ankle plantar flexor and dorsiflexor moment impulses were positively and negatively related to the braking impulse, respectively (Table 3-2, plantar flexor coefficient = 0.12,  $p < 0.001$ ; dorsiflexor coefficient = -0.047,  $p < 0.001$ ). During the propulsive phase, the knee flexor moment impulse was positively related to the propulsive impulse (Table 3-2, coefficient = 0.021,  $p < 0.001$ ) and the ankle plantar flexor moment impulse was positively related to the propulsive impulse (Table 3-2, coefficient = 0.14,  $p < 0.001$ ). Rate of acceleration or deceleration did not significantly change the relationships between braking and propulsive impulses with joint moment impulses.

Table 3-2: Linear mixed model coefficients and intercepts (Int.) to predict braking and propulsive impulses from joint moment impulses generated during accelerated and decelerated walking. Significance of the model coefficients are indicated by \* ( $p < 0.05$ ), and † ( $p < 0.001$ ).

	<b>Braking Impulse</b>		<b>Propulsive Impulse</b>	
	<b>Coefficient</b>	<b>Int.</b>	<b>Coefficient</b>	<b>Int.</b>
<b>Hip Extensor Impulse</b>	<b>0.24†</b>	-0.028	-0.92	0.088
<b>Hip Flexor Impulse</b>	-0.25	0.022	0.033	0.0048
<b>Knee Extensor Impulse</b>	<b>0.12*</b>	0.00037	0.0015	0.0024
<b>Knee Flexor Impulse</b>	0.0076	0.0014	<b>0.021†</b>	-0.00006
<b>Ankle Plantar Flexor Impulse</b>	<b>0.12†</b>	0.00077	<b>0.14†</b>	0.0043
<b>Ankle Dorsiflexor Impulse</b>	<b>-0.047†</b>	0.0027	-0.0035	-0.00096

## DISCUSSION

The primary purpose of this study was to identify relationships between walking speed and AP impulses, step length, and step frequency during accelerated and decelerated walking on a treadmill. The hypothesis that braking and propulsive impulses

would increase with speed from 0.4 to 1.8 m/s was supported (Fig. 3-2). This result is consistent with a previous study that found braking and propulsive impulses increase with increasing steady-state speeds from 1.0 to 2.0 m/s during overground walking (Nilsson and Thorstensson, 1989). Average braking and propulsive impulses of steady-state trials were achieved during accelerated and decelerated walking, suggesting that these quantities may be measured at steady-state speeds to estimate these measures in accelerated and decelerated walking. The hypothesis that step length and frequency would increase with walking speed was supported and consistent with previous studies at steady-state speeds (Cavagna and Franzetti, 1986; Nilsson and Thorstensson, 1987). Subjects were able to modulate step length and frequency while accelerating and decelerating to attain step lengths and frequencies within three standard deviations of their average values during steady-state trials (Fig. 3-3). Over this range of moderate steady-state speeds, healthy walkers have been shown to choose step frequencies that minimize the rate of metabolic energy expenditure (Zarrugh and Radcliffe, 1978; Umberger and Martin, 2007). Therefore, these results suggest that subjects may also modulate step frequency to minimize metabolic cost while accelerating and decelerating.

The braking impulse had a greater positive relationship with walking speed than the propulsive impulse at each rate of acceleration and deceleration (Fig. 3-2), suggesting that subjects modulate their braking impulse more than the propulsive impulse to change speed. Similarly, Orendurff et al. (2008b) found that subjects accelerated and decelerated across a speed range of 1.0 to 1.4 m/s by either decreasing (acceleration) or increasing (deceleration) the early stance braking impulse, which was modulated by the plantar flexor ankle moment. In agreement with Orendurff et al. (2008b), the plantar flexor ankle moment was related to braking in the current study (i.e., the ankle plantar flexor and dorsi flexor moment impulses were positively and negatively related to the braking impulse,



respectively). However, in the present study the hip and knee extensor moments were also positively related to braking. This finding supported the hypothesis that the hip and knee extensor moments would positively relate to the braking impulse and agreed with previous simulation analyses of steady-state walking over a range of speeds (Neptune et al., 2008; Liu et al., 2008). Although not reported by Orendurff et al. (2008b), the propulsive impulse was found to increase with walking speed. The hypothesis that the ankle plantar flexor moment would positively relate to the propulsive impulse was supported, and is consistent with the functional role of the plantar flexors to provide forward propulsion (Kepple et al., 1997; Neptune et al., 2001; McGowan et al., 2009). Also, increased force by gastrocnemius to provide swing initiation as speed increased (Neptune et al., 2008) may have contributed to the positive relationship between the knee flexor moment and propulsive impulse.

The rate of acceleration or deceleration did not have a strong effect on the relationships between braking and propulsive impulses with walking speed. Although differences existed due to rate, the range of the model coefficients was small. For example, model coefficients to predict the braking impulse from walking speed ranged only from 0.0099 (Table 3-1,  $-0.12 \text{ m/s}^2$ ) to 0.0143 (Table 3-1,  $0.0099 + 0.0044 = 0.0143$  at  $0.06 \text{ m/s}^2$ ). Thus, at a walking speed of  $1.0 \text{ m/s}$ , the predicted braking impulses were 0.0289 and 0.0259 N-m/BW at rates of  $-0.12 \text{ m/s}^2$  and  $0.06 \text{ m/s}^2$ , respectively. In addition, the effect of rate on the relationships between walking speed and step length and step frequency were not significant for most conditions, and was small for those conditions that were significant. Model coefficients to predict step length from walking speed ranged only from 0.34 during deceleration at  $0.12 \text{ m/s}^2$  to 0.304 during acceleration at  $0.03 \text{ m/s}^2$  (Table 3-1,  $0.34 + -0.036 = 0.304$ ). Similarly, model coefficients to predict step frequency from walking speed ranged only from 0.73 to 0.80. These results suggest

that rate is not an important factor in modulating AP impulses, step length and step frequency during accelerated and decelerated walking by nondisabled subjects.

An important delimitation of this study is that data were collected on a treadmill. The use of the instrumented treadmill allowed for speed to be controlled over a wide range of values during accelerated and decelerated walking, which is difficult to achieve overground. A recent study compared the AP impulse between overground and treadmill walking at steady-state speeds and found there is no fundamental difference in propulsion mechanics (Goldberg et al., 2008). However, a non-inertial reference frame (e.g., the accelerating treadmill) exerts an inertial force on a subject due to the acceleration of the treadmill belt such that acceleration on a treadmill may be subtly different from overground. This inertial force, which is greater for higher rates of acceleration or deceleration, may have contributed to the small differences in the relationships between AP impulses and speed due to rate. The range of speeds studied and potential differences in accelerated and decelerated walking on a treadmill versus overground may account for the additional relationships reported in the current study that were not observed by Ordendurff et al. (2008b).

## **CONCLUSION**

Braking and propulsive impulses were positively related to walking speed during acceleration and deceleration on a treadmill. The braking impulse had a greater positive relationship with walking speed than the propulsive impulse, suggesting that subjects modulate the braking impulse more than the propulsive impulse to change speed. Hip and knee extensor, and ankle plantar flexor moment impulses were positively related to the braking impulse, and knee flexor and ankle plantar flexor moment impulses were

positively related to the propulsive impulse. Step length and frequency increased with walking speed and were near subjects' preferred step length and frequency at constant speeds suggesting economical energy expenditure by healthy subjects during non steady-state walking. The outcomes of this work provide the foundation to investigate motor coordination during acceleration and deceleration in pathological subjects (e.g., post-stroke) in response to the increased task demands of non steady-state walking.

## **Conclusions**

### **SUMMARY**

The overall goal of this work was to investigate muscle coordination and mechanical work production in hemiparetic walking and mechanisms of acceleration and deceleration in nondisabled walking. Musculoskeletal modeling and simulation analyses were used to compare individual muscle contributions to important subtasks of walking (Chapter 1) and muscle mechanical work (Chapter 2) by two representative hemiparetic subjects (limited community and community walkers) during pre-swing to a speed and age-matched control. Experimental data collected during accelerated and decelerated walking from nondisabled subjects were analyzed to identify relationships between walking speed and anterior-posterior ground reaction forces, step length and frequency and joint moments as a framework for future investigations of non-steady state walking in hemiparetic subjects (Chapter 3).

The simulation analyses identified decreased paretic soleus and gastrocnemius contributions to forward propulsion and power generation as the primary impairment in the limited community walker compared to the speed-matched control subject. Comparison of muscle mechanical work showed that total paretic and non-paretic fiber work was increased in the limited community walker compared to the control such that the limited community walker would expend more metabolic energy during pre-swing if they performed work with the same efficiency as the control subject. Increased fiber work was primarily related to decreased fiber and tendon work by paretic soleus and gastrocnemius requiring compensatory work by other muscles. Also, experimental analyses of accelerated and decelerated walking by nondisabled subjects showed that the ankle plantar flexor moment was positively related to braking and propulsive impulses,

which increased with speed. Thus, deficits in the paretic plantar flexors limit forward propulsion, may explain why hemiparetic walkers have an increased metabolic cost compared to nondisabled walkers at matched speeds, and would limit the ability of hemiparetic walkers to accelerate and decelerate. Rehabilitation strategies aimed at diminishing paretic plantar flexor deficits have much potential to improve forward propulsion, decrease metabolic cost and improve the ability to modulate speed in the limited community walker and those with similar deficits.

For the community walker, simulation analyses showed that paretic muscles had the net effect to absorb energy from the paretic leg during pre-swing suggesting that deficits in swing initiation are a primary impairment. Specifically, the paretic gastrocnemius and hip flexors (i.e., iliacus, psoas and sartorius) contributed less to swing initiation in the community walker compared to the speed-matched control subject. Total paretic and non-paretic fiber work was increased in the community walker compared to the control, primarily due to increased work by the hip abductors and adductors. Because step length and step frequency were positively related to walking speed in nondisabled accelerated and decelerated walking, impaired paretic swing initiation would likely limit the community walker's ability to accelerate and decelerate. Thus, deficits of the paretic gastrocnemius and hip flexors limit swing initiation and likely limit acceleration and deceleration, while increased work by the paretic hip abductors and adductors would increase the metabolic cost of walking in the community walker compared to the speed-matched control subject. Post-stroke rehabilitation strategies that promote paretic swing initiation and walking kinematics and kinetics similar to nondisabled walkers would improve walking function during steady and non-steady state conditions and decrease metabolic cost in the community walker and those with similar deficits.

## **FUTURE WORK**

### ***Evaluate Effectiveness of Post-stroke Rehabilitation***

Focused rehabilitation and evaluation of rehabilitation effectiveness is needed to support the results of the simulation analyses of post-stroke hemiparetic walking. Paretic plantar flexor deficits limited forward propulsion and power generation and contributed to increased mechanical work in the limited community walker compared to the speed matched control (Chapters 1 and 2). Thus, hemiparetic subjects walking with similar kinematics and kinetics as the limited community walker would benefit from rehabilitation strategies focused on increasing paretic plantar flexor output during pre-swing. Because paretic leg extension is important for increasing paretic plantar flexor contributions to propulsion during pre-swing (Peterson et al., 2010), emphasizing paretic hip extension in pre-swing with manual guidance during body-weight-support treadmill training as suggested by Mulroy et al. (2010) would be most beneficial. In order to determine whether this rehabilitation is indeed beneficial for hemiparetic subjects with paretic plantar flexor deficits, pre and post-rehabilitation experimental and simulation analyses are needed to assess whether paretic plantar flexor contributions to forward propulsion increased and total paretic and non-paretic mechanical work decreased due to rehabilitation.

For the community walker, the paretic gastrocnemius and hip flexors contributed less to swing initiation and the paretic hip abductors and adductors did more mechanical work compared to the speed matched control (Chapters 1 and 2). Previously, treadmill training at fast speeds resulted in increased paretic leg kinetic energy at toe-off suggesting that paretic leg swing initiation was improved (Chen et al., 2005b). Thus, treadmill training at fast speeds with manual assistance to decrease paretic hip circumduction (i.e., decrease hip abductor and adductor work) may be a beneficial

rehabilitation strategy for hemiparetic walkers with similar deficits to the community walker. Pre and post-rehabilitation experimental and simulation analyses are needed to assess whether paretic gastrocnemius and hip flexor contributions to swing initiation increased and total paretic and non-paretic mechanical work decreased due to rehabilitation for hemiparetic subjects with deficits similar to the community walker.

### ***Expand Simulation Analyses of Hemiparetic Walking***

This study generated the first three-dimensional simulations of post-stroke hemiparetic walking. However, the simulation analyses were limited to the paretic pre-swing phase. Impaired muscle contributions to important subtasks of walking during other phases of the gait cycle likely exist in hemiparetic walking. For example, decreased paretic weight acceptance and stance time has been previously reported in hemiparetic subjects (e.g., Turnbull et al., 1996) such that identifying individual muscle contributions to vertical support from paretic heel strike to toe-off is necessary future work. Furthermore, much mechanical work is done during the single support phase, which accounts for approximately 44 percent of the total metabolic cost expended during the nondisabled gait cycle (Umberger, 2010). In addition, leg swing represents approximately 29 percent of the total metabolic cost (Umberger, 2010). Therefore, comparing muscle mechanical work generated by hemiparetic subjects to speed matched controls during single support and swing provide additional insight into the increased metabolic cost of hemiparetic walking.

Two hemiparetic subjects were analyzed in the current studies (Chapters 1 and 2) that were representative of the limited community and community functional groups. However, the post-stroke population is very heterogeneous such that other limited

community and community walkers may not walk with similar kinetics and kinematics as the representative subjects, and therefore would not likely have the same deficits as those identified. Also, some hemiparetic subjects walk at extremely slow self-selected speeds (e.g., household walkers =  $<0.4$  m/s). Thus, future work should include generating simulations of more hemiparetic subjects to investigate muscle coordination and mechanical work production in this population.

### ***Further Understanding of Accelerated and Decelerated Walking***

Nondisabled subjects were able to increase (decrease) braking and propulsive impulses and step length and frequency to increase (decrease) speed during accelerated (decelerated) walking on a treadmill (Chapter 3). In general, nondisabled subjects accelerated and decelerated with step frequencies within three standard deviations of their mean values during steady-state trials suggesting efficient energy expenditure since nondisabled subjects walk with step frequencies that minimize metabolic cost during steady-state walking. However, it is expected that hemiparetic subjects (and other patient populations) would be less able to modulate braking and propulsive impulses and step length and frequency to increase or decrease speed compared to nondisabled subjects. Also, the greater metabolic cost of hemiparetic walking compared to controls at matched speeds may be exacerbated with the increased task demands of accelerated and decelerated walking. Experimental data of accelerated and decelerated walking by hemiparetic subjects are needed to compare non steady-state hemiparetic walking to nondisabled controls.

Relationships between joint moment impulses and braking and propulsive impulses were identified during accelerated and decelerated walking by nondisabled



subjects (Chapter 3). However, individual muscle function is difficult to interpret experimentally because several muscles contribute to the net joint moment. Musculoskeletal modeling and simulation analyses of accelerated and decelerated walking by nondisabled subjects to quantify individual muscle contributions to specific subtasks would provide additional insight into the biomechanical mechanisms at the individual muscle level necessary to increase or decrease speed. Finally, modeling and simulation analyses of accelerated and decelerated walking by hemiparetic subjects are needed to fully understand how paretic and non-paretic muscle contributions to important walking subtasks may differ from nondisabled subjects during accelerated and decelerated walking. These studies would provide rationale for post-stroke rehabilitation strategies to improve the ability to change speeds by hemiparetic walkers.

## Appendix 1

### Musculotendon Regression Equations

Generating forward dynamic simulations is computationally expensive. In the current studies (Chapters 1 and 2), 516 parameters (6 excitation parameters per 43 muscles per leg) were optimized to simulate hemiparetic walking. The optimization algorithm (Goffe, 1994) used to determine the muscle excitations necessary to reproduce the experimental kinematics and ground reaction forces required a large number of iterations to converge to an optimal solution (Fig. A1-1). Complex surfaces (e.g., wrapping surfaces) are needed to accurately replicate musculotendon moment arms and lengths, but these complex surfaces increase simulation time. Thus, to reduce the computational expense, the time required to execute a simulation was decreased by fitting muscle moment arms and musculotendon lengths with polynomial regression equations and removing the patella (structure with wrapping surfaces) from the musculoskeletal model. In addition, this allowed the removal of the planar knee model with prescribed motion, which was replaced with a revolute joint that is computationally more efficient.

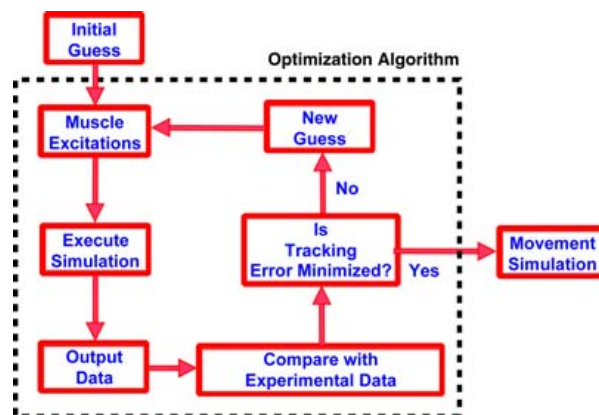


Figure A1-1: Schematic of a simulated annealing algorithm that determined the muscle excitation patterns that minimized differences between simulated and experimentally measured kinematics and ground reaction forces.

Regression equations were determined using a least-squares fitting method (Menegaldo et al., 2004). Musculotendon length and moment arm fitting equations can be expressed as:

$$F(Q_1, Q_2, Q_3, Q_4) = a_1 + a_2 f_1(Q_1, Q_2, Q_3, Q_4) + a_3 f_2(Q_1, Q_2, Q_3, Q_4) + \dots + a_n f_{n-1}(Q_1, Q_2, Q_3, Q_4) \quad \text{Eq. A1-1}$$

where  $F$  represents a musculotendon's moment arms ( $r_i$ ) or length ( $L_{mt}$ ),  $Q_i$  is a generalized coordinate of the model,  $a_i$  are coefficients to be determined,  $f_i$  are predetermined non-linear polynomial functions and  $n$  is a positive integer. In the lower extremity, every musculotendon actuator crosses one or two joints and its length and moment arm depends on the generalized coordinates (GC) of the corresponding joints. Because the maximum number of GCs for all muscles was four (biarticular muscles that cross the hip and knee), fitting equations with one to four GCs dependency were used (Table A1-1). If  $k$  samples of data are available, matrix  $A$  and coefficient and function vectors  $\mathbf{a}$  and  $\mathbf{b}$  can be constructed.

$$A = \begin{bmatrix} \mathbf{1} & f_1(\mathbf{1}) & \dots & f_{n-1}(\mathbf{1}) \\ \vdots & \vdots & \ddots & \vdots \\ \mathbf{1} & f_1(\mathbf{k}) & \dots & f_{n-1}(\mathbf{k}) \end{bmatrix} \quad \text{Eq. A1-2}$$

$$\mathbf{a} = [a_1, a_2, \dots, a_n]^T \quad \text{Eq. A1-3}$$

$$\mathbf{b} = [F_1, F_2, \dots, F_k]^T \quad \text{Eq. A1-4}$$

Using the least squares normal equation, the coefficients can be estimated from Eq. A1-5 where  $^+$  represents a pseudo-inverse matrix.

$$\mathbf{a} = (A^T A)^+ A^T \mathbf{b} \quad \text{Eq. A1-5}$$

Table A1-1: Fitting equations for musculotendon lengths ( $L_{mt}$ ) and moment arms ( $R_i$ ) depending on the number of generalized coordinates (GCs) from Menegaldo et al. (2004).

Number of GCs	Equation Number	Fitting Equations
4	1	$L_{mt}, R_1, R_2, R_3, R_4(Q_1, Q_2, Q_3, Q_4) = a_1 + a_2 Q_1 + a_3 Q_2 + a_4 Q_3 + a_5 Q_4 + a_6 Q_1^2 + a_7 Q_2^2 + a_8 Q_3^2 + a_9 Q_4^2 + a_{10} Q_1^3 + a_{11} Q_2^3 + a_{12} Q_3^3 + a_{13} Q_4^3$
	2	$L_{mt}, R_1, R_2, R_3, R_4(Q_1, Q_2, Q_3, Q_4) = a_1 + a_2 Q_1 + a_3 Q_2 + a_4 Q_3 + a_5 Q_4 + a_6 Q_1 Q_2 + a_7 Q_1 Q_3 + a_8 Q_1 Q_4 + a_9 Q_2 Q_3 + a_{10} Q_2 Q_4 + a_{11} Q_3 Q_4$
	3	$L_{mt}, R_1, R_2, R_3, R_4(Q_1, Q_2, Q_3, Q_4) = a_1 + a_2 Q_1 + a_3 Q_2 + a_4 Q_3 + a_5 Q_4$
	4	$L_{mt}, R_1, R_2, R_3, R_4(Q_1, Q_2, Q_3, Q_4) = a_1 + a_2 Q_1 + a_3 Q_2 + a_4 Q_3 + a_5 Q_4 + a_6 Q_1^2 + a_7 Q_2^2 + a_8 Q_3^2 + a_9 Q_4^2 + a_{10} Q_1 Q_2 Q_3 Q_4$
3	1	$L_{mt}, R_1, R_2, R_3(Q_1, Q_2, Q_3) = a_1 + a_2 Q_1 + a_3 Q_2 + a_4 Q_3 + a_5 Q_1^2 + a_6 Q_2^2 + a_7 Q_3^2 + a_8 Q_1^3 + a_9 Q_2^3 + a_{10} Q_3^3$
	2	$L_{mt}, R_1, R_2, R_3(Q_1, Q_2, Q_3) = a_1 + a_2 Q_1 + a_3 Q_2 + a_4 Q_3 + a_5 Q_1 Q_2 + a_6 Q_1 Q_3 + a_7 Q_2 Q_3$
	3	$L_{mt}, R_1, R_2, R_3(Q_1, Q_2, Q_3) = a_1 + a_2 Q_1 + a_3 Q_2 + a_4 Q_3$
	4	$L_{mt}, R_1, R_2, R_3(Q_1, Q_2, Q_3) = a_1 + a_2 Q_1 + a_3 Q_2 + a_4 Q_3 + a_5 Q_1^2 + a_6 Q_2^2 + a_7 Q_3^2 + a_8 Q_1 Q_2 Q_3$
2	1	$L_{mt}, R_1, R_2(Q_1, Q_2) = a_1 + a_2 Q_1 + a_3 Q_2 + a_4 Q_1^2 + a_5 Q_2^2 + a_6 Q_1^3 + a_7 Q_2^3$
	2	$L_{mt}, R_1, R_2(Q_1, Q_2) = a_1 + a_2 Q_1 + a_3 Q_2 + a_4 Q_1 Q_2$
	3	$L_{mt}, R_1, R_2(Q_1, Q_2) = a_1 + a_2 Q_1 + a_3 Q_2$
	4	$L_{mt}, R_1, R_2, R_3(Q_1, Q_2, Q_3) = a_1 + a_2 Q_1 + a_3 Q_2 + a_4 Q_1^2 + a_5 Q_2^2 + a_6 Q_1 Q_2$
1	1	$L_{mt}, R_1(Q_1) = a_1 + a_2 Q_1 + a_3 Q_1^2 + a_4 Q_1^3$
	2	$L_{mt}, R_1(Q_1) = a_1 + a_2 Q_1 + a_3 Q_1^2$
	3	$L_{mt}, R_1(Q_1) = a_1 + a_2 Q_1$

MATLAB code provided by Menegaldo et al. (2004) were used to generate input files to SIMM to obtain data samples for regression fitting. All combinations of the GCs were sampled with 20 points across the range of motion expected for hemiparetic walking (Table A1-2). For muscles dependent on one, two, and three GCs, 20, 400, and 8000 points were generated, respectively. For muscles dependent on four GCs, data were sampled by 15 points such that 50,625 points were generated. Musculotendon actuators were placed into one of six groups based on the GCs spanned (Table A1-3).

Table A1-2: Generalized coordinates and the range of motion over which data were sampled to compute regression coefficients.

<b>Generalized coordinate</b>	<b>Minimum (deg)</b>	<b>Maximum (deg)</b>
Hip flexion (HF)	-40 extension	60 flexion
Hip abduction (HA)	-30 abduction	30 adduction
Hip rotation (HR)	-30 external	30 internal
Knee angle (KA)	-100 flexion	10 extension
Ankle angle (AA)	-30 plantar flexion	30 dorsiflexion
Subtalar angle (SA)	-40 eversion	40 inversion
Metatarsal angle (MA)	-5 flexion	40 extension

Table A1-3: Selected muscle groups according to dependence on the same generatlized coordinates (GCs).

<b>Group</b>	<b>Number of GCs dependent on</b>	<b>Muscle name</b>
1	3: (HF, HA, HR)	Anterior, Middle and Posterior Gluteus Medius, Anterior, Middle and Posterior Gluteus Minimus, Adductor Longus, Adductor Brevis, Pectineus, Superior, Middle and Inferior Adductor Magnus, Iliacus, Psoas, Quadratus Femoris, Gemellus, Piriformis, Tensor Fasciae Lata
2	4: (HF, HA, HR, KA)	Semitendinosus, Semimembranosus, Gracilis, Biceps Femoris Long Head, Rectus Femoris, Sartorius
3	1: (KA)	Biceps Femoris Short Head, Vastus Medialis, Lateralis, and Intermedius
4	3: (KA, AA, SA)	Medial and Lateral Gastrocnemius
5	2: (AA, SA)	Soleus, Tibialis Anterior, Tibialis Posterior, Peroneus Brevis, Peroneus Tertius, Peroneus Longus
6	3: (AA, SA, MA)	Flexor Digitorum Longus, Flexor Hallucis Longus, Extensor Digitorum Longus, Extensor Hallucis Longus

Table A1-4: Regression coefficients for Group 1 muscles dependent on 3 generalized coordinates to estimate musculotendon lengths ( $L_{mt}$ ) and hip flexion, hip abduction, and hip rotation moment arms ( $R_{HF}$ ,  $R_{HA}$ ,  $R_{HR}$ ) using the equations (Eq.) given in Table A1-1.

$L_{mt}$	Anterior GMED	Middle GMED	Posterior GMED	Anterior GMIN	Middle GMIN	Posterior GMIN	Quadratus Femoris
Eq.	2	2	2	1	1	1	1
a <sub>1</sub>	0.12122	0.12938	0.10894	0.082448	0.082488	0.08617	0.069484
a <sub>2</sub>	0.00024	0.000333	0.000383	3.4e-005	0.0001	0.000179	-6e-005
a <sub>3</sub>	0.000807	0.000728	0.000584	0.00071	0.000705	0.00063	-0.000664
a <sub>4</sub>	-0.000344	0.000113	0.000491	-0.000323	-0.000119	0.000135	0.000568
a <sub>5</sub>	-2e-006	-2e-006	-3e-006	-1e-006	-1e-006	-1e-006	7e-006
a <sub>6</sub>	-2e-006	0	-2e-006	-2e-006	-3e-006	-3e-006	-2e-006
a <sub>7</sub>	2e-006	5e-006	3e-006	2e-006	2e-006	1e-006	-2e-006
a <sub>8</sub>				0	0	0	0
a <sub>9</sub>				0	0	0	0
a <sub>10</sub>				0	0	0	0
$R_{HF}$							
Eq.	2	1	1	2	2	1	2
a <sub>1</sub>	-0.012853	-0.022313	-0.023811	-0.001885	-0.005371	-0.010559	0.004048
a <sub>2</sub>	0.000278	9.9e-005	-9.5e-005	0.000153	0.00015	8.8e-005	-0.000697
a <sub>3</sub>	-1.6e-005	0.000124	0.000179	-1.1e-005	2e-005	5.8e-005	0.000264
a <sub>4</sub>	-9.9e-005	1.7e-005	0.000108	-5.6e-005	-4.4e-005	5e-006	0.000143
a <sub>5</sub>	0	3e-006	4e-006	0	-1e-006	1e-006	-1e-005
a <sub>6</sub>	-1e-006	2e-006	1e-006	0	0	0	8e-006
a <sub>7</sub>	4e-006	0	0	3e-006	3e-006	0	-6e-006
a <sub>8</sub>		0	0			0	
a <sub>9</sub>		0	0			0	
a <sub>10</sub>		0	0			0	

R <sub>HA</sub>							
Eq.	2	2	1	1	1	1	1
a1	-0.0443	-0.041252	-0.035316	-0.042243	-0.042452	-0.038376	0.041961
a2	-2.8e-005	0.000117	0.000206	-1.5e-005	1.8e-005	6.8e-005	0.000324
a3	0.000148	0.000343	0.000397	0.000233	0.000302	0.000348	0.000191
a4	-0.00039	-0.000293	-0.000151	-0.000238	-0.000156	-6.6e-005	1.8e-005
a5	4e-006	3e-006	-1e-006	0	0	0	-5e-006
a6	4e-006	3e-006	2e-006	3e-006	2e-006	2e-006	-3e-006
a7	3e-006	3e-006	6e-006	6e-006	7e-006	6e-006	-3e-006
a8			0	0	0	0	0
a9			0	0	0	0	0
a10			0	0	0	0	0

R <sub>HR</sub>							
Eq.	2	2	2	2	2	2	2
a1	0.019431	-0.006366	-0.027599	0.017645	0.006687	-0.007338	-0.034153
a2	-0.000106	1.8e-005	0.00011	-5.5e-005	-4.5e-005	5e-006	0.000247
a3	-0.000374	-0.000289	-0.00018	-0.000213	-0.000156	-9e-005	0.000104
a4	-0.000159	-1.5e-005	2.6e-005	-0.000175	-0.000183	-7.1e-005	0.000186
a5	4e-006	3e-006	1e-006	3e-006	3e-006	2e-006	-7e-006
a6	-1e-006	0	0	-1e-006	0	1e-006	3e-006
a7	1.2e-005	1.3e-005	1.2e-005	1.2e-005	1.3e-005	1.2e-005	-6e-006

L <sub>mt</sub>	Anterior GMAX	Middle GMAX	Posterior GMAX	Adductor Longus	Adductor Brevis	Pectineus	Tensor Fasciae Lata
Eq.	2	1	2	2	2	2	1
a1	0.19873	0.20962	0.23726	0.21714	0.13616	0.10276	0.53545
a2	0.000689	0.000908	0.001146	-0.000531	-9.8e-005	-0.000354	-0.000581
a3	0.000463	0.000173	-0.000778	-0.000998	-0.000973	-0.000509	0.000816
a4	0.000359	0.000407	0.000504	-0.000121	-5.6e-005	-7.3e-005	-4.8e-005
a5	-2e-006	-1e-006	6e-006	1e-006	2e-006	-1e-006	-7e-006
a6	-2e-006	-1e-006	-1.5e-005	-1.7e-005	-1.5e-005	-9e-006	-6e-006

a7	6e-006	4e-006	1e-006	0	0	-1e-006	3e-006
a8		0					0
a9		0					0
a10		0					0

R<sub>HF</sub>

Eq.	1	1	1	2	2	2	2
a1	-0.045584	-0.055697	-0.073446	0.031423	0.008836	0.019807	0.031837
a2	0.000173	0.000171	-0.000166	-0.000318	-0.00037	-8.7e-005	0.000721
a3	0.000143	4.2e-005	-0.000276	9.4e-005	5.4e-005	0.00015	-4e-005
a4	0.00012	0.000245	0.000921	0.000923	0.000811	0.000456	-0.000336
a5	5e-006	5e-006	1.6e-005	-1.9e-005	-1.8e-005	-9e-006	2e-006
a6	2e-006	0	-1e-006	0	-2e-006	3e-006	0
a7	3e-006	9e-006	5e-006	-2e-006	-2e-006	0.019807	1.6e-005
a8	0	0	0				
a9	0	0	0				
a10	0	0	0				

R<sub>HA</sub>

Eq.	2	2	1	1	1	1	2
a1	-0.026266	-0.010009	0.050122	0.066614	0.064746	0.032962	-0.04585
a2	0.00013	4.4e-005	-0.000334	0.000152	6e-005	0.000206	-1.4e-005
a3	0.000328	0.000124	-0.000145	0.000138	0.000305	0.000196	0.000708
a4	-0.0004	-9e-005	-0.000105	1.8e-005	8e-006	5.4e-005	0.000216
a5	4e-006	0	-4e-006	-9e-006	-1e-005	-4e-006	-4e-006
a6	7e-006	3e-006	-9e-006	-8e-006	-5e-006	-3e-006	1.6e-005
a7	2e-006	-1e-006	-3e-006	0	0	0	-1e-006
a8			0	0	0	0	
a9			0	0	0	0	
a10			0	0	0	0	



$R_{HR}$							
Eq.	2	2	2	2	1	2	2
a1	-0.019886	-0.021157	-0.027237	0.006721	0.003829	0.004081	0.006071
a2	9.1e-005	0.000102	0.000797	0.000974	0.000963	0.000504	-0.000327
a3	-0.000398	-9.5e-005	-1.5e-005	2.6e-005	1.5e-005	4.9e-005	0.00021
a4	-0.000415	-0.000687	-0.00022	0.000155	0.00032	0.00023	-0.000322
a5	7e-006	3e-006	-4e-006	-1e-006	1e-006	0	1.5e-005
a6	7e-006	1.8e-005	1.6e-005	-7e-006	-1e-006	-4e-006	-7e-006
a7	1.2e-005	4e-006	-5e-006	0	-1e-006	0	1e-005
a8					0		
a9					0		
a10					0		

$L_{mt}$	Superior AMG	Middle AMG	Inferior AMG	Iliacus	Psoas	Piriformis	Gemellus
Eq.	2	2	2	1	1	1	1
a1	0.12026	0.1998	0.34267	0.20596	0.2571	0.13634	0.064391
a2	0.000145	0.000382	0.000271	-0.000554	-0.000528	0.000158	-2.1e-005
a3	-0.001109	-0.000993	-0.000864	3.3e-005	-7.8e-005	0.000317	-0.000198
a4	5.7e-005	2.8e-005	-1e-005	-6.6e-005	-8.3e-005	0.000491	0.000542
a5	3e-006	5e-006	4e-006	-3e-006	-3e-006	1e-006	1e-006
a6	-1.4e-005	-1.4e-005	-1.5e-005	-1e-006	-1e-006	-2e-006	-1e-006
a7	1e-006	2e-006	2e-006	2e-006	2e-006	-2e-006	-2e-006
a8				0	0	0	0
a9				0	0	0	0
a10				0	0	0	0

$R_{HF}$							
Eq.	2	2	2	1	1	1	2
a1	0.000331	-0.011725	-0.006084	0.03368	0.031963	-0.009111	0.00122
a2	-0.000761	-0.000807	-0.000823	0.000328	0.0003	-0.000101	-0.00016
a3	6.2e-005	-3.9e-005	-1.2e-005	-1.1e-005	1.3e-005	7.7e-005	4.4e-005
a4	0.000748	0.0008	0.000851	2.2e-005	0.000153	6.6e-005	-3e-006

a5	-2.1e-005	-1.8e-005	-1.8e-005	-2e-006	-2e-006	2e-006	-1e-006
a6	-3e-006	-5e-006	-4e-006	0	0	0	2e-006
a7	-8e-006	-1.1e-005	-1.2e-005	-6e-006	-6e-006	0	-1e-006
a8				0	0	0	
a9				0	0	0	
a10				0	0	0	

R<sub>HA</sub>

Eq.	1	1	1	2	2	1	2
a1	0.07565	0.067832	0.059159	-0.001735	0.004133	-0.019729	0.010637
a2	-1.3e-005	-0.000129	-5.9e-005	-1.1e-005	1.7e-005	9.1e-005	3.8e-005
a3	9e-005	-0.000514	-0.000812	0.000118	0.000108	0.000268	0.000156
a4	-7.1e-005	-0.000134	-0.000136	1.5e-005	1.9e-005	2e-005	-3.9e-005
a5	-1.3e-005	-1e-005	-1e-005	1e-006	1e-006	0	-1e-006
a6	-9e-006	-1.2e-005	-1e-005	3e-006	2e-006	1e-006	-1e-006
a7	-2e-006	-1e-006	0	0	0	3e-006	-1e-006
a8	0	0	0			0	
a9	0	0	0			0	
a10	0	0	0			0	

R<sub>HR</sub>

Eq.	2	2	2	2	2	2	1
a1	-0.003207	-0.001561	0.000586	0.003383	0.002983	-0.027926	-0.031936
a2	0.000791	0.000802	0.000856	9e-006	0.000116	7.1e-005	-3e-006
a3	3e-006	-1.5e-005	-5e-006	1.4e-005	1.7e-005	4e-006	-4.2e-005
a4	0.000335	0.000143	-3.6e-005	-7.5e-005	-6e-005	0.000183	0.000261
a5	-7e-006	-1.2e-005	-1.3e-005	2e-006	2e-006	0	1e-006
a6	1e-006	4e-006	3e-006	-1.2e-005	-1.1e-005	0	0
a7	-3e-006	-2e-006	0.000586	1e-006	0	5e-006	2e-006
a8							0
a9							0
a10							0

Table A1-5: Regression coefficients for Group 2 muscles dependent on 4 generalized coordinates to estimate musculotendon lengths ( $L_{mt}$ ) and hip flexion, hip abduction, hip rotation, and knee angle moment arms ( $R_{HF}$ ,  $R_{HA}$ ,  $R_{HR}$ ,  $R_{KA}$ ) using the equations (Eq.) given in Table A1-1.

$L_{mt}$	Semi-membranosus	Semi-tendinosus	Biceps Fem. Long Head	Sartorius	Gracilis	Rectus Femoris
Eq.	1	1	1	4	2	4
a1	0.41514	0.4642	13	0.56825	0.45159	0.40992
a2	0.000794	0.000933	0.44096	-0.00072	0.000131	-0.000648
a3	-0.000197	-0.000335	0.000873	0.000402	-0.00082	0.00018
a4	-4.5e-005	-6.5e-005	-0.000325	0.000194	8e-005	5.1e-005
a5	0.00044	0.000731	9.2e-005	4e-005	0.00064	-0.000809
a6	6e-006	7e-006	0.000219	-7e-006	1e-006	-3e-006
a7	5e-006	6e-006	5e-006	-8e-006	-1.6e-05	-4e-006
a8	0	0	4e-006	0	0	2e-006
a9	-8e-006	-5e-006	0	-3e-006	1e-006	-3e-006
a10	0	0	-1.1e-005	0	0	0.40992
a11	0	0	0			
a12	0	0	0			
a13	0	0	0			
$R_{HF}$						
Eq.	4	4	4	2	2	1
a1	-0.049162	-0.056283	-0.054583	0.039583	0.001715	0.042149
a2	-0.000625	-0.000762	-0.000592	0.000821	-0.00086	0.00053
a3	-2.4e-005	-4.8e-005	-3.7e-005	-3.6e-005	9.8e-005	4e-005
a4	0.000199	0.000332	0.000251	-0.00051	0.000834	-0.000183
a5	-5.8e-005	-4.2e-005	-6.3e-005	0	-1.4e-05	2.1e-005
a6	9e-006	1.1e-005	9e-006	9e-006	-1.8e-05	-5e-006
a7	1e-006	1e-006	1e-006	-1e-006	-2e-006	-1e-006
a8	7e-006	8e-006	7e-006	0	0	-5e-006
a9	0	-1e-006	0	1.5e-005	-1.3e-05	0
a10	0	0	0	0	0	0
a11				0	0	0
a12						0
a13						0
$R_{HA}$						
Eq.	2	2	2	2	4	2
a1	0.010981	0.018599	0.017679	-0.02316	0.056692	-0.010448
a2	-3.8e-005	-5.3e-005	-6.4e-005	4.5e-005	0.000103	4.5e-005
a3	-0.000564	-0.000719	-0.000489	0.000906	-0.00085	0.000484
a4	6.3e-005	0.000113	3.6e-005	1.5e-005	-5.2e-005	7.5e-005

a5	3e-006	2e-006	-7e-006	0	-6e-006	1e-006
a6	1e-006	2e-006	1e-006	-1e-006	-9e-006	-2e-006
a7	-9e-006	-1.2e-005	-9e-006	1.5e-005	-1e-005	9e-006
a8	0	0	0	0	0	0
a9	0	0	0	1e-006	0	1e-006
a10	0	0	0	0	0	0
a11	-1e-006	0	-1e-006	0	0	0

R<sub>IHR</sub>

Eq.	2	2	2	2	2	2
a1	0.000767	-0.000225	-0.005803	-0.00552	-0.00441	-0.001448
a2	0.000206	0.000348	0.000255	-0.00053	0.000865	-0.000181
a3	6.2e-005	0.000112	3.5e-005	1.4e-005	7.1e-005	7.4e-005
a4	-9.9e-005	-0.00017	-3.8e-005	7.2e-005	-6.1e-05	-9e-005
a5	8e-006	-9e-006	3.9e-005	0	1.4e-005	-9e-006
a6	-1e-005	-1.2e-005	-9e-006	1.5e-005	-1.3e-05	9e-006
a7	1.4e-005	1.6e-005	1.5e-005	-1.2e-005	1e-006	-1e-005
a8	0	0	0	0	0	0
a9	0	0	-1e-006	-3e-006	0	0
a10	-1e-006	0	-1e-006	0	0	0
a11	1e-006	0	2e-006	0	0	0

R<sub>KA</sub>

Eq.	1	4	1	1	1	1
a1	-0.026321	-0.042167	-0.014082	-0.00153	-0.02467	0.042061
a2	-2.5e-005	1.6e-005	-5.3e-005	0	-1.3e-05	3e-005
a3	0	3e-006	-1.2e-005	0	-2e-006	3e-006
a4	7e-006	-9e-006	3.8e-005	0	1.1e-005	-1.2e-005
a5	0.000809	0.000505	0.001043	0.000355	0.000539	-0.000429
a6	0	0	1e-006	0	0	0
a7	0	0	0	0	0	0
a8	0	0	1e-006	0	0	0
a9	3e-006	8e-006	1e-006	0	4e-006	-2e-005
a10	0	0	0	0	0	0
a11	0	0	0	0	0	0
a12	0	0	0	0	0	0
a13	0	0	0	0	0	0

Table A1-6: Regression coefficients for Group 3 muscles dependent on 1 generalized coordinate to estimate musculotendon lengths ( $L_{mt}$ ) and knee angle moment arms ( $R_{KA}$ ) using the equations (Eq.) given in Table A1-1.

$L_{mt}$	<b>Vastus Medialis</b>	<b>Vastus Lateralis</b>	<b>Vastus Intermedius</b>	<b>Biceps Fem. Short Head</b>
Eq.	2	1	1	1
a1	0.17273	0.20073	0.18251	0.25884
a2	-0.000679	-0.000656	-0.000756	6.5e-005
a3	-1e-006	-1e-006	-3e-006	-9e-006
a4		0	0	0
$R_{KA}$				
Eq.	1	1	1	1
a1	0.036804	0.033036	0.039485	-0.004308
a2	-0.000212	-0.0005	-0.000163	0.000905
a3	-1.1e-005	-1.7e-005	-1.2e-005	0
a4	0	0	0	0

Table A1-7: Regression coefficients for Group 4 muscles dependent on 3 generalized coordinates to estimate musculotendon lengths ( $L_{mt}$ ) and knee, ankle and subtalar angle moment arms ( $R_{KA}$ ,  $R_{AA}$ ,  $R_{SA}$ ) using the equations (Eq.) given in Table A1-1.

$L_{mt}$	<b>Medial Gastrocnemius</b>	<b>Lateral Gastrocnemius</b>
Eq.	1	1
a1	0.45032	0.44749
a2	0.000182	0.000219
a3	0.000709	0.000726
a4	-2.6e-005	-7.7e-005
a5	0	0
a6	-2e-006	-2e-006
a7	2e-006	2e-006
a8	0	0
a9	0	0
a10	0	0

$R_{KA}$		
Eq.	3	3
a1	-0.014631	-0.016594
a2	-0.000169	-0.000232
a3	0	0
a4	0	0

$R_{AA}$		
Eq.	1	1
a1	-0.041733	-0.042777
a2	0	0
a3	0.000205	0.00022
a4	5.1e-005	4.6e-005
a5	0	0
a6	6e-006	6e-006
a7	2e-006	2e-006
a8	0	0
a9	0	0
a10	0	0

$R_{SA}$		
Eq.	2	2
a1	0.001373	0.004013
a2	0	0
a3	4.6e-005	4.2e-005
a4	-0.00028	-0.000276
a5	0	0
a6	0	0
a7	4e-006	4e-006

Table A1-8: Regression coefficients for Group 5 muscles dependent on 2 generalized coordinates to estimate musculotendon lengths ( $L_{mt}$ ) and ankle and subtalar angle moment arms ( $R_{AA}$ ,  $R_{SA}$ ) using the equations (Eq.) given in Table A1-1.

$L_{mt}$	<b>Soleus</b>	<b>Tibialis Posterior</b>	<b>Tibialis Anterior</b>	<b>Peroneus Brevis</b>	<b>Peroneus Longus</b>	<b>Peroneus Tertius</b>
Eq.	4	4	4	2	1	4
a1	0.29079	0.34528	0.30357	0.2106	0.39533	0.17804
a2	0.000681	0.000193	-0.000668	6.9e-005	0.000157	-0.0004
a3	-6e-005	-0.00031	-0.000222	0.000459	0.000483	0.0003
a4	-2e-006	-1e-006	-1e-006	1e-006	0	0
a5	2e-006	1e-006	-1e-006		0	1e-006
a6	-1e-006	1e-006	1e-006		0	-6e-006
a7					0	

$R_{AA}$						
Eq.	4	4	4	4	4	4
a1	-0.041235	-0.011592	0.042213	-0.004837	-0.009827	0.026731
a2	0.000257	9e-005	7.4e-005	-2.3e-005	-1.5e-005	-4.8e-005
a3	3.7e-005	-8e-005	-3.8e-005	-7.6e-005	-5.4e-005	0.000333
a4	5e-006	1e-006	-5e-006	0	2e-006	-3e-006
a5	2e-006	1e-006	-5e-006	1e-006	2e-006	-5e-006
a6	-2e-006	-3e-006	2e-006	7e-006	7e-006	8e-006

$R_{SA}$						
Eq.	4	1	4	1	1	4
a1	0.003966	0.019908	0.012948	-0.031675	-0.030373	-0.019456
a2	3.5e-005	-8e-005	-5.4e-005	-0.000115	-6.4e-005	0.000334
a3	-0.000264	-7.9e-005	0.000105	0.000219	0.000191	-8.3e-005
a4	-1e-006	-2e-006	1e-006	5e-006	5e-006	4e-006
a5	-1e-006	-4e-006	-2e-006	1.1e-005	9e-006	3e-006
a6	4e-006	0	-1e-005	0	0	-1.1e-005
a7		0		0	0	

Table A1-9: Regression coefficients for Group 6 muscles dependent on 3 generalized coordinates to estimate musculotendon lengths ( $L_{mt}$ ) and ankle, subtalar and metatarsal angle moment arms ( $R_{AA}$ ,  $R_{SA}$ ,  $R_{MA}$ ) using the equations (Eq.) given in Table A1-1.

	<b>Flex. Digitorum</b>	<b>Flex. Hallucis</b>	<b>Ext. Digitorum</b>	<b>Ext. Hallucis</b>
$L_{mt}$	<b>Longus</b>	<b>Longus</b>	<b>Longus</b>	<b>Longus</b>
Eq.	3	3	4	4
a1	0.43041	0.41534	0.45388	0.42225
a2	-0.000424	-0.000352	0.000238	-9.8e-005
a3	5.6e-005	5.9e-005	-6.4e-005	-7.7e-005
a4	0.000246	0.000362	-0.000825	-0.000844
a5			-1e-006	-1e-006
a6			0	0
a7			0	-1e-006
a8			0	0
<b><math>R_{AA}</math></b>				
Eq.	1	1	3	3
a1	-0.01301	-0.018401	0.035077	0.035927
a2	-0.000125	-0.000111	0.000135	-8.7e-005
a3	0	0	0	0
a4	8.5e-005	9.4e-005	-2.4e-005	2.8e-005
a5	0	1e-006		
a6	0	0		
a7	3e-006	3e-006		
a8	0	0		
a9	0	0		
a10	0	0		
<b><math>R_{SA}</math></b>				
Eq.	4	4	3	1
a1	0.021011	0.017527	-0.012012	0.006088
a2	-3.1e-005	-5.1e-005	5.9e-005	5.8e-005
a3	0	0	0	0
a4	-2.3e-005	-3.1e-005	0.00012	-9.3e-005
a5	-6e-006	-5e-006		-1e-006
a6	0	0		0
a7	-3e-006	-2e-006		-1e-006
a8	0	0		0
a9				0
a10				0



$R_{MA}$				
Eq.	4	3	4	4
a1	-0.005695	-0.005935	0.006546	0.007954
a2	0	0	0	0
a3	2.8e-005	-1e-006	2.4e-005	3.5e-005
a4	0	0	0	0
a5	0		0	0
a6	0		0	0
a7	0		0	0
a8	0		0	0

## Appendix 2

### Experimental Setup for Accelerated and Decelerated Walking

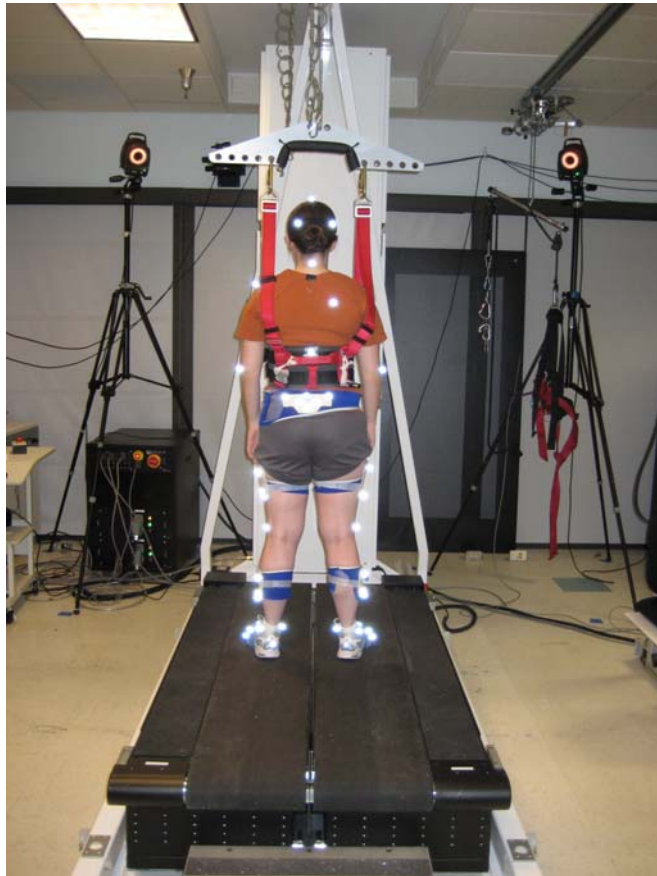


Figure A2-1: Kinematic and GRF data were collected during treadmill walking at the VA-UF Human Motor Performance Laboratory, VA Medical Center at Gainesville, Florida. Marker trajectories were recorded with a twelve-camera motion capture system (Vicon) and GRF data were measured as subjects walked on a split-belt instrumented treadmill. A safety harness that did not provide body weight support was worn during all trials to protect subjects in case of a loss of balance.

## Appendix 3

### Accelerated and Decelerated Walking Data

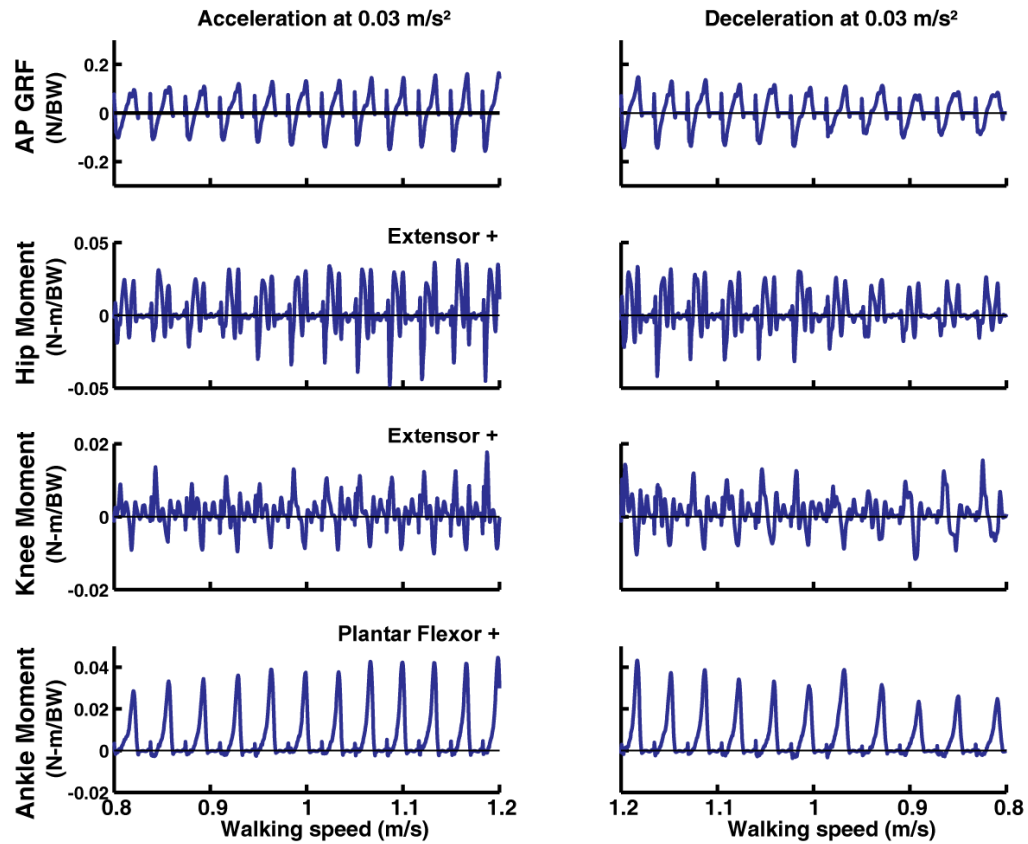


Figure A3-1: Anterior-posterior ground reaction forces (AP GRFs), hip, knee and ankle moments across speeds of 0.8 to 1.2 m/s during a representative acceleration and deceleration trial at 0.03 m/s<sup>2</sup>.

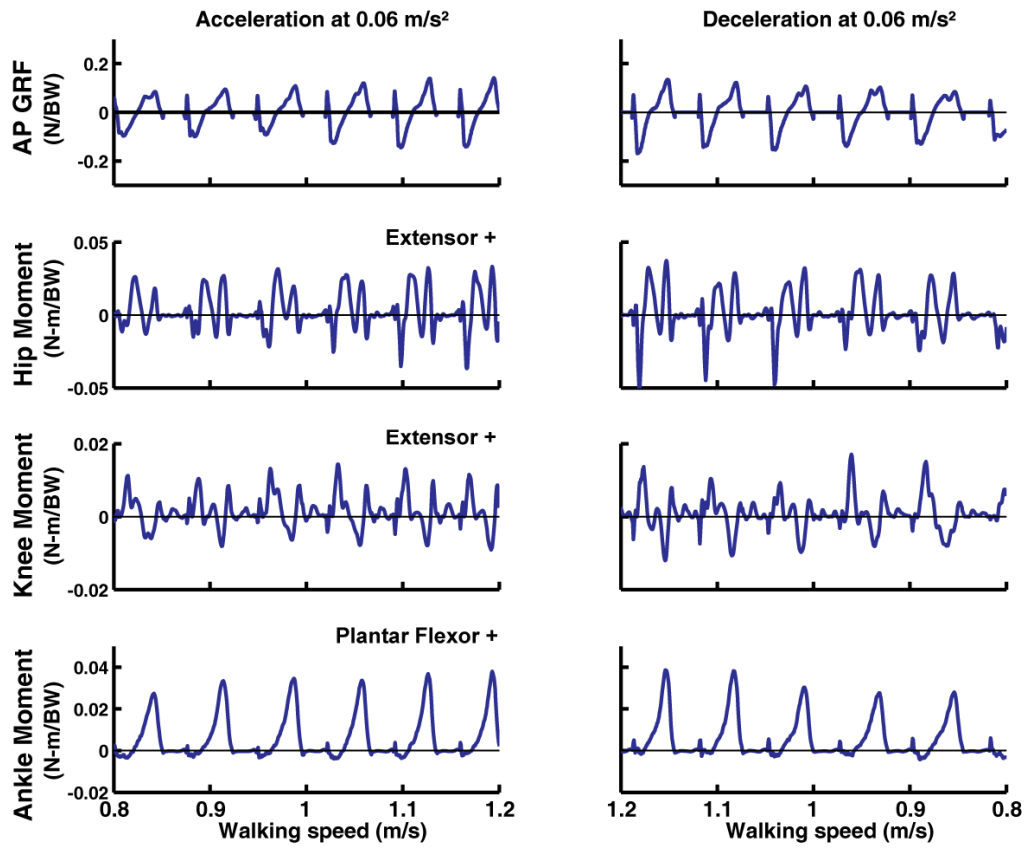


Figure A3-2: Anterior-posterior ground reaction forces (AP GRFs), hip, knee and ankle moments across speeds of 0.8 to 1.2 m/s during a representative acceleration and deceleration trial at 0.06 m/s<sup>2</sup>.

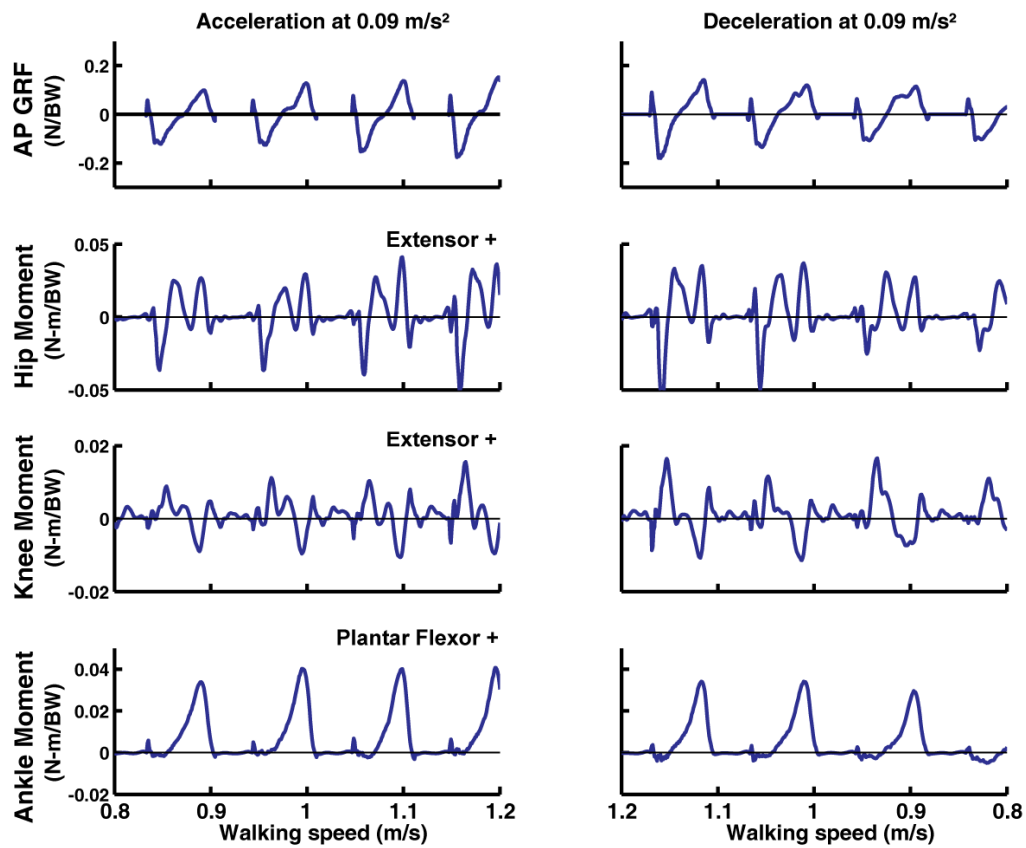


Figure A3-3: Anterior-posterior ground reaction forces (AP GRFs), hip, knee and ankle moments across speeds of 0.8 to 1.2 m/s during a representative acceleration and deceleration trial at 0.09 m/s<sup>2</sup>.

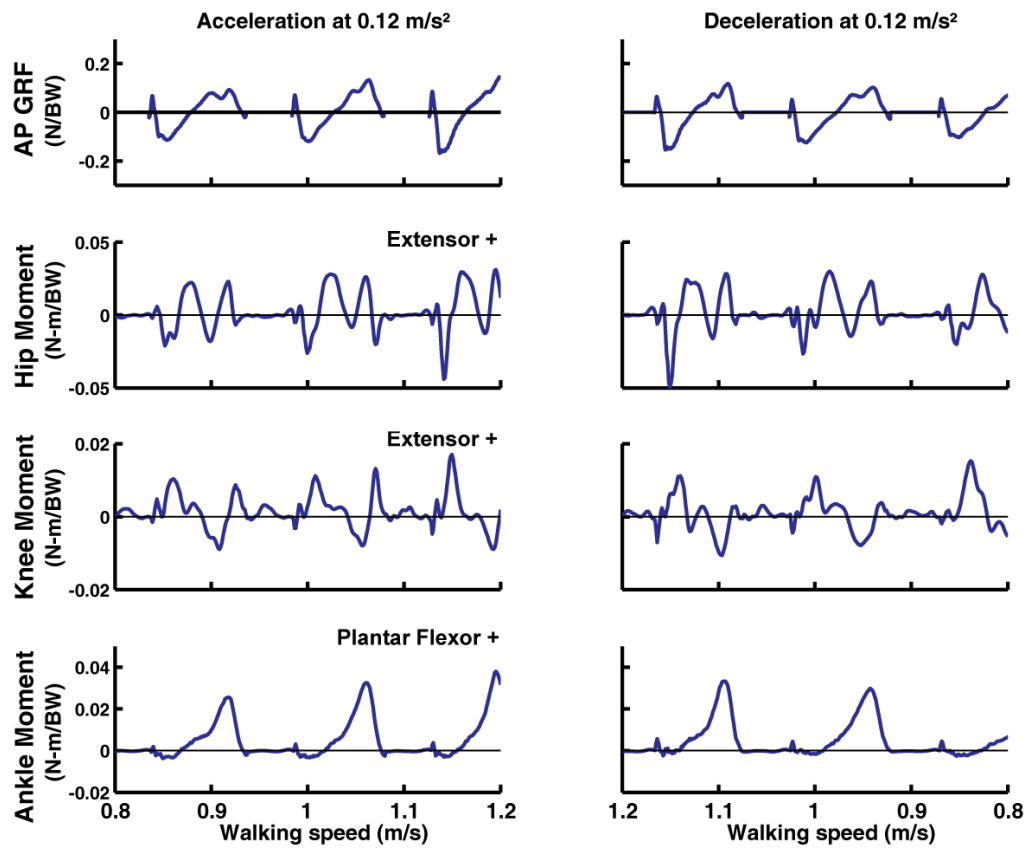


Figure A3-4: Anterior-posterior ground reaction forces (AP GRFs), hip, knee and ankle moments across speeds of 0.8 to 1.2 m/s during a representative acceleration and deceleration trial at 0.12 m/s<sup>2</sup>.

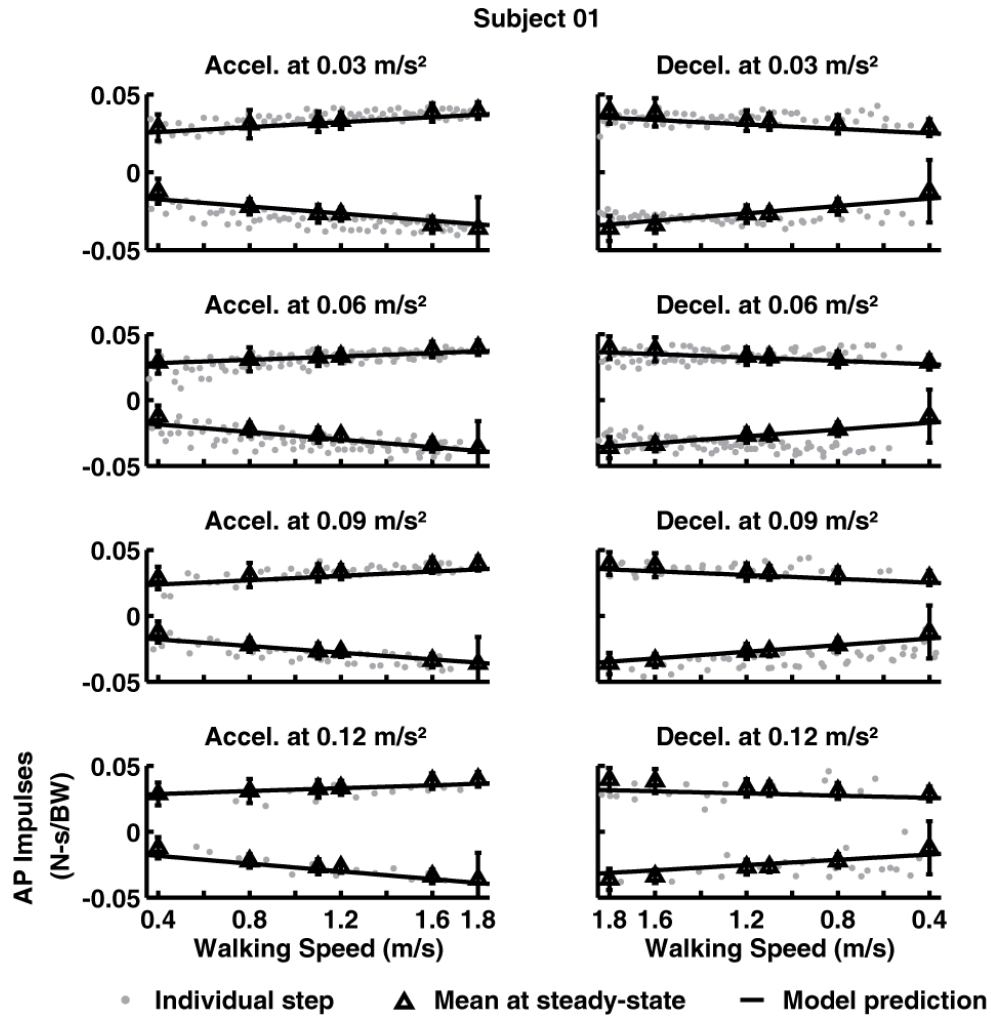


Figure A3-5: Linear mixed regression models were generated from data collected from ten subjects and are compared to individual steps for subject 01 at each rate and subject 01's mean anterior-posterior ground reaction force (AP) impulses (error bars are  $\pm 3$  standard deviations) at steady-state speeds. Subject 01's self-selected walking speed was 1.1 m/s.

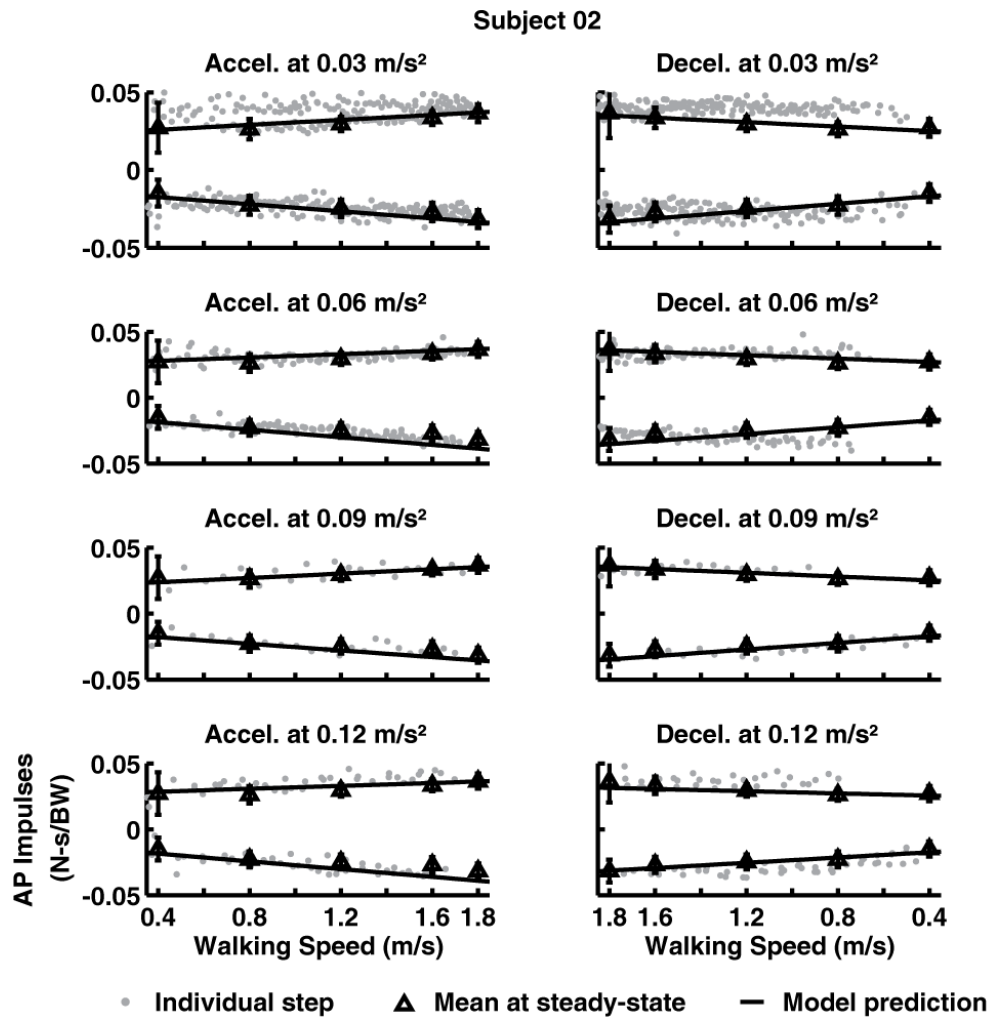


Figure A3-6: Linear mixed regression models were generated from data collected from ten subjects and are compared to individual steps for subject 02 at each rate and subject 02's mean anterior-posterior ground reaction force (AP) impulses (error bars are  $\pm 3$  standard deviations) at steady-state speeds. Subject 02's self-selected walking speed was 1.2 m/s.



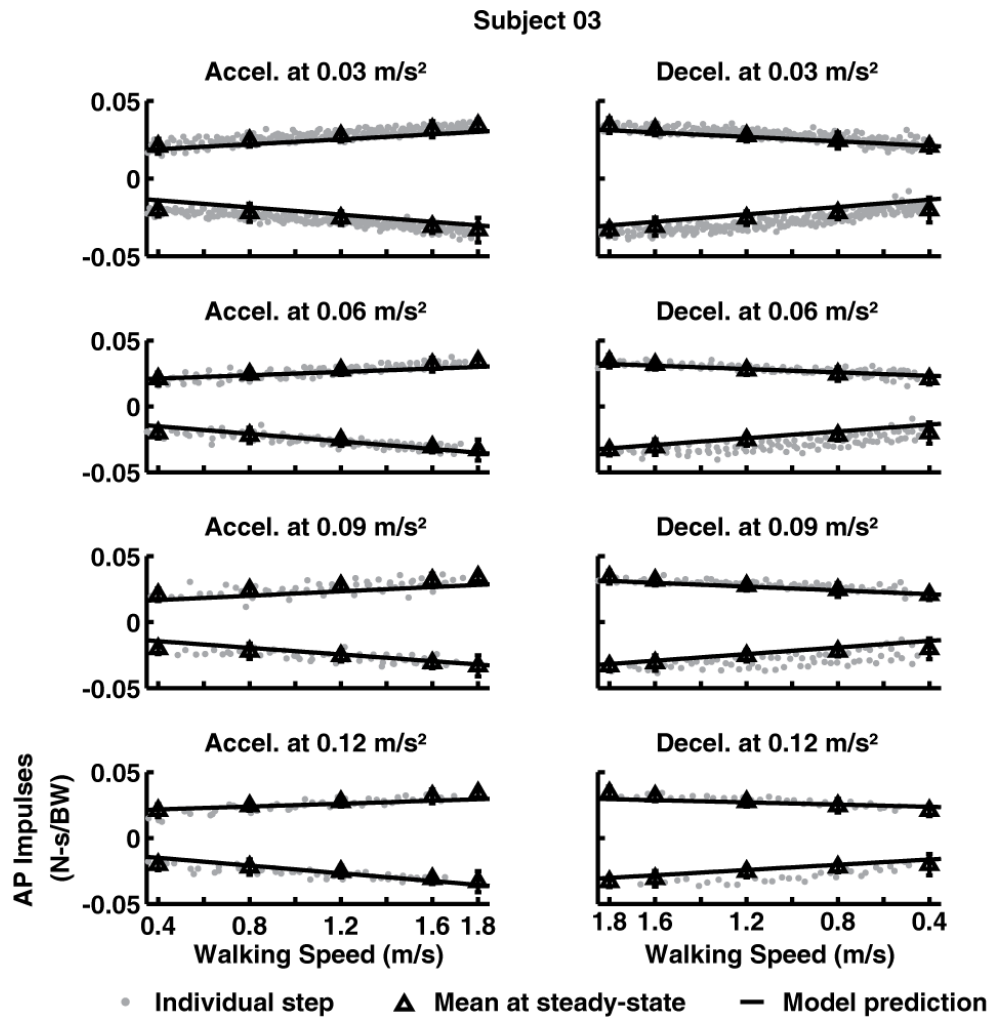


Figure A3-7: Linear mixed regression models were generated from data collected from ten subjects and are compared to individual steps for subject 03 at each rate and subject 03's mean anterior-posterior ground reaction force (AP) impulses (error bars are  $\pm 3$  standard deviations) at steady-state speeds. Subject 03's self-selected walking speed was 1.2 m/s.

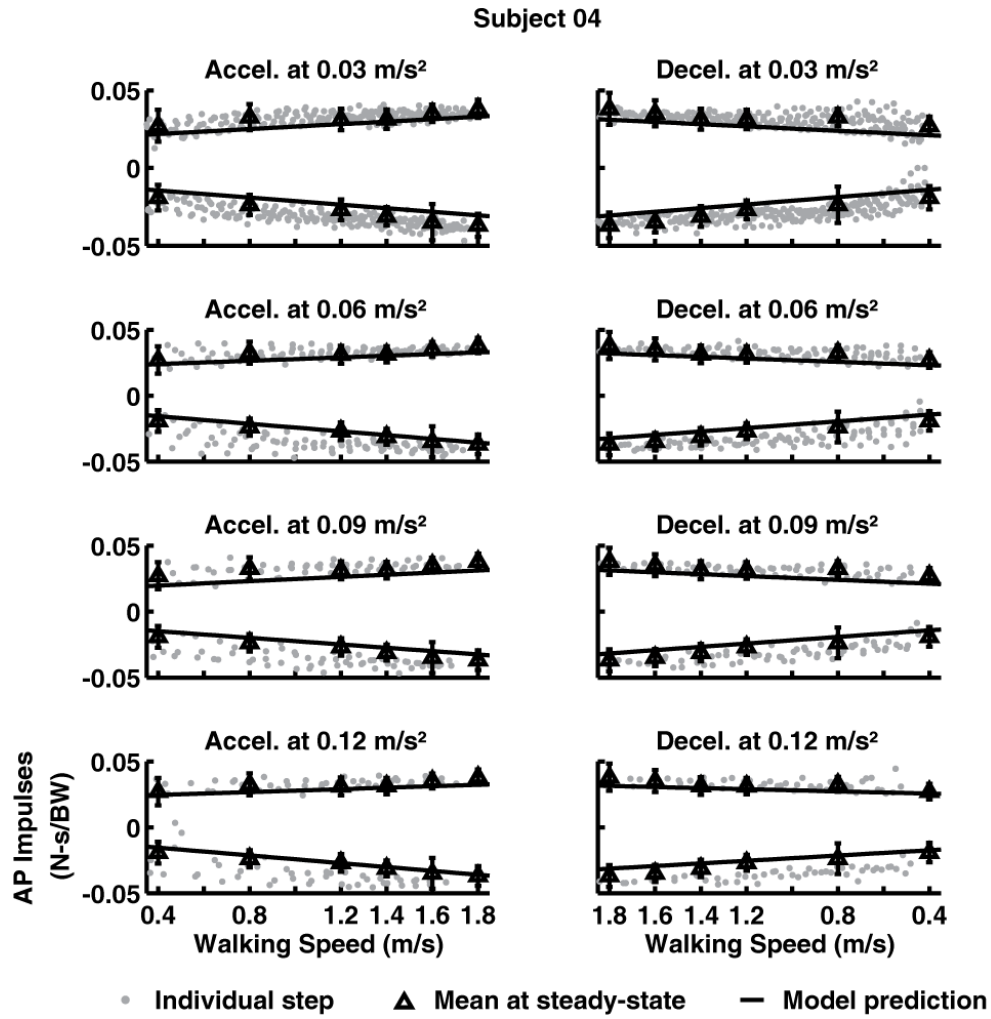


Figure A3-8: Linear mixed regression models were generated from data collected from ten subjects and are compared to individual steps for subject 04 at each rate and subject 04's mean anterior-posterior ground reaction force (AP) impulses (error bars are  $\pm 3$  standard deviations) at steady-state speeds. Subject 04's self-selected walking speed was 1.4 m/s.

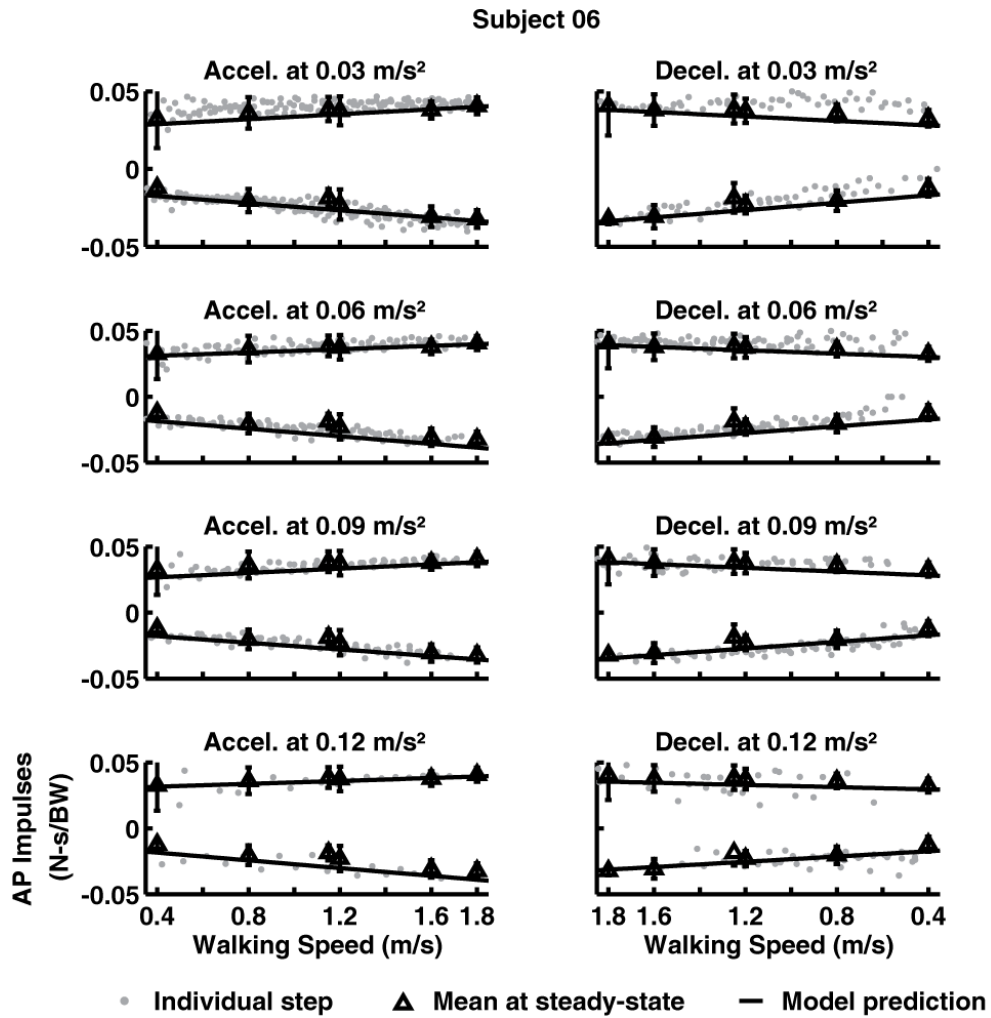


Figure A3-9: Linear mixed regression models were generated from data collected from ten subjects and are compared to individual steps for subject 06 at each rate and subject 06's mean anterior-posterior ground reaction force (AP) impulses (error bars are  $\pm 3$  standard deviations) at steady-state speeds. Subject 06's self-selected walking speed was 1.15 m/s.

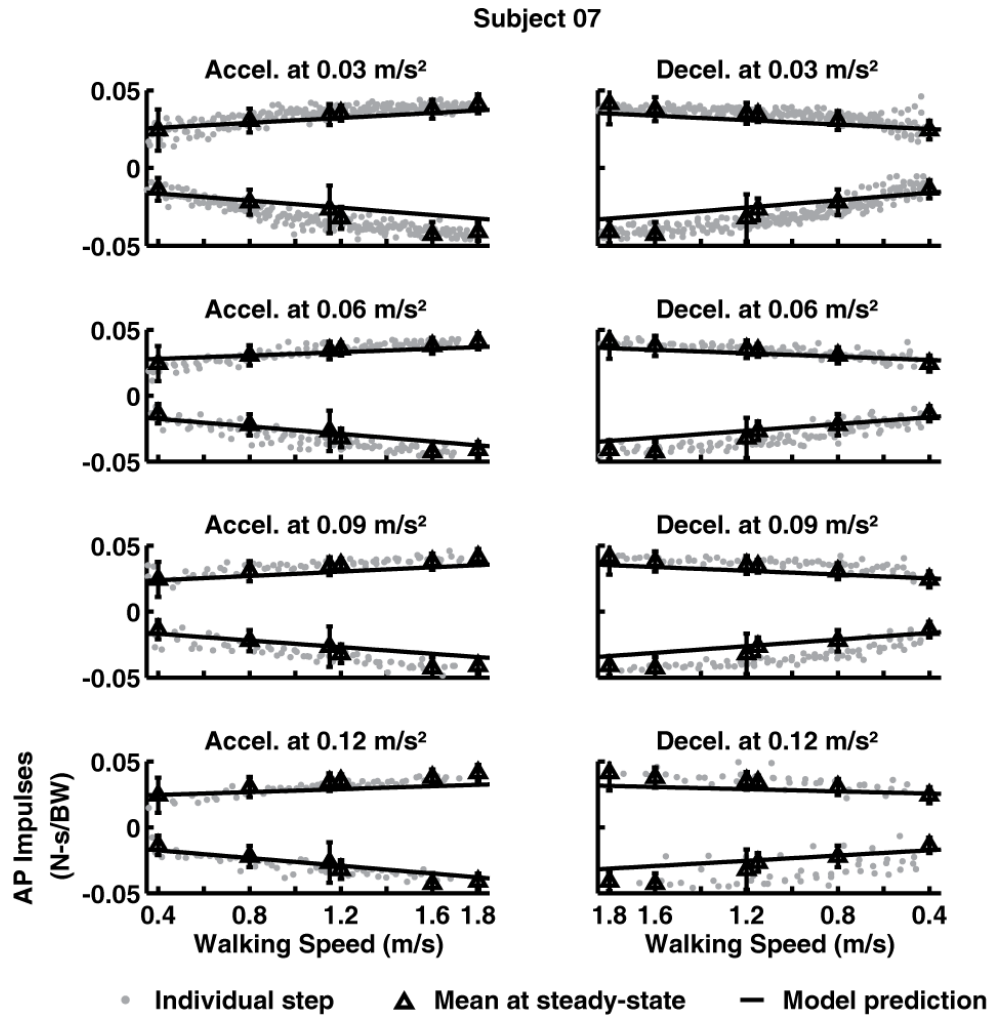


Figure A3-10: Linear mixed regression models were generated from data collected from ten subjects and are compared to individual steps for subject 07 at each rate and subject 07's mean anterior-posterior ground reaction force (AP) impulses (error bars are  $\pm 3$  standard deviations) at steady-state speeds. Subject 07's self-selected walking speed was 1.15 m/s.

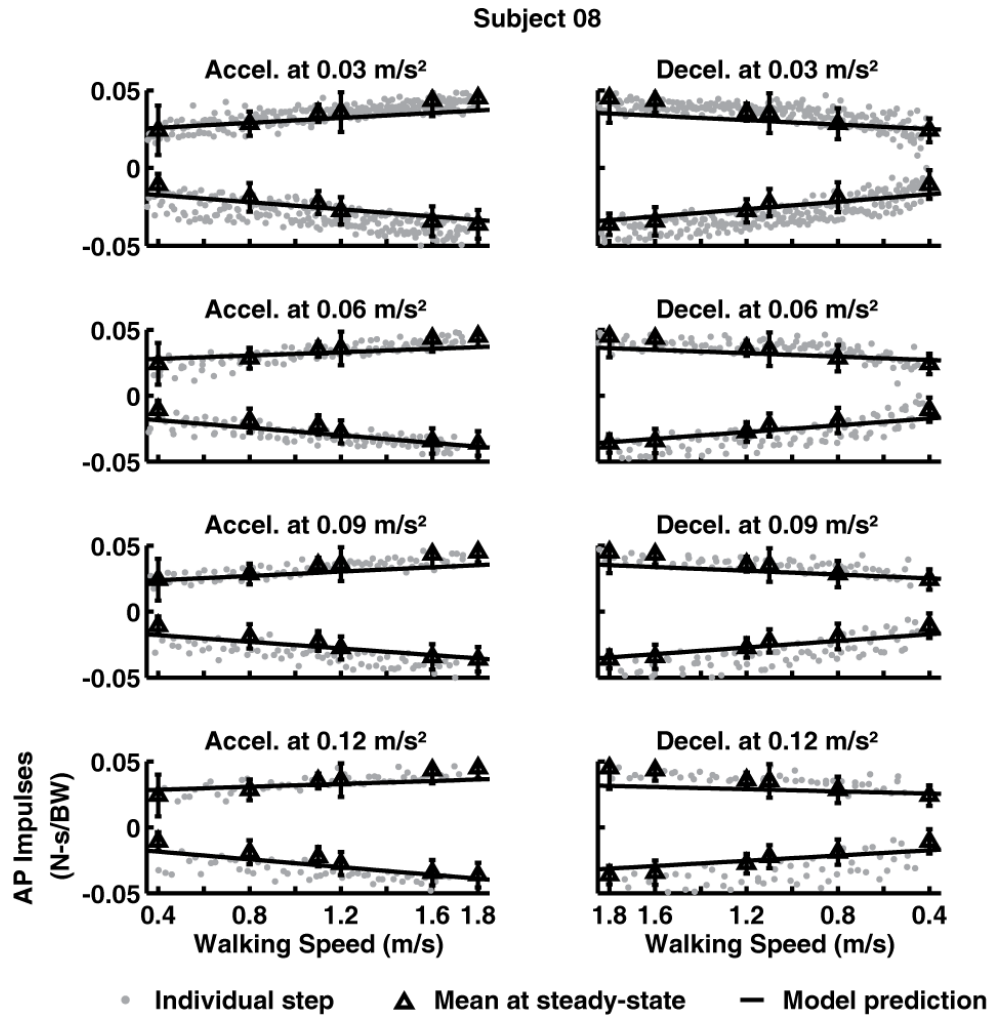


Figure A3-11: Linear mixed regression models were generated from data collected from ten subjects and are compared to individual steps for subject 08 at each rate and subject 08's mean anterior-posterior ground reaction force (AP) impulses (error bars are  $\pm 3$  standard deviations) at steady-state speeds. Subject 08's self-selected walking speed was 1.1 m/s.

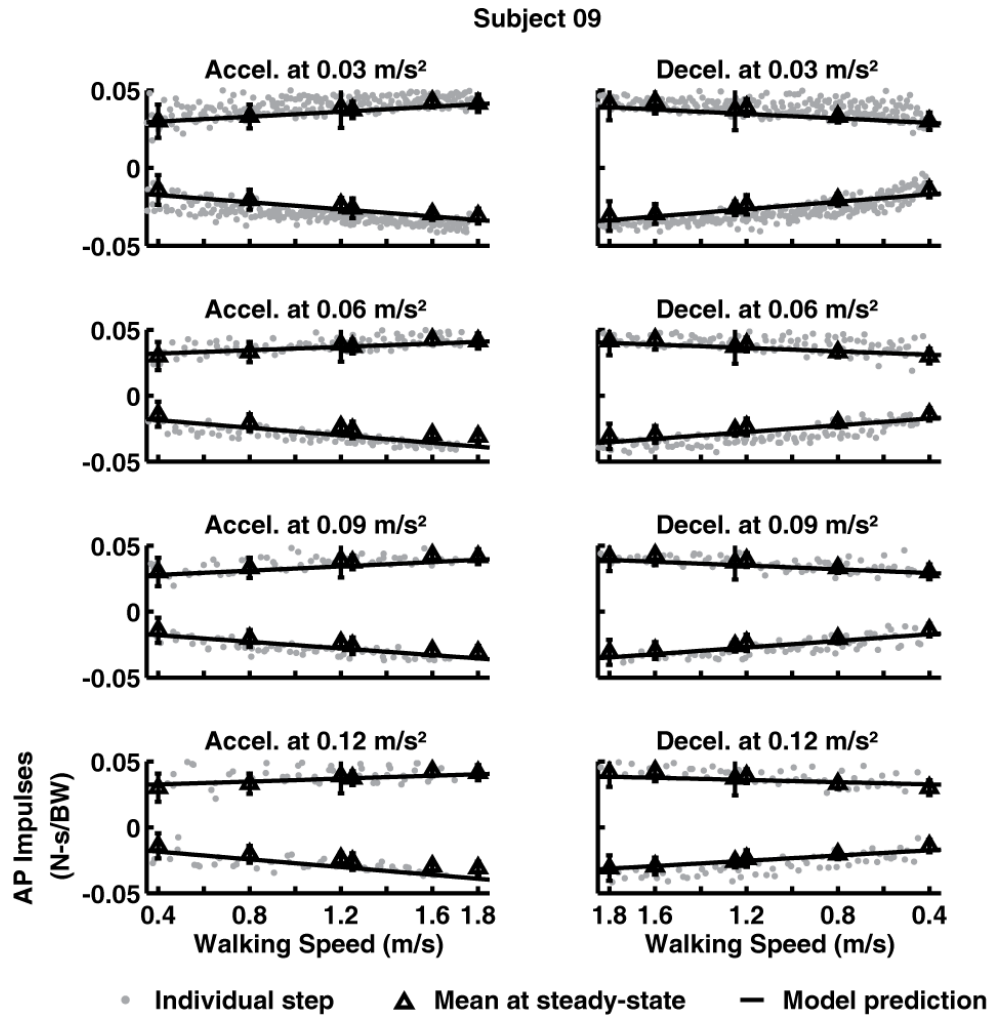


Figure A3-12: Linear mixed regression models were generated from data collected from ten subjects and are compared to individual steps for subject 09 at each rate and subject 09's mean anterior-posterior ground reaction force (AP) impulses (error bars are  $\pm 3$  standard deviations) at steady-state speeds. Subject 09's self-selected walking speed was 1.25 m/s.

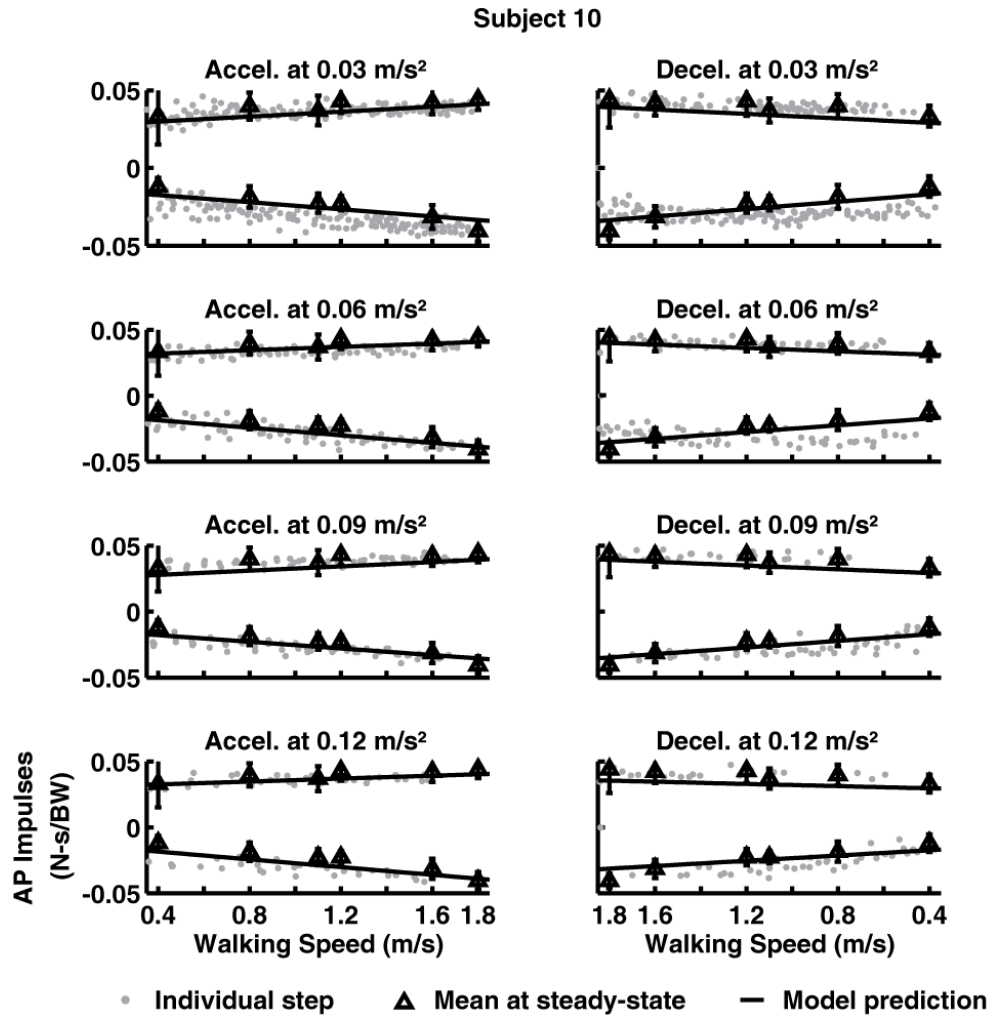


Figure A3-13: Linear mixed regression models were generated from data collected from ten subjects and are compared to individual steps for subject 10 at each rate and subject 10's mean anterior-posterior ground reaction force (AP) impulses (error bars are  $\pm 3$  standard deviations) at steady-state speeds. Subject 10's self-selected walking speed was 1.1 m/s.

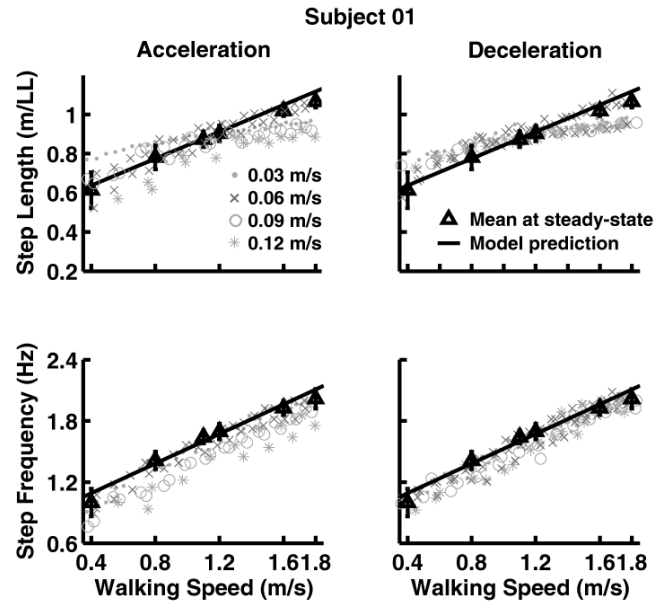


Figure A3-14: Linear models generated from data across ten subjects compared to mean step lengths (normalized by leg length (LL)) and frequencies ( $\pm 3$  standard deviations) by subject 01 at steady-state speeds and individual steps.

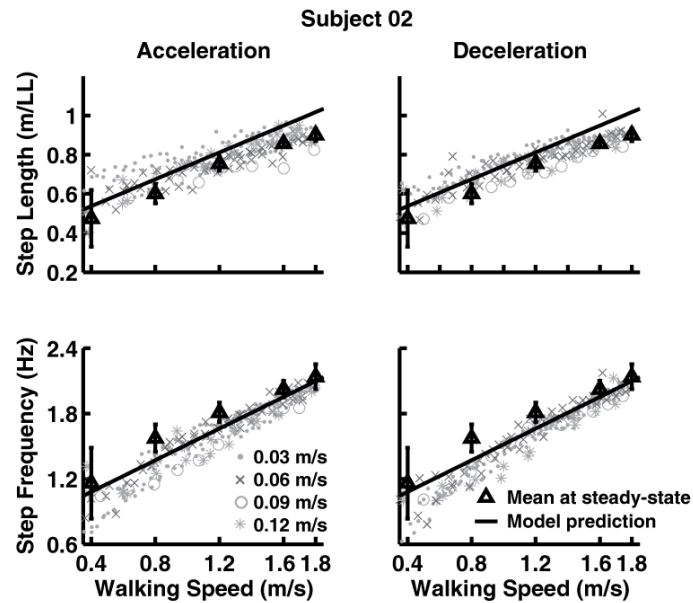


Figure A3-15: Linear models generated from data across ten subjects compared to mean step lengths (normalized by leg length (LL)) and frequencies ( $\pm 3$  standard deviations) by subject 02 at steady-state speeds and individual steps.



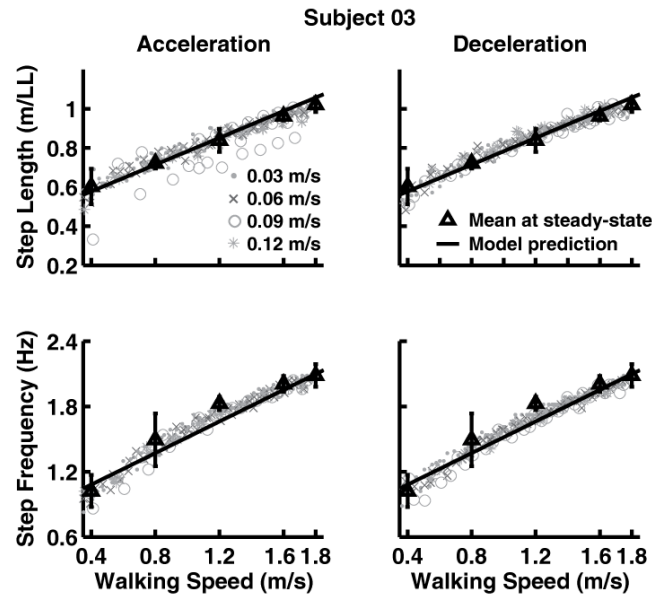


Figure A3-16: Linear models generated from data across ten subjects compared to mean step lengths (normalized by leg length (LL)) and frequencies ( $\pm 3$  standard deviations) by subject 03 at steady-state speeds and individual steps.

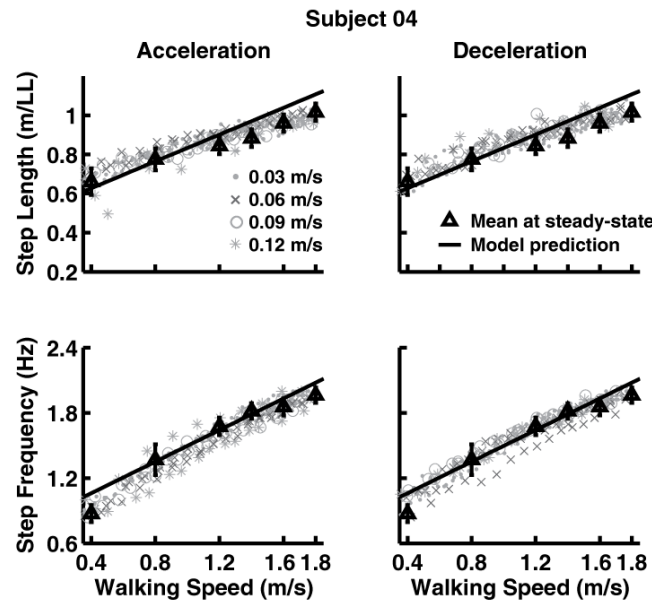


Figure A3-17: Linear models generated from data across ten subjects compared to mean step lengths (normalized by leg length (LL)) and frequencies ( $\pm 3$  standard deviations) by subject 04 at steady-state speeds and individual steps.

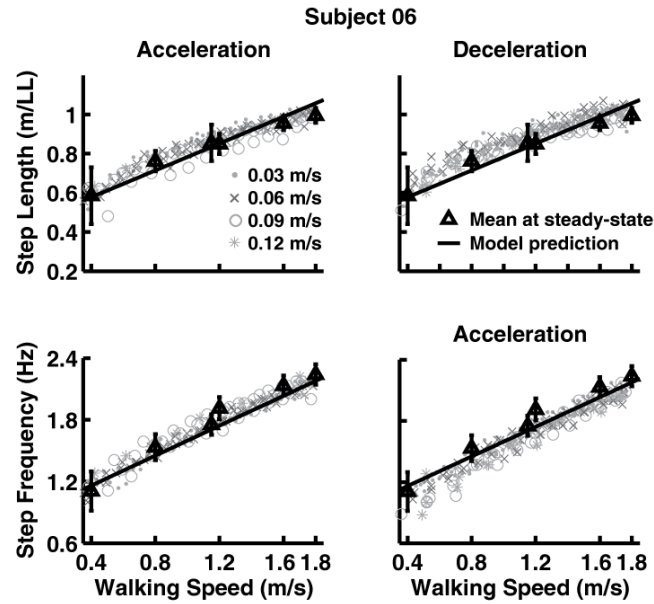


Figure A3-18: Linear models generated from data across ten subjects compared to mean step lengths (normalized by leg length (LL)) and frequencies ( $\pm 3$  standard deviations) by subject 06 at steady-state speeds and individual steps.

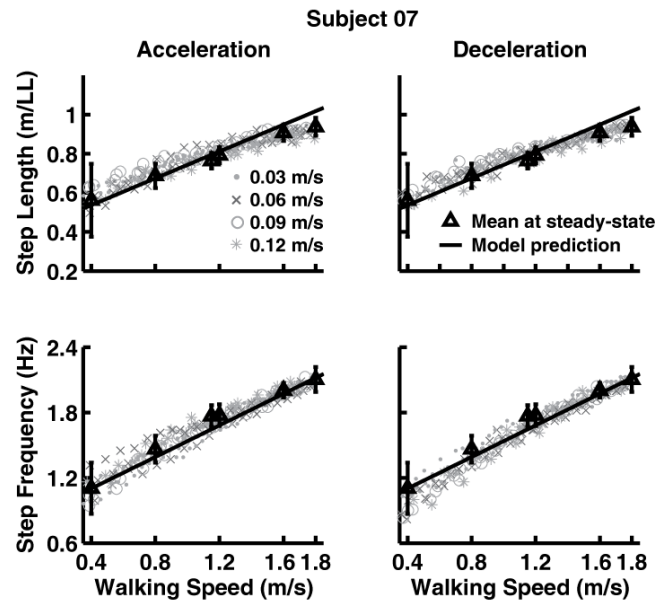


Figure A3-19: Linear models generated from data across ten subjects compared to mean step lengths (normalized by leg length (LL)) and frequencies ( $\pm 3$  standard deviations) by subject 07 at steady-state speeds and individual steps.

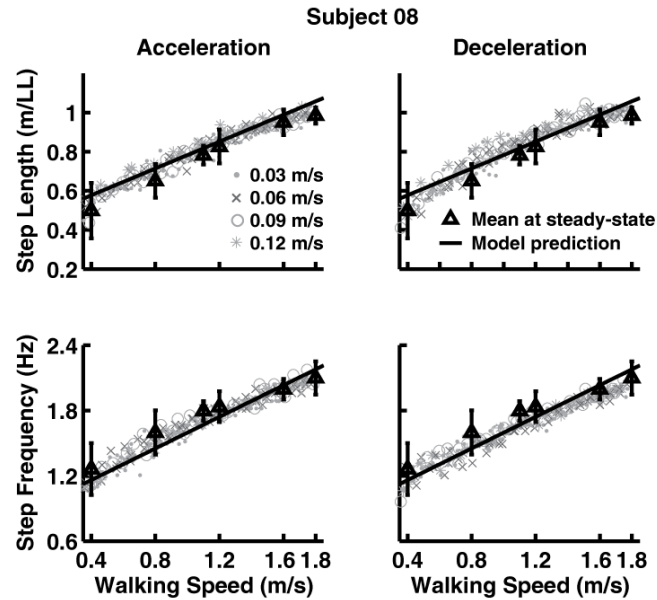


Figure A3-20: Linear models generated from data across ten subjects compared to mean step lengths (normalized by leg length (LL)) and frequencies ( $\pm 3$  standard deviations) by subject 08 at steady-state speeds and individual steps.

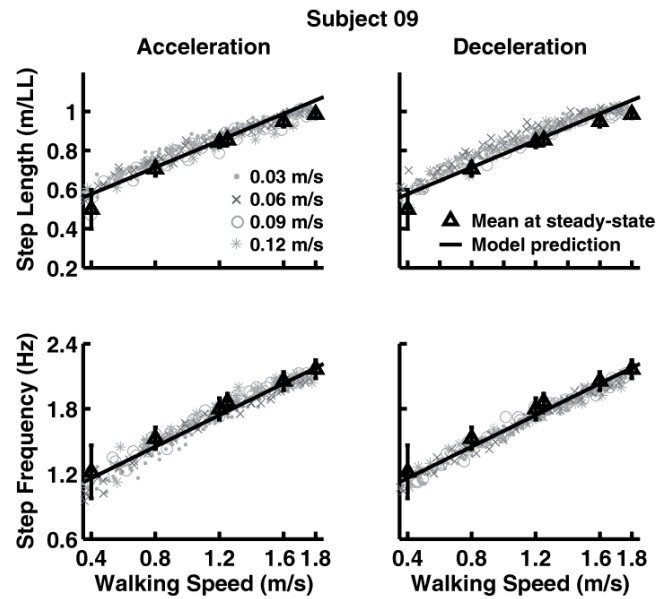


Figure A3-21: Linear models generated from data across ten subjects compared to mean step lengths (normalized by leg length (LL)) and frequencies ( $\pm 3$  standard deviations) by subject 09 at steady-state speeds and individual steps.

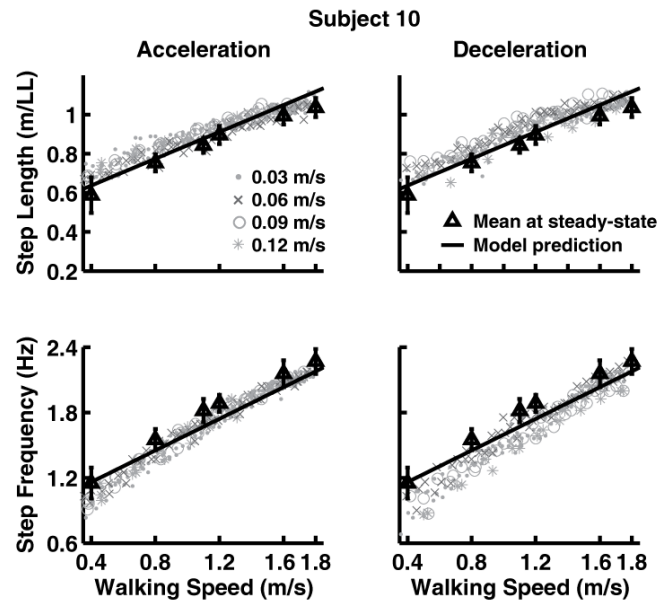


Figure A3-22: Linear models generated from data across ten subjects compared to mean step lengths (normalized by leg length (LL)) and frequencies ( $\pm 3$  standard deviations) by subject 10 at steady-state speeds and individual steps.

## References

- Anderson, F. C., 1999. A dynamic optimization solution for a complete cycle of normal gait. Austin, TX, The University of Texas at Austin.
- Association, A. H., 1997. Heart and Stroke Facts, Dallas, TX: AHA. 2010.
- Audu, M. L. and Davy, D. T., 1985. The influence of muscle model complexity in musculoskeletal motion modeling. *J Biomech Eng* 107, 147-57.
- Balasubramanian, C. K., Bowden, M. G., Neptune, R. R. and Kautz, S. A., 2007. Relationship between step length asymmetry and walking performance in subjects with chronic hemiparesis. *Arch Phys Med Rehabil* 88, 43-9.
- Biewener, A. A., Farley, C. T., Roberts, T. J. and Temaner, M., 2004. Muscle mechanical advantage of human walking and running: implications for energy cost. *J Appl Physiol* 97, 2266-74.
- Bowden, M. G., Balasubramanian, C. K., Neptune, R. R. and Kautz, S. A., 2006. Anterior-posterior ground reaction forces as a measure of paretic leg contribution in hemiparetic walking. *Stroke* 37, 872-6.
- Brouwer, B., Parvataneni, K. and Olney, S. J., 2009. A comparison of gait biomechanics and metabolic requirements of overground and treadmill walking in people with stroke. *Clin Biomech (Bristol, Avon)* 24, 729-34.
- Cavagna, G. A. and Franzetti, P., 1986. The determinants of the step frequency in walking in humans. *J Physiol* 373, 235-42.
- Chen, G. and Patten, C., 2008. Joint moment work during the stance-to-swing transition in hemiparetic subjects. *J Biomech* 41, 877-83.
- Chen, G., Patten, C., Kothari, D. H. and Zajac, F. E., 2005. Gait differences between individuals with post-stroke hemiparesis and non-disabled controls at matched speeds. *Gait Posture* 22, 51-6.
- Chen, G., Patten, C., Kothari, D. H. and Zajac, F. E., 2005a. Gait differences between individuals with post-stroke hemiparesis and non-disabled controls at matched speeds. *Gait Posture* 22, 51-6.
- Chen, G., Patten, C., Kothari, D. H. and Zajac, F. E., 2005b. Gait deviations associated with post-stroke hemiparesis: improvement during treadmill walking using weight support, speed, support stiffness, and handrail hold. *Gait Posture* 22, 57-62.
- Corriveau, H., Hebert, R., Raiche, M. and Prince, F., 2004. Evaluation of postural stability in the elderly with stroke. *Arch Phys Med Rehabil* 85, 1095-101.
- De Quervain, I. A., Simon, S. R., Leurgans, S., Pease, W. S. and McAllister, D., 1996. Gait pattern in the early recovery period after stroke. *J Bone Joint Surg Am* 78, 1506-14.

- Delp, S. L., Loan, J. P., Hoy, M. G., Zajac, F. E., Topp, E. L. and Rosen, J. M., 1990. An interactive graphics-based model of the lower extremity to study orthopaedic surgical procedures. *IEEE Trans Biomed Eng* 37, 757-67.
- Den Otter, A. R., Geurts, A. C., Mulder, T. and Duysens, J., 2004. Speed related changes in muscle activity from normal to very slow walking speeds. *Gait Posture* 19, 270-8.
- Den Otter, A. R., Geurts, A. C., Mulder, T. and Duysens, J., 2007. Abnormalities in the temporal patterning of lower extremity muscle activity in hemiparetic gait. *Gait Posture* 25, 342-52.
- Detrembleur, C., Dierick, F., Stoquart, G., Chantaine, F. and Lejeune, T., 2003. Energy cost, mechanical work, and efficiency of hemiparetic walking. *Gait Posture* 18, 47-55.
- Diedrich, F. J. and Warren, W. H., Jr., 1995. Why change gaits? Dynamics of the walk-run transition. *J Exp Psychol Hum Percept Perform* 21, 183-202.
- Fregly, B. J. and Zajac, F. E., 1996. A state-space analysis of mechanical energy generation, absorption, and transfer during pedaling. *J Biomech* 29, 81-90.
- Goffe, W. L., Ferrier, G.D., and Rogers, J., 1994. Global optimization of statistical functions with simulated annealing. *Journal of Econometrics* 60, 65-99.
- Goldberg, E. J., Kautz, S. A. and Neptune, R. R., 2008. Can treadmill walking be used to assess propulsion generation? *J Biomech* 41, 1805-8.
- Goldberg, E. J. and Neptune, R. R., 2007. Compensatory strategies during normal walking in response to muscle weakness and increased hip joint stiffness. *Gait Posture* 25, 360-7.
- Hsu, A. L., Tang, P. F. and Jan, M. H., 2003. Analysis of impairments influencing gait velocity and asymmetry of hemiplegic patients after mild to moderate stroke. *Arch Phys Med Rehabil* 84, 1185-93.
- Hunt, A. E., Smith, R. M. and Torode, M., 2001. Extrinsic muscle activity, foot motion and ankle joint moments during the stance phase of walking. *Foot Ankle Int* 22, 31-41.
- Ishikawa, M., Komi, P. V., Grey, M. J., Lepola, V. and Bruggemann, G. P., 2005. Muscle-tendon interaction and elastic energy usage in human walking. *J Appl Physiol* 99, 603-8.
- Jonkers, I., Delp, S. and Patten, C., 2009. Capacity to increase walking speed is limited by impaired hip and ankle power generation in lower functioning persons post-stroke. *Gait Posture* 29, 129-37.

- Kautz, S. A. and Neptune, R. R., 2002. Biomechanical determinants of pedaling energetics: internal and external work are not independent. *Exerc Sport Sci Rev* 30, 159-65.
- Kepple, T. M., Siegel, K. L. and Stanhope, S. J., 1997. Relative contributions of the lower extremity joint moments to forward progression and support during gait. *Gait Posture* 6, 1-8.
- Knutsson, E. and Richards, C., 1979. Different types of disturbed motor control in gait of hemiparetic patients. *Brain* 102, 405-30.
- Lamontagne, A., Malouin, F., Richards, C. L. and Dumas, F., 2002. Mechanisms of disturbed motor control in ankle weakness during gait after stroke. *Gait Posture* 15, 244-55.
- Li, L. and Hamill, J., 2002. Characteristics of the vertical ground reaction force component prior to gait transition. *Res Q Exerc Sport* 73, 229-37.
- Liu, M. Q., Anderson, F. C., Pandy, M. G. and Delp, S. L., 2006. Muscles that support the body also modulate forward progression during walking. *J Biomech* 39, 2623-30.
- Liu, M. Q., Anderson, F. C., Schwartz, M. H. and Delp, S. L., 2008. Muscle contributions to support and progression over a range of walking speeds. *J Biomech* 41, 3243-52.
- Martin, P. E. and Marsh, A. P., 1992. Step length and frequency effects on ground reaction forces during walking. *J Biomech* 25, 1237-9.
- McGowan, C. P., Kram, R. and Neptune, R. R., 2009. Modulation of leg muscle function in response to altered demand for body support and forward propulsion during walking. *J Biomech* 42, 850-6.
- McGowan, C. P., Neptune, R. R. and Kram, R., 2008. Independent effects of weight and mass on plantar flexor activity during walking: implications for their contributions to body support and forward propulsion. *J Appl Physiol* 105, 486-94.
- Menegaldo, L. L., de Toledo Fleury, A. and Weber, H. I., 2004. Moment arms and musculotendon lengths estimation for a three-dimensional lower-limb model. *J Biomech* 37, 1447-53.
- Morita, S., Yamamoto, H. and Furuya, K., 1995. Gait analysis of hemiplegic patients by measurement of ground reaction force. *Scand J Rehabil Med* 27, 37-42.
- Mulroy, S. J., Klassen, T., Gronley, J. K., Eberly, V. J., Brown, D. A. and Sullivan, K. J., 2010. Gait parameters associated with responsiveness to treadmill training with body-weight support after stroke: an exploratory study. *Phys Ther* 90, 209-23.

- Nadeau, S., Gravel, D., Arsenault, A. B. and Bourbonnais, D., 1999. Plantarflexor weakness as a limiting factor of gait speed in stroke subjects and the compensating role of hip flexors. *Clin Biomech (Bristol, Avon)* 14, 125-35.
- Neptune, R. R., Kautz, S. A. and Zajac, F. E., 2001. Contributions of the individual ankle plantar flexors to support, forward progression and swing initiation during walking. *J Biomech* 34, 1387-98.
- Neptune, R. R., Sasaki, K. and Kautz, S. A., 2008. The effect of walking speed on muscle function and mechanical energetics. *Gait Posture* 28, 135-43.
- Neptune, R. R., Wright, I. C. and Van Den Bogert, A. J., 2000. A Method for Numerical Simulation of Single Limb Ground Contact Events: Application to Heel-Toe Running. *Comput Methods Biomech Biomed Engin* 3, 321-334.
- Neptune, R. R., Zajac, F. E. and Kautz, S. A., 2004. Muscle force redistributes segmental power for body progression during walking. *Gait Posture* 19, 194-205.
- Neptune, R. R., Zajac, F. E. and Kautz, S. A., 2004a. Muscle force redistributes segmental power for body progression during walking. *Gait Posture* 19, 194-205.
- Neptune, R. R., Zajac, F. E. and Kautz, S. A., 2004b. Muscle mechanical work requirements during normal walking: the energetic cost of raising the body's center-of-mass is significant. *J Biomech* 37, 817-25.
- Niam, S., Cheung, W., Sullivan, P. E., Kent, S. and Gu, X., 1999. Balance and physical impairments after stroke. *Arch Phys Med Rehabil* 80, 1227-33.
- Nilsson, J. and Thorstensson, A., 1987. Adaptability in frequency and amplitude of leg movements during human locomotion at different speeds. *Acta Physiol Scand* 129, 107-14.
- Nilsson, J. and Thorstensson, A., 1989. Ground reaction forces at different speeds of human walking and running. *Acta Physiol Scand* 136, 217-27.
- Olney, S. J., Griffin, M. P., Monga, T. N. and McBride, I. D., 1991. Work and power in gait of stroke patients. *Arch Phys Med Rehabil* 72, 309-14.
- Orendurff, M. S., Bernatz, G. C., Schoen, J. A. and Klute, G. K., 2008b. Kinetic mechanisms to alter walking speed. *Gait Posture* 27, 603-10.
- Orendurff, M. S., Schoen, J. A., Bernatz, G. C., Segal, A. D. and Klute, G. K., 2008a. How humans walk: bout duration, steps per bout, and rest duration. *J Rehabil Res Dev* 45, 1077-89.
- Parvataneni, K., Ploeg, L., Olney, S. J. and Brouwer, B., 2009. Kinematic, kinetic and metabolic parameters of treadmill versus overground walking in healthy older adults. *Clin Biomech (Bristol, Avon)* 24, 95-100.
- Perry, J., 1993. Determinants of muscle function in the spastic lower extremity. *Clin Orthop Relat Res*, 10-26.



- Perry, J., Garrett, M., Gronley, J. K. and Mulroy, S. J., 1995. Classification of walking handicap in the stroke population. *Stroke* 26, 982-9.
- Peterson, C. L., Cheng, J., Kautz, S. A. and Neptune, R. R., 2010. Leg extension is an important predictor of paretic leg propulsion in hemiparetic walking. *Gait Posture*, in press.
- Raasch, C. C., Zajac, F. E., Ma, B. and Levine, W. S., 1997. Muscle coordination of maximum-speed pedaling. *J Biomech* 30, 595-602.
- Sasaki, K., Neptune, R. R. and Kautz, S. A., 2009. The relationships between muscle, external, internal and joint mechanical work during normal walking. *J Exp Biol* 212, 738-44.
- Segers, V., Aerts, P., Lenoir, M. and De Clercq, D., 2006. Spatiotemporal characteristics of the walk-to-run and run-to-walk transition when gradually changing speed. *Gait Posture* 24, 247-54.
- Svantesson, U., Takahashi, H., Carlsson, U., Danielsson, A. and Sunnerhagen, K. S., 2000. Muscle and tendon stiffness in patients with upper motor neuron lesion following a stroke. *Eur J Appl Physiol* 82, 275-9.
- Thorstensson, A. and Rotherthson, H., 1987. Adaptations to changing speed in human locomotion: speed of transition between walking and running. *Acta Physiol Scand* 131, 211-4.
- Turnbull, G. I., Charteris, J. and Wall, J. C., 1996. Deficiencies in standing weight shifts by ambulant hemiplegic subjects. *Arch Phys Med Rehabil* 77, 356-62.
- Turns, L. J., Neptune, R. R. and Kautz, S. A., 2007. Relationships between muscle activity and anteroposterior ground reaction forces in hemiparetic walking. *Arch Phys Med Rehabil* 88, 1127-35.
- Umberger, B. R., 2010. Stance and swing phase costs in human walking. *J R Soc Interface*.
- Umberger, B. R., 2010. Stance and swing phase costs in human walking. *J R Soc Interface*.
- Umberger, B. R. and Martin, P. E., 2007. Mechanical power and efficiency of level walking with different stride rates. *J Exp Biol* 210, 3255-65.
- Winters, J. M. and Stark, L., 1988. Estimated mechanical properties of synergistic muscles involved in movements of a variety of human joints. *J Biomech* 21, 1027-41.
- Zajac, F. E., 1989. Muscle and tendon: properties, models, scaling, and application to biomechanics and motor control. *Crit Rev Biomed Eng* 17, 359-411.
- Zajac, F. E., 1993. Muscle coordination of movement: a perspective. *J Biomech* 26 Suppl 1, 109-24.

- Zajac, F. E., Neptune, R. R. and Kautz, S. A., 2002. Biomechanics and muscle coordination of human walking. Part I: introduction to concepts, power transfer, dynamics and simulations. *Gait Posture* 16, 215-32.
- Zajac, F. E., Neptune, R. R. and Kautz, S. A., 2003. Biomechanics and muscle coordination of human walking: part II: lessons from dynamical simulations and clinical implications. *Gait Posture* 17, 1-17.
- Zamparo, P., Francescato, M. P., De Luca, G., Lovati, L. and di Prampero, P. E., 1995. The energy cost of level walking in patients with hemiplegia. *Scand J Med Sci Sports* 5, 348-52.
- Zarrugh, M. Y. and Radcliffe, C. W., 1978. Predicting metabolic cost of level walking. *Eur J Appl Physiol Occup Physiol* 38, 215-23.

## **Vita**

Carrie Lynn Peterson was born in Ann Arbor, MI on June 10, 1981, the daughter of Paul and Jane Peterson. In 1999, she graduated from Vicksburg High School and entered the University of Michigan in Ann Arbor, MI. During the summers from 2000 to 2003, she worked at Eaton Corporation in Galesburg, MI as an engineering intern. Carrie received a Bachelor of Science in Mechanical Engineering from The University of Michigan in 2004. She worked in the Biomechanics Research Laboratory at The University of Michigan during the summer and Fall of 2004 as an undergraduate research assistant. In 2005, she entered the graduate program in Mechanical Engineering at The University of Texas at Austin and received the degree Master of Science in Engineering in 2007.

Permanent address: 9328 Arrowhead Dr, Scotts, MI 49088

This dissertation was typed by the author.